Open access • Book Chapter • DOI:10.1520/STP27119S

Fatigue Crack Propagation in Rail Steels — Source link

CE Feddersen, David Broek

Institutions: Battelle Memorial Institute

Published on: 01 Jan 1978 - ASTM special technical publications (ASTM International)

Topics: Paris' law, Fracture mechanics and Pearlite

REPORT NO. FRA/ORD-77/14

FATIGUE CRACK PROPAGATION IN RAIL STEELS

C.E. Feddersen
R.D. Buchheit
D. Broek

BATTELLE COLUMBUS LABORATORIES
505 King Avenue
Columbus OH 43201

JUNE 1977
INTERIM REPORT

Prepared for

U.S. DEPARTMENT OF TRANSPORTATION
FEDERAL RAILROAD ADMINISTRATION
Research and Development
Washington DC 20590

Technical Report Documentation Page

1. Report No.	2. Government Accession No.	3. Recipient's Catalog No.
FRA/ORD-77/14		

4. Title and Subtitle	5. Report Date
FATIGUE CRACK PROPAGATION IN RAIL STEELS	June 1977
	6. Performing Organization Code
7. Author(s) G.E. Feddersen, R.D. Buchheit, D. Broek	8. Performing Organization Report No. DOT-TSC-FRA-77-3
9. Performing Organization Name and Address Battelle Columbus Laboratories* 505 King Avenue Columbus OH 43201	10. Work Unit No. (TRAIS) RR719/R7321 11. Contract or Grant No. DOT-TSC-1076
12. Sponsoring Agency Name and Address U.S. Department of Transportation Federal Railroad Administration Research and Development Washington DC 20590	13. Type of Report and Period Covered Interim Report July 1975 - July 1976 14. Sponsoring Agency Code

15. Supplementary Notes

*Under contract to: U.S. Department of Transportation
Transportation Systems Center
Kendall Square
Cambridge MA 02142

16. Abstract

In order to establish safe inspection periods of railroad rails information on fatigue crack growth rates is required. These data should come from a sufficiently large sample of rails presently in service. The reported research consisted of the generation and analysis of fatigue crack growth data of 66 rail samples taken from existing track all over the United States. Additional information concerns mechanical properties, chemical composition, microstructure, and fractographic features.

A statistical analysis was performed to evaluate possible correlations with fatigue crack growth properties and microstructural parameters. Weak correlations were found with carbon, manganese and oxygen content, and with the fraction of pearlite.

A subsequent phase of this research program is laid out.

17. Key Words	18. Distribution Statement
Rail, Cracks, Fatigue Crack Propagation, Chemical Composition, Mechanical Properties, Microstructure, Fractography	DOCUMENT IS AVAILABLE TO THE U.S. PUBLIC THROUGH THE NATIONAL TECHNICAL INFORMATION SERVICE, SPRINGFIELD, VIRGINIA 22161

19. Security Classif. (of this report)	20. Security Classif. (of this page)	22. Price
Unclassified	Unclassified	PC A06-A01

Form DOT F 1700.7 (8-72) Reproduction of completed page authorized

PREFACE

This report presents the results of the first phase of a program on Rail Material Failure Characterization. It has been prepared by Battelle's Columbus Laboratories (BCL) under Contract DOT-TSC-1076 for the Transportation Systems Center (TSC) of the Department of Transportation. The work was conducted under the technical direction of Mr. Roger Steele of TSC.

The results of this phase of the program are the basis for the lay out of the second phase. The objective of the second phase is the development of a computational rail failure model. This model, in conjunction with the results of ongoing studies on Engineering Stress Analysis of Rails and on Wheel-Rail-Loads when incorporated into a reliability analyses will enable establishment of safe inspection schedules.

The cooperation of the American Association of Railroads (AAR) and the various railroads (Boston & Maine Railroad Company, Chessie System, Denver and Rio Grande Western Railroad Company, Penn Central Railroad Company, Southern Pacific Transportation Company, and Union Pacific Railroad Company) in acquiring rail samples is gratefully acknowledged. The cooperation and assistance of Mr. Roger Steele of TSC, Mr. Omar Deel and Mr. David Utah of BCL were of great value to the program.

METRIC CONVERSION FACTORS

Approximate Conversions to Metric Measures

Symbol	When You Know	Multiply by	To Find	Symbol
		LENGTH		
in	inches	2.5	centimeters	cm
ft	feet	30	centimeters	cm
yd	yards	0.9	meters	m
mi	miles	1.6	kilometers	km
		AREA		
in^2	square inches	6.5	square centimeters	cm^2
ft^2	square feet	0.09	square meters	m^2
yd^2	square yards	0.8	square meters	m^2
mi^2	square miles	2.6	square kilometers	km^2
	acres	0.4	hectares	ha
		MASS (weight)		
oz	ounces	28	grams	g
lb	pounds	0.45	kilograms	kg
	short tons (2000 lb)	0.9	tonnes	t
		VOLUME		
tsp	teaspoons	5	milliliters	ml
Tbsp	tablespoons	15	milliliters	ml
fl oz	fluid ounces	30	milliliters	ml
c	cups	0.24	liters	l
pt	pints	0.47	liters	l
qt	quarts	0.95	liters	l
gal	gallons	3.8	liters	l
ft^3	cubic feet	0.03	cubic meters	m^3
yd^3	cubic yards	0.76	cubic meters	m^3
		TEMPERATURE (exact)		
	Fahrenheit temperature	5/9 (after subtracting 32)	Celsius temperature	°C

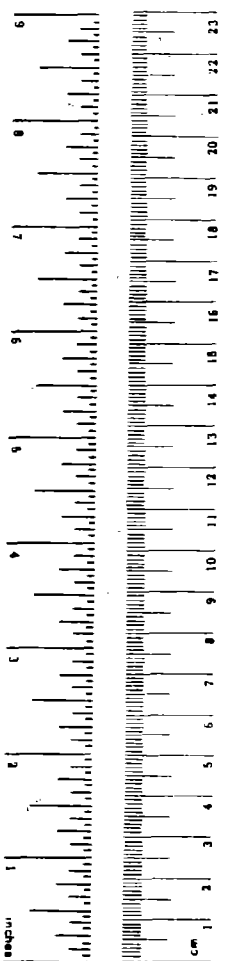

Approximate Conversions from Metric Measures

Symbol	When You Know	Multiply by	To Find	Symbol
		LENGTH		
mm	millimeters	0.04	inches	in
cm	centimeters	0.4	inches	in
m	meters	3.3	feet	ft
m	meters	1.1	yards	yd
km	kilometers	0.6	miles	mi
		AREA		
cm^2	square centimeters	0.16	square inches	in^2
m^2	square meters	1.2	square yards	yd^2
km^2	square kilometers	0.4	square miles	mi^2
ha	hectares (10,000 m^2)	2.5	acres	
		MASS (weight)		
g	grams	0.035	ounces	oz
kg	kilograms	2.2	pounds	lb
t	tonnes (1000 kg)	1.1	short tons	
		VOLUME		
ml	milliliters	0.03	fluid ounces	fl oz
l	liters	2.1	pints	pt
l	liters	1.06	quarts	qt
l	liters	0.26	gallons	gal
m^3	cubic meters	35	cubic feet	ft^3
m^3	cubic meters	1.3	cubic yards	yd^3
		TEMPERATURE (exact)		
°C	Celsius temperature	9/5 (then add 32)	Fahrenheit temperature	°F

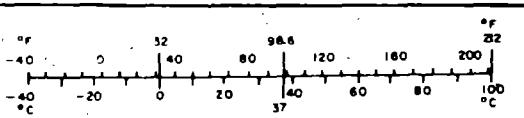

TABLE OF CONTENTS

LIST OF FIGURES

LIST OF FIGURES (Continued)

LIST OF TABLES

LIST OF TABLES (Continued)

EXPLANATORY NOTE

This report conveys preliminary information on the crack growth behavior of a sample of rail steels (66 rails) taken from the population currently in use in the United States. Ultimately, this information will be used to predict the flaw growth behavior of actual rails in service under various loading and support conditions. A more comprehensive treatment of the subject, with additional test data, will be available later in 1977. This interim report is being issued at this time to provide other investigators working in the field with the results which have been generated thus far.

1. INTRODUCTION

Fatigue cracks in railroad rails can be the cause of rail failures and subsequent derailments. Prevention of these failures relies on timely detection of fatigue cracks when they are still small and not likely to cause failures. In order to establish safe inspection periods, data are required on the available time for crack detection, i.e., the time it takes for a small detectable crack to grow to a critical size that can cause rail failure. Therefore, the rate of fatigue-crack propagation has to be known.

One portion of the Federal Railroad Administration's (FRA) Track Performance Improvement Program is the development of a predictive rail failure model that enables a determination of optimal inspection periods through a calculation of fatigue-crack-propagation behavior. The research reported here concerns the first phase of a program to develop this rail failure model.

In order to predict fatigue-crack growth and failures under a service load environment, fatigue-crack-rate data are required. These data should come from a sufficiently large sample of rails presently in service to properly evaluate the statistical variability of fatigue-crack-growth properties. The first phase of this program consisted of the generation and analysis of fatigue-crack-growth data of 66 rail samples of various age, make, and weight. The samples were taken from existing track from all sections of the United States.

This report presents the crack-growth data for the 66 rail samples. Also presented are chemical compositions, mechanical properties, and some data on microstructure and fractographic features. A statistical analysis was performed to evaluate possible correlation between one or more of these parameters and the resistance to fatigue-crack propagation.

On the basis of the present results, the 66 samples were divided into three broad categories of rate behavior. Further characterization of the three categories will be conducted; i.e., the effect of parameters such as stress ratio, temperature, and microstructural orientation be experimentally evaluated. The behavior under variable amplitude loading also will be investigated. Subsequently, the computational failure model will be developed after which the results will be reported.

2. RAIL MATERIALS: SAMPLE SOURCE AND DESCRIPTION

At the outset of this program, an effort was made to assemble a representa-give sampling of rail materials which are presently, and will continue to be, in service on U. S. railroads. Variations of rail size, rail producer, and year of production were the primary selection criteria. Eleven of the major railroad organizations were contacted for contributions of rail samples. Directly or indirectly samples were received from the following organizations:

- Association of American Railroads
- Boston and Maine Railroad Company
- Chessie System
- Denver and Rio Grande Western Railroad Company
- Penn Central Railroad Company
- Southern Pacific Transportation Company
- Transportation Systems Center
- Union Pacific Railroad Company.

A total of 66 material samples were received representing sizes from 85 lb/yd to 140 lb/yd, produced over a period from 1911 to 1975 in both U. S. and Japanese mills. The samples were given identification numbers from 001 to 066. Basic information on the samples is presented in Table 1.

3. METALLOGRAPHIC CHARACTERIZATIONS

3.1 CHEMICAL ANALYSES

Specifications for the chemical composition of rail steels vary slightly with the rail size (expressed as the weight per yard of rail). The ASTM Standard Specification for Carbon-Steel Rails, ASTM Designation: A1-68a, states the following chemical requirements:

Element, percent	Nominal Weight, lb/yd			
	61-80	81-90	91-120	121 and Over
Carbon	0.55-0.68	0.64-0.77	0.67-0.80	0.69-0.82
Manganese	0.60-0.90	0.60-0.90	0.70-1.00	0.70-1.00
Phosphorus, max	0.04	0.04	0.04	0.04
Silicon	0.10-0.23	0.10-0.23	0.10-0.23	0.10-0.23.

TABLE 1. RAIL MATERIALS INVENTORY

BCL Sequence Number	Receipt Date	Source	Source Number	Wt. or Section Number	Type	Controlled Cool	Mill Brand	Year Rolled	Month Rolled	Sample Length	Remarks
001	10/10/75	TSC	418	130			BSCO	1929	11	34-7/8	Steelton Open Hearth Med. Mang. Ht. 83530 AREA
002			521	85				1911		34	Maryland ASCE
003			399	130				1929	11	37-1/8	Steelton Open Hearth Med. Mang. Ht. 81366 AREA
004			100	85			BSCO	1920		36	Steelton Open Hearth ASCE
005			398	130				1929	9	35-3/8	Steelton Open Hearth Med. Mang. Ht. 81692 AREA
006			VD-1	115	RE			1974		35-1/2	Vacuum Degassed, Sydney VT Rail, New 115 lb A&M
007			VD-2	115	RE			1974		36-1/8	Vacuum Degassed, Sydney VT Rail, New 115 lb A&M
008			535	85				1924		35-5/8	Lackawanna Open Hearth ASCE
009			442	130				1929		36-1/8	Steelton Open Hearth Med. Mang. Ht. 83549
010			539	85				1919		36-1/4	Lackawanna Ht. 850 ASCE
011	10/14/75	AAR	UP-3-4	1330	RE	Yes	CF&I	1965	11	63-1/2	
012			UP-I-1	1330	RE		CF&I	1955	12	47-1/2	
013			PC-1-1	127DM			Illinois	1954	1	60-1/2	
014			UP-1-14	1330	RE	Yes	CF&I	1955	11	48	
015			UP-1-20	1330	RE	Yes	CF&I	1949	2	47-1/2	
016			UP-2A-9	133		Yes	CF&I	1957	5	50-1/2	
017			UP-2A-8	133			CF&I	1957	1	48	
018			UP-2A-2	1330	RE	Yes	CF&I	1953	4	40	
019			UP-3-5	1330	RE	Yes	CF&I	1965	11	40-3/4	
020			SF-2-3	119			CF&I	1957	11	47	
021			UP-1-27	1330	RE	Yes	CF&I	1955	11	42-1/4	
022			UP-2A-21	1330	RE	Yes	CF&I	1956	3	51-1/2	
023			UP-2A-17	133		Yes	CF&I	1957	1	52	
024			UP-2A-22	1330	RE	Yes	CF&I	1956	1	51-1/2	
025			UP-3-1	1330	RE	Yes	USS	1966	7	46-3/4	
026			UP-2A-15	1330	RE	Yes	CF&I	1957	1	49-3/4	
027			UP-1-6	133			CF&I	1956	12	46	
028			UP-2A-18	1330	RE	Yes	CF&I	1953	31	50	
029			SF-2-2	119		Yes	CF&I	1958	11	39-3/4	
030			SF-2-6	119			CF&I	1958	11	48-1/4	
031			UP-I-7	133			CF&I	1956	12	36-3/4	
032			UP-2A-20	13331	RE	Yes	USS	1953	3	47-3/4	
033			UP-I-12	133			CF&I	1955	11	46-1/2	
034			SF-2-5	1190		Yes		1957	1	46-3/4	
035	12/4/75	Denver & Rio Grande	165	1150	RE	Yes	CF&I	1955	5	35-3/4	Heat CH 9332 D3 Defect IDO S, Defect No. 165
036			143	112	RE		CF&I	1939	2	34-3/4	Heat 10053 820CH Defect BHJ 2, Defect No. 143
037			601	1155		Yes	CF&I	1943	12	40-1/4	Heat CC 2060 E5 Defect TDDS, Defect No. 601
038			158	1121			CF&I	1930	9	37-3/4	Heat 16422 E 6 IM Defect TDDS, Defect No. 158
039			215	90			CF&I	1924	4	36-1/4	Heat 2521 C, Defect TDDS, Defect No. 215
040			499	100			CF&I	1928	3	36	Heat 2996 B 19, Defect VSH 4 inch (sub for BH) Defect No. 499
041			155	1150	RE	Yes	CF&I	1953	3	36-1/4	Heat 15198 FJ Defect HSH, Defect No. 155
042			496	100			CF&I	1928	3	36	Heat 3004 81 Defect TDDS, Defect No. 496
043			179	90			CF&I	1921	3	36	Heat 1368, Defect BAJZ, Defect No. 179
044			24	110	RE		CF&I	1936	3	36-1/4	Heat 13116 A10 Defect TDDS, Defect No. 24
045			199	110	RE		CF&I	1930	2	35-1/2	Heat 11121 Defect HSH 5 inch (sub for BH) Defect No. 199
046				136	RE	Yes	CF&I	1966	2	36	Linde Flame Hardened Rail
047	2/9/76	Chessie		130	RE		Beth.			36	
048				122	CB	Yes	Beth.	1965		36	
049				115	RE	Yes	USS	1950		36	
050				132	RE	Yes	USS	1948		36	
051				130	RE		Inland	1931		36	
052				100	ARAB		USS	1916		36	
053				140	RE	Yes	USS	1956		36	
054				131	RE		USS	1935		36	
055				131	RE		Beth.	1947	9	36	Heat 86462 F-11
056				132	RE		Beth.	1949	5	36	Heat CH 81294 F-11
057				140	RE		Beth.	1953	1	36	Heat CH 83673 C-5
058				140	RE		Beth.	1974		36	Fully Heat Treated, Heat 68674 2-19
059	3/1/76	Chessie		133			USS	1967		36	Sperry detected Defect Heat 95-P-134 B27 (Curvemaster)
060				124			Beth.	1975	11	36	Heat 162724-A-21
061				124			Beth.	1975	11	36	Heat 162729-A-12
062				124			Beth.	1975	12	36	Heat 187006-A-32
063				124			Beth.	1975	12	36	Heat 175105-A-6
064				124			Nippon	1975	7	36	Heat A-39262 D-2
065				124			Nippon	1975	7	36	Heat A-39780-D-5
066				124			Nippon	1975	7	36	Heat A-39376 C-7

No specification for the sulfur content is given by the ASTM Standard, but it states "that thoroughly deoxidized steel will be furnished and that, in every stage of manufacture, strict adherence to the standards of best practice of the individual mill will be observed". On this basis, it is reasonable to assume that the sulfur content of rail steels should be controlled by the mill to a maximum of about 0.050 weight percent.

Chemical analyses of each of the 66 rail samples were made for total carbon, manganese, silicon, and sulfur in percent by weight, and for hydrogen and oxygen in parts per million (ppm). The results of the analyses are presented in Table 2. Duplicate and, in some instances, triplicate analyses were made for hydrogen and oxygen and these are shown individually in the table.

Four rail steels, Samples 001, 003, 005, and 009, were designated by the suppliers as medium manganese steels. The manganese contents of three of these steels (Samples 001, 005, and 009) were within a range, 1.36 to 1.48 percent, normally associated with medium manganese steels. However, the manganese content of Sample 003, 0.76 weight percent, was within the standard chemical requirements for its rail size. A fourth rail steel, Sample 038, contained a manganese content of 1.48 weight percent, which means that it is a medium manganese steel also. Since the chemical requirements for the medium manganese steels were not available for rail steels, an assessment of these values in the total range of compositional variation cannot be made.

An analysis of the composition data presented in Table 2 indicates that the compositions of several rail samples, excluding the medium manganese steels, do not meet the chemical requirements contained in the ASTM Standard and the assumed maximum sulfur content. Table 3 lists the samples which do not meet the requirements and the manner in which they deviate from the requirements.

With the exception of Sample 053, the hydrogen content determined in each of the 66 rails was between 0.2 and 1.1 ppm. The hydrogen content of Sample 053 was reported to be 6.1 and 6.5 ppm in two determinations. The concentration of hydrogen in all other rails was characteristic of residual levels of hydrogen concentrations present in steels. Since hydrogen will effuse from steel at ambient temperatures over a period of time, it would be expected that rails of early vintage that may have had high hydrogen contents when placed into service would now contain only residual amounts.

The oxygen contents of the 66 rails were generally well below 100 ppm. The only exceptions were rail Samples 004 and 045 which contained averages of 538 and 333 ppm of oxygen, respectively. These oxygen contents are considerably higher than normal for silicon deoxidized rail steels.

TABLE 2. RESULTS OF CHEMICAL ANALYSES OF RAIL SAMPLES 001 THROUGH 066

Rail Sample	Size, lb/yd	Elemental Content, weight percent				Hydrogen, ppm	Oxygen, ppm
		C	Mn	Si	S		
001	130	0.63	1.48	0.21	0.022	0.8, 1.0	100, 96
002	85	0.74	0.61	0.07	0.154	0.8, 0.9	46, 48
003	130	0.77	0.76	0.20	0.036	0.4, 0.5	71, 69
004	85	0.67	0.62	0.30	0.052	0.7, 0.5	519, 435, 659
005	130	0.63	1.36	0.21	0.033	0.6, 0.8	52, 54
006	115	0.72	0.97	0.10	0.028	0.4, 0.4	23, 25
007	115	0.73	0.93	0.18	0.037	0.4, 0.3	24, 26
008	85	0.66	0.94	0.20	0.029	0.8, 0.8	57, 61
009	130	0.61	1.46	0.29	0.039	0.7, 0.7	56, 59
010	85	0.63	0.74	0.14	0.028	1.1, 0.9	132, 138
011	133	0.73	0.81	0.19	0.028	0.4, 0.4	57, 51, 56
012	133	0.79	0.84	0.18	0.029	0.8, 0.7	54, 58
013	127	0.74	0.89	0.24	0.028	0.8, 1.0	51, 47
014	133	0.78	0.74	0.17	0.014	0.8, 0.8	86, 84
015	133	0.76	0.82	0.19	0.033	0.6, 0.6	54, 54
016	133	0.81	0.93	0.17	0.044	0.6, 0.8	39, 43
017	133	0.79	0.85	0.26	0.048	0.9, 1.0	44, 43
018	133	0.75	0.89	0.17	0.046	0.7, 0.6	45, 43
019	133	0.74	0.88	0.21	0.038	0.4, 0.4	38, 36
020	119	0.75	0.83	0.15	0.033	0.8, 0.7	34, 32
021	133	0.79	0.90	0.21	0.024	0.7, 0.6	41, 45
022	133	0.78	0.87	0.20	0.028	0.4, 0.5	46, 47
023	133	0.79	0.92	0.21	0.040	0.6, 0.7	39, 35, 46
024	133	0.81	0.83	0.12	0.030	1.0, 0.7	26, 28
025	133	0.80	0.91	0.23	0.016	0.7, 0.7	29, 27
026	133	0.78	0.94	0.17	0.050	0.5, 0.5	47, 46
027	133	0.78	0.87	0.23	0.022	0.7, 0.6	45, 45
028	133	0.71	0.90	0.17	0.022	0.7, 1.0	79, 53, 69
029	119	0.72	0.89	0.19	0.046	0.5, 0.6	45, 43
030	119	0.80	0.90	0.16	0.028	0.5, 0.7	52, 54
031	133	0.79	0.76	0.15	0.022	0.5, 0.4	53, 49
032	133	0.80	0.94	0.18	0.035	0.5, 0.5	63, 61
033	133	0.78	0.92	0.23	0.025	0.6, 0.5	37, 35
034	119	0.77	1.04	0.17	0.023	0.5, 0.7	38, 38
035	115	0.76	0.80	0.23	0.028	0.5, 0.4	27, 27
036	112	0.75	0.81	0.18	0.016	0.4, 0.5	57, 54
037	115	0.72	0.93	0.25	0.017	0.4, 0.5	86, 67, 61
038	112	0.57	1.48	0.16	0.029	0.3, 0.3	78, 82
039	90	0.71	0.81	0.17	0.028	0.3, 0.3	81, 107, 168
040	100	0.58	0.64	0.08	0.030	0.4, 0.4	39, 34
041	115	0.77	0.81	0.21	0.043	0.4, 0.3	91, 93
042	100	0.63	0.71	0.08	0.026	0.3, 0.4	49, 36, 64
043	90	0.75	0.81	0.15	0.032	0.6, 0.4	84, 85

TABLE 2. (Continued)

Rail Sample	Size, lb/yd	Elemental Content, weight percent				Hydrogen, ppm	Oxygen, ppm
		C	Mn	Si	S		
044	110	0.78	0.88	0.20	0.016	0.3, 0.3	84 86
045	110	0.65	0.65	0.21	0.027	0.6, 0.5	342, 286, 372
046	133	0.78	0.90	0.20	0.027	0.2, 0.3	49, 48
047	130	0.76	0.46	0.11	0.044	1.1, 0.7	43, 41
048	122	0.79	0.95	0.17	0.022	0.7, 0.6	58, 61
049	115	0.80	0.89	0.11	0.040	0.9, 1.1	48, 50
050	133	0.75	0.91	0.20	0.036	0.5, 0.6	56, 56
051	130	0.84	0.72	0.19	0.016	0.6, 0.5	47, 51
052	100	0.72	0.90	0.19	0.021	0.4, 0.4	52, 54
053	140	0.85	0.91	0.18	0.032	6.1, 6.5	44, 44
054	131	0.78	0.76	0.20	0.021	1.0, 0.6	36, 32
055	131	0.78	0.90	0.17	0.028	0.8, 0.8	33, 35
056	132	0.80	0.90	0.19	0.039	0.7, 0.7	44, 46
057	140	0.77	0.94	0.16	0.028	0.7, 0.9	58, 46, 50
058	140	0.83	0.84	0.18	0.048	0.4, 0.5	47, 44
059	133	0.83	0.98	0.14	0.024	0.4, 0.3	22, 25
060	124	0.80	0.90	0.12	0.013	0.5, 0.4	56, 36, 47
061	124	0.80	0.91	0.12	0.015	0.4, 0.7	46, 46
062	124	0.79	0.84	0.08	0.017	0.3, 0.6	45, 51, 48
063	124	0.79	0.86	0.12	0.033	0.3, 0.3	49, 59, 64
064	124	0.76	0.85	0.18	0.018	0.6, 0.6	43, 49, 54
065	124	0.82	0.90	0.17	0.016	0.3, 0.3	41, 42
066	124	0.75	0.90	0.18	0.019	0.4, 0.7	37, 36

TABLE 3. RAIL SAMPLES NOT WITHIN CHEMICAL REQUIREMENTS

Rail Sample	High C	Low C	High Mn	Low Mn	High Si	Low Si	High S
002				X		X	X
004					X		X
008		X					
010		X					
013					X		
017					X		
034			X				
037					X		
040		X		X		X	
042		X				X	
045		X		X			
047				X			
051	X						
053	X						
058	X						
059	X						
062						X	

3.2 MACROSTRUCTURES

Most of the 66 rail samples exhibited uniform macrostructures throughout their full cross sections. The principle variances in the macrostructures among the rail samples were differences in fineness or coarseness. These differences may be related to the prior austenite grain size and/or the pearlite colony size. Typical macrostructures observed are exemplified by the photomacrographs in Figures 1 and 2, Samples 027 and 019, respectively. Figure 1 shows a typical coarse-textured macrostructure which was observed in 19 rail samples (Samples 007, 012, 014 through 018, 020 through 024, 027 through 032, and 042). Figure 2 shows a fine-textured macrostructure which was observed in the remaining 47 rail samples, except for Sample 058. Sample 058 had a macrostructure which exhibited very little of a structural pattern as shown in Figure 3.

The macrostructures of Samples 046 and 059 showed that the running surfaces apparently had been heat treated. The heat-treated surface of Sample 059 is evident in Figure 4. The surface heat treatment suggested that these two samples were from the ends of rails that were end-hardened, a process commonly used to reduce wheel batter at the rail joint.

The macrostructure of Sample 002 showed that its running surface apparently had been repaired by the mechanical removal of surface damage and subsequent deposition of weld metal. The repair weld in this sample is evident in Figure 5.

The macrostructure of Sample 001 showed evidence of a high inclusion content and internal fissuring, both conditions being located primarily in the web section and at the bottom of the head section. These conditions can be seen in Figure 6.

Cracks were observed in the macrostructures of Samples 061, 062, and 063. The cracks in these three rails were located centrally in the web below the rail head. All three cracks extended through the entire thickness (1 inch) of the transverse cross sections. The cracks are believed to be the remains of shrinkage porosity formed in the steels during solidification of the original ingots. The cracks are visible in the photomacrographs of Samples 061, 062, and 063 shown in Figures 7, 8, and 9, respectively. Sample 062 exhibited decarburization around the crack as indicated by the white zone in Figure 8.

Some chemical segregation in the central zone of the web rail section was indicated by the macrostructures of Samples 003, 025, 040, 060, 061, 062, and 063. An example of this condition is shown by the photomacrograph of Sample 003 in Figure 10. Similar conditions of chemical segregation exist in Figures 7, 8, and 9.

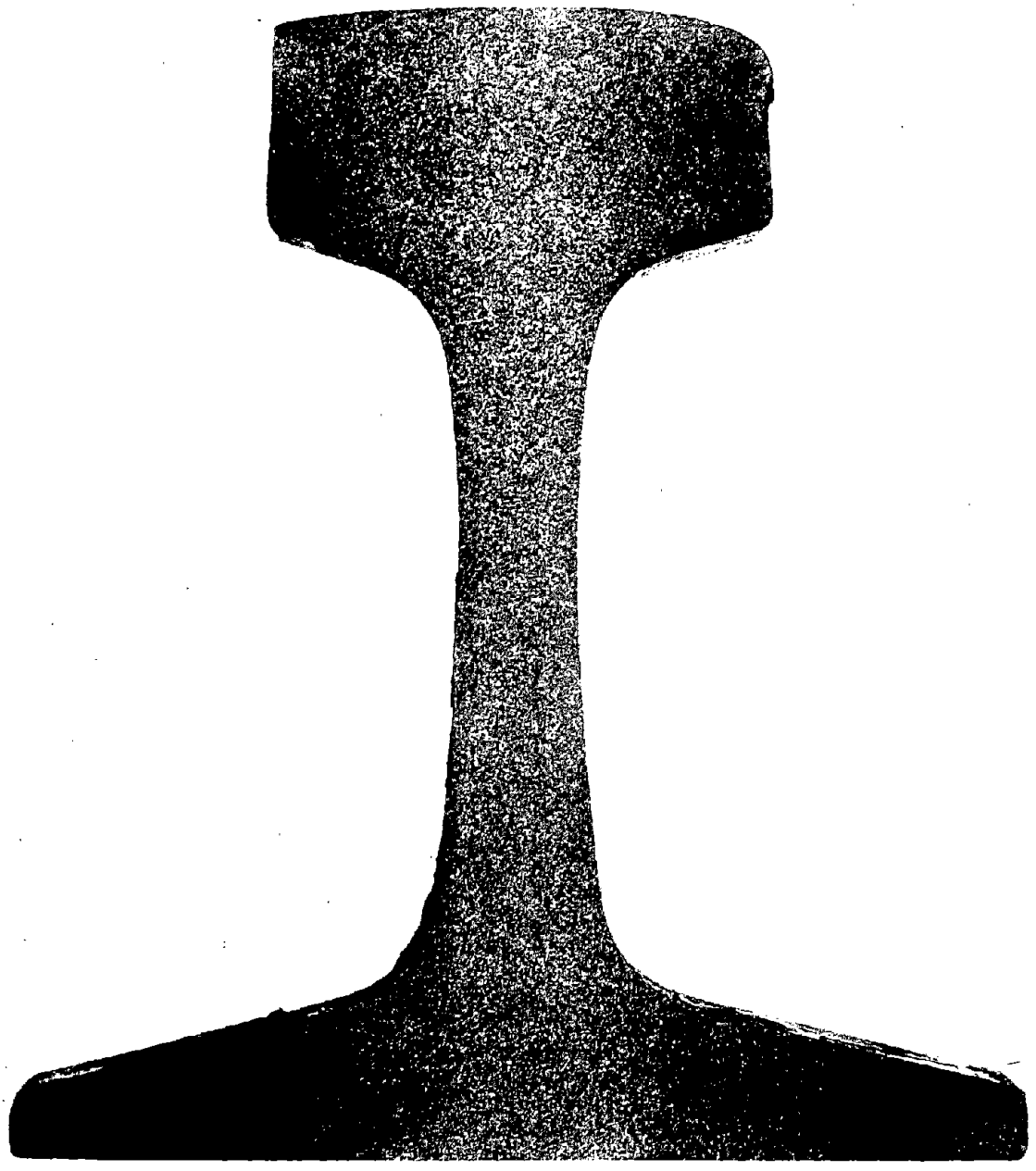

1X

FIGURE 1. TYPICAL COARSE-TEXTURED MACROSTRUCTURE OF RAILS - SAMPLE 027

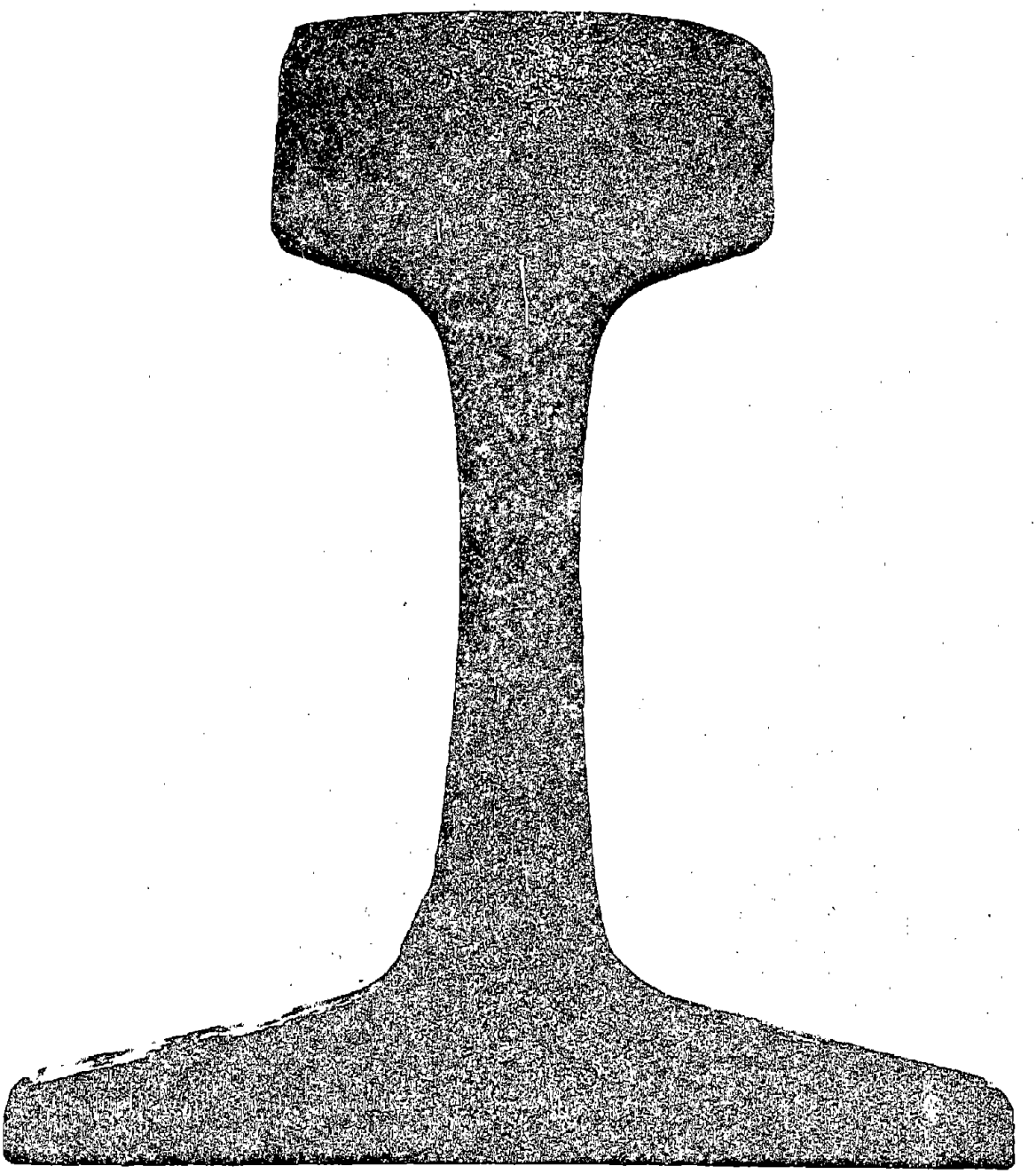

1X

FIGURE 2. TYPICAL FINE-TEXTURED MACROSTRUCTURE OF RAILS - SAMPLE 019

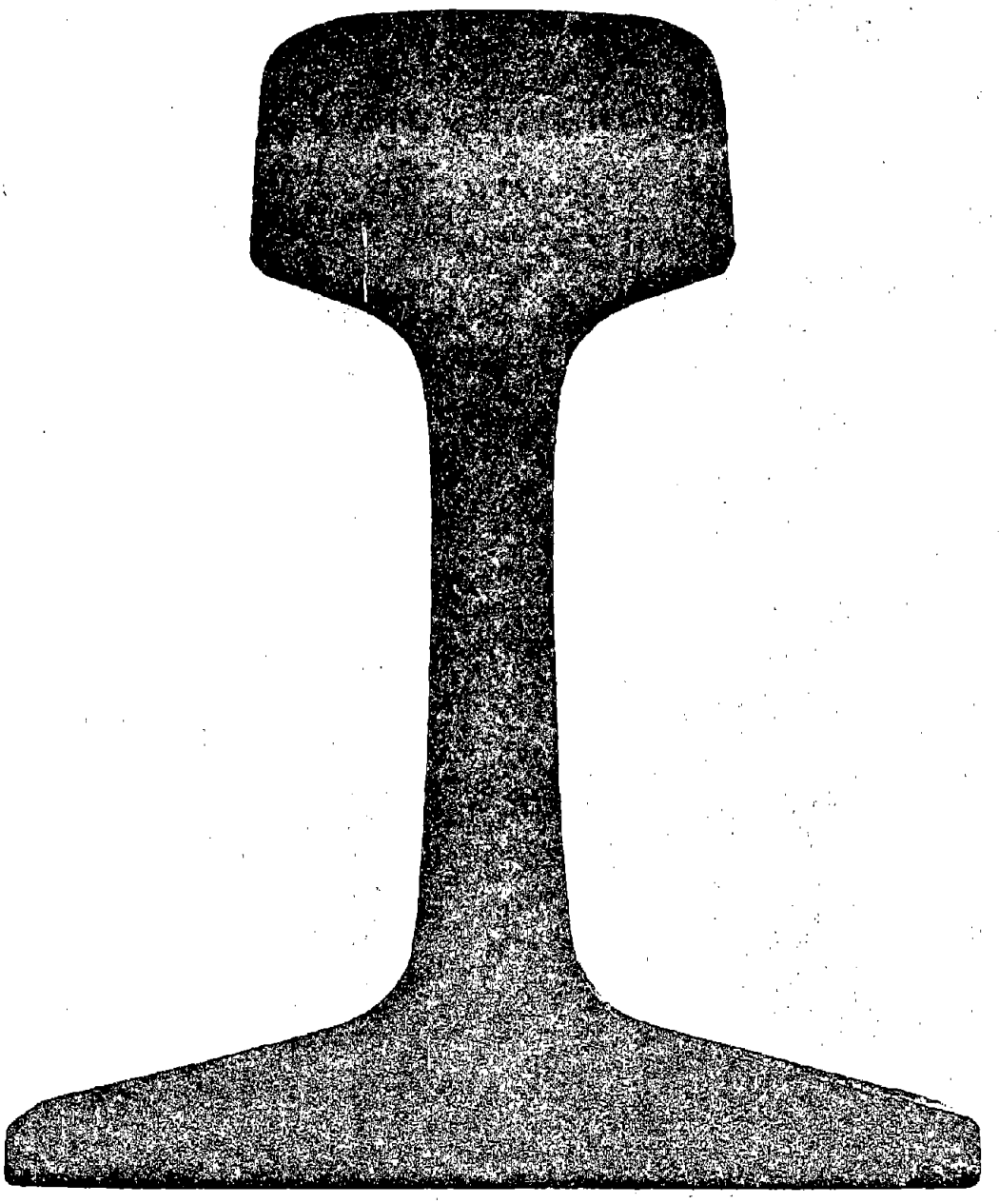

1X

FIGURE 3. MACROSTRUCTURE OF RAIL SAMPLE 058
Note lack of any structural pattern.

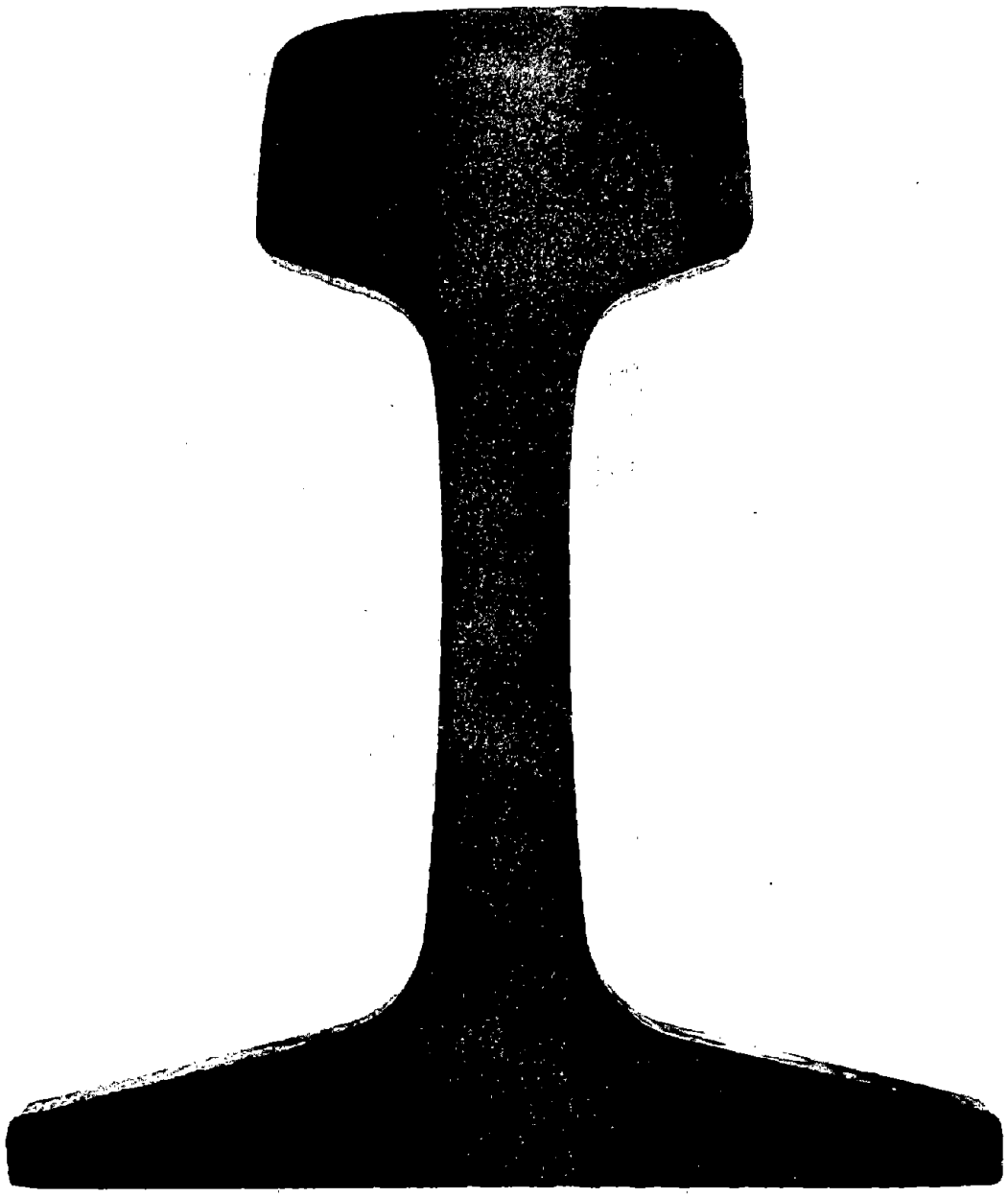

1X

FIGURE 4. MACROSTRUCTURE OF A HEAT-TREATED RUNNING SURFACE - RAIL SAMPLE 059

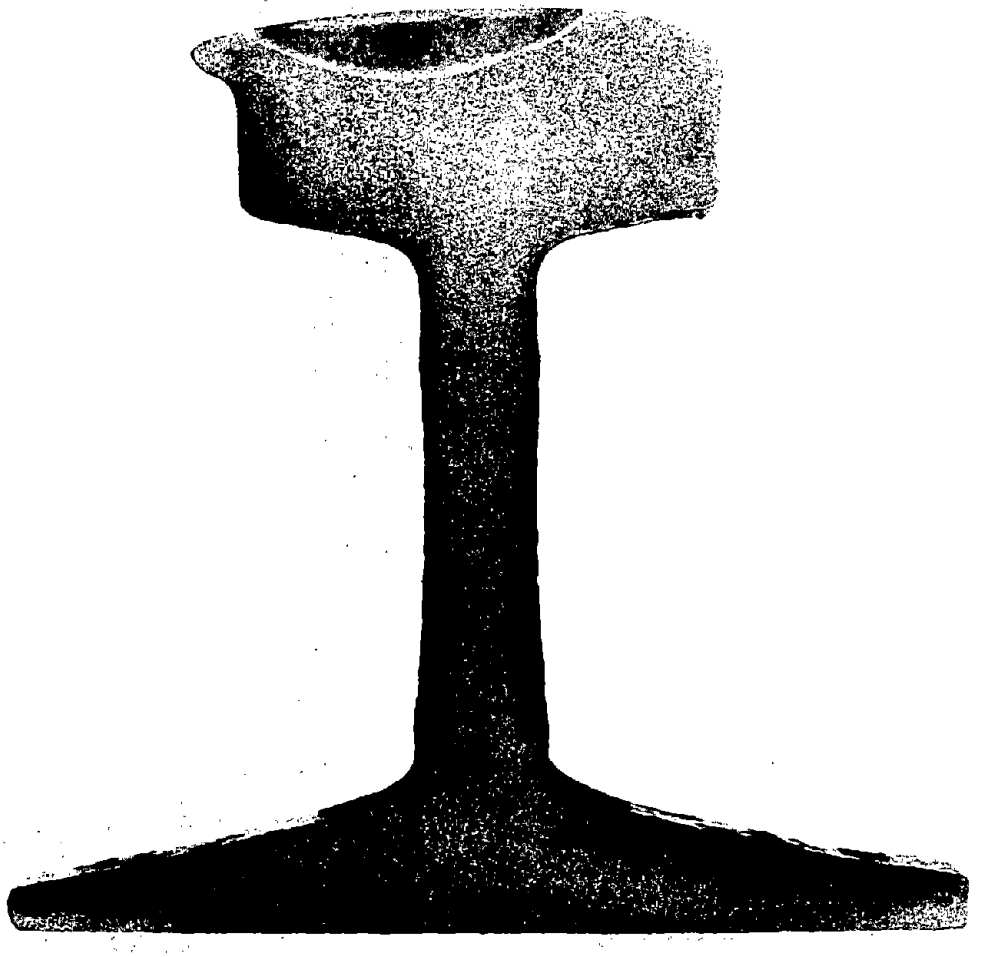

1X

FIGURE 5. MACROSTRUCTURE OF A REPAIRED RUNNING SURFACE - RAIL SAMPLE 002

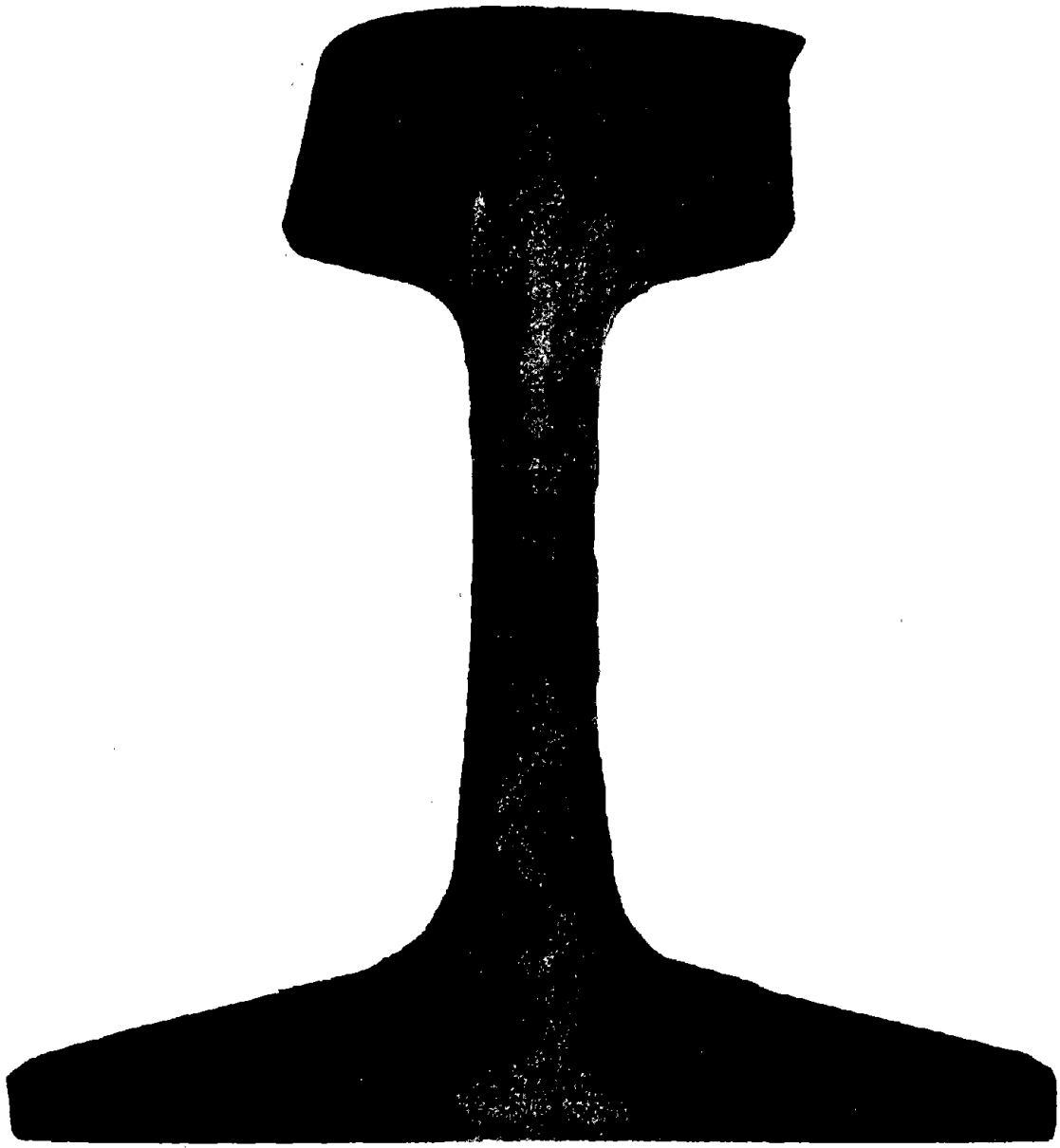

1X

FIGURE 6. MACROSTRUCTURE OF RAIL SAMPLE 001
Note internal fissures.

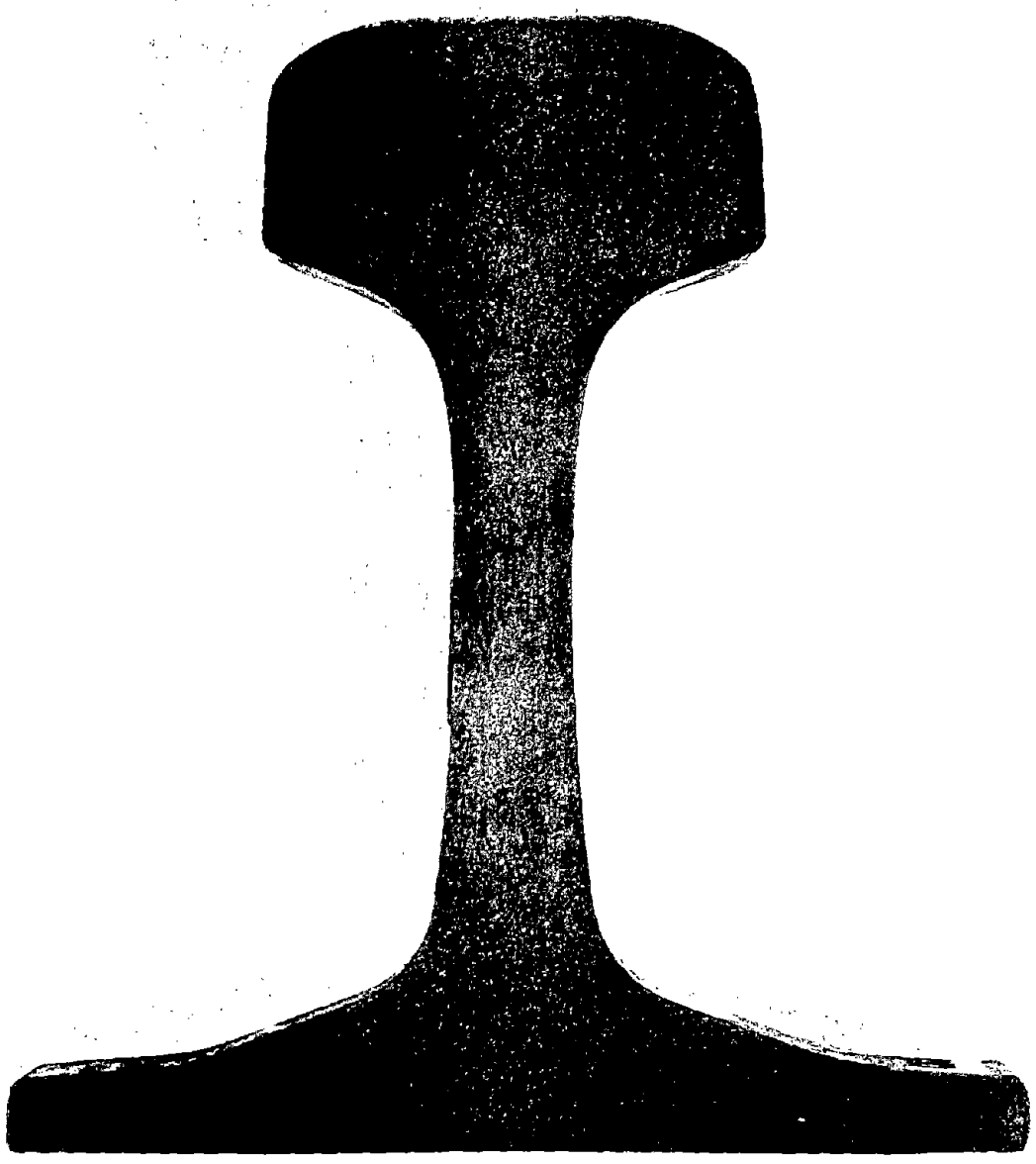

1X

FIGURE 7. MACROSTRUCTURE OF RAIL SAMPLE 061
Note crack in the web.

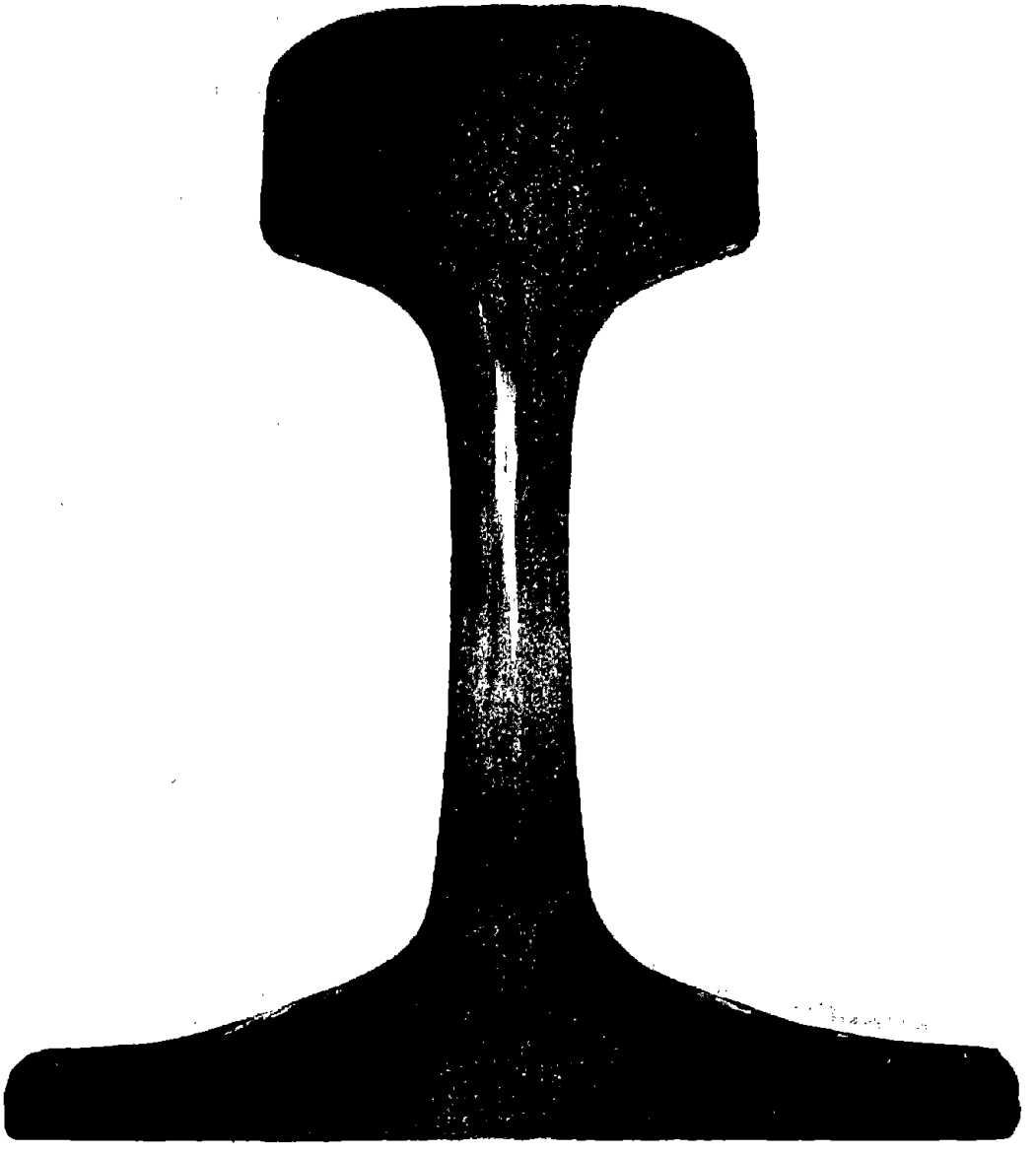

1X

FIGURE 8. MACROSTRUCTURE OF RAIL SAMPLE 062
Note segregation and crack in the web.

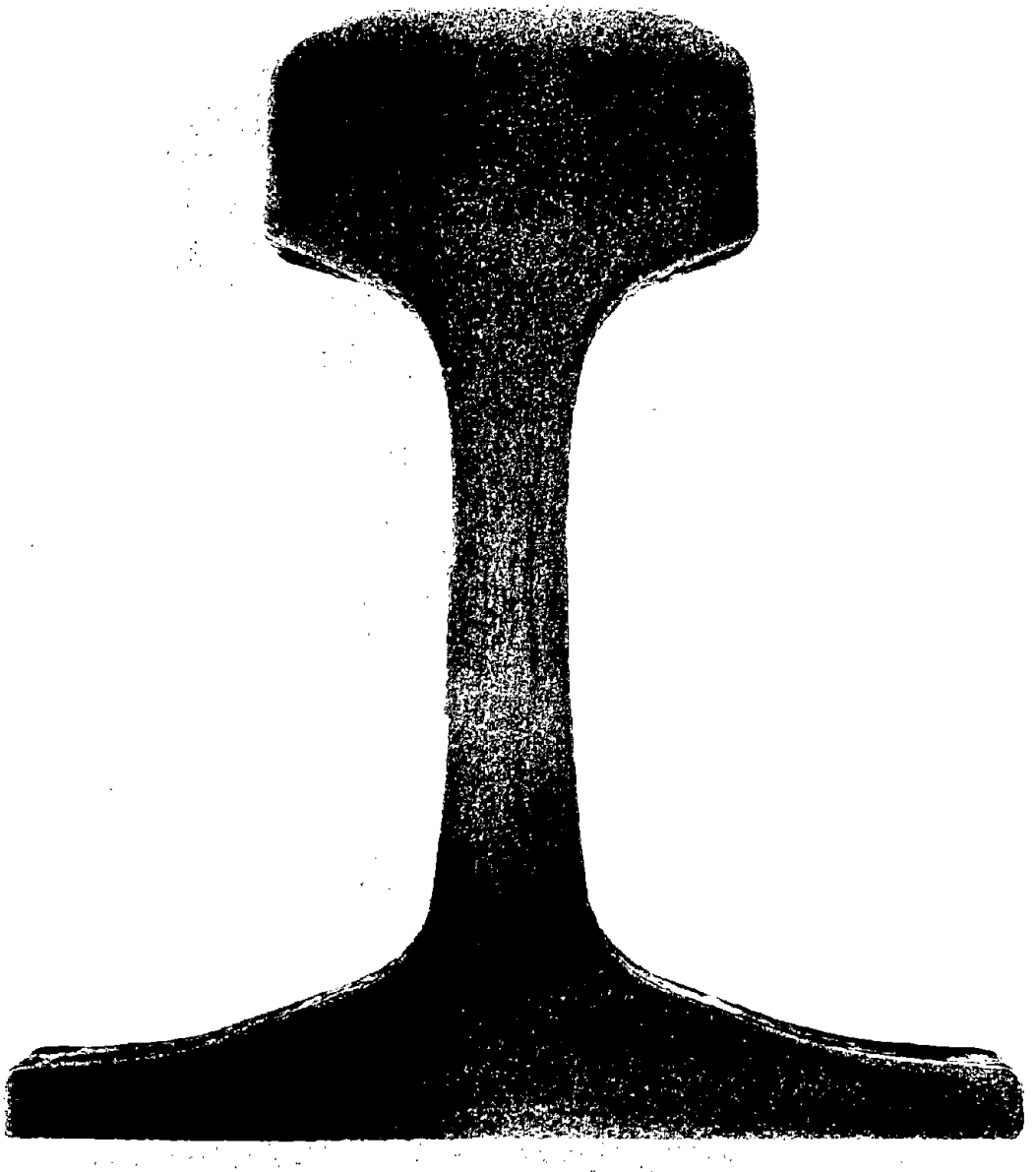

1X

FIGURE 9. MACROSTRUCTURE OF RAIL SAMPLE 063

Note hairline crack in the central area of the web.

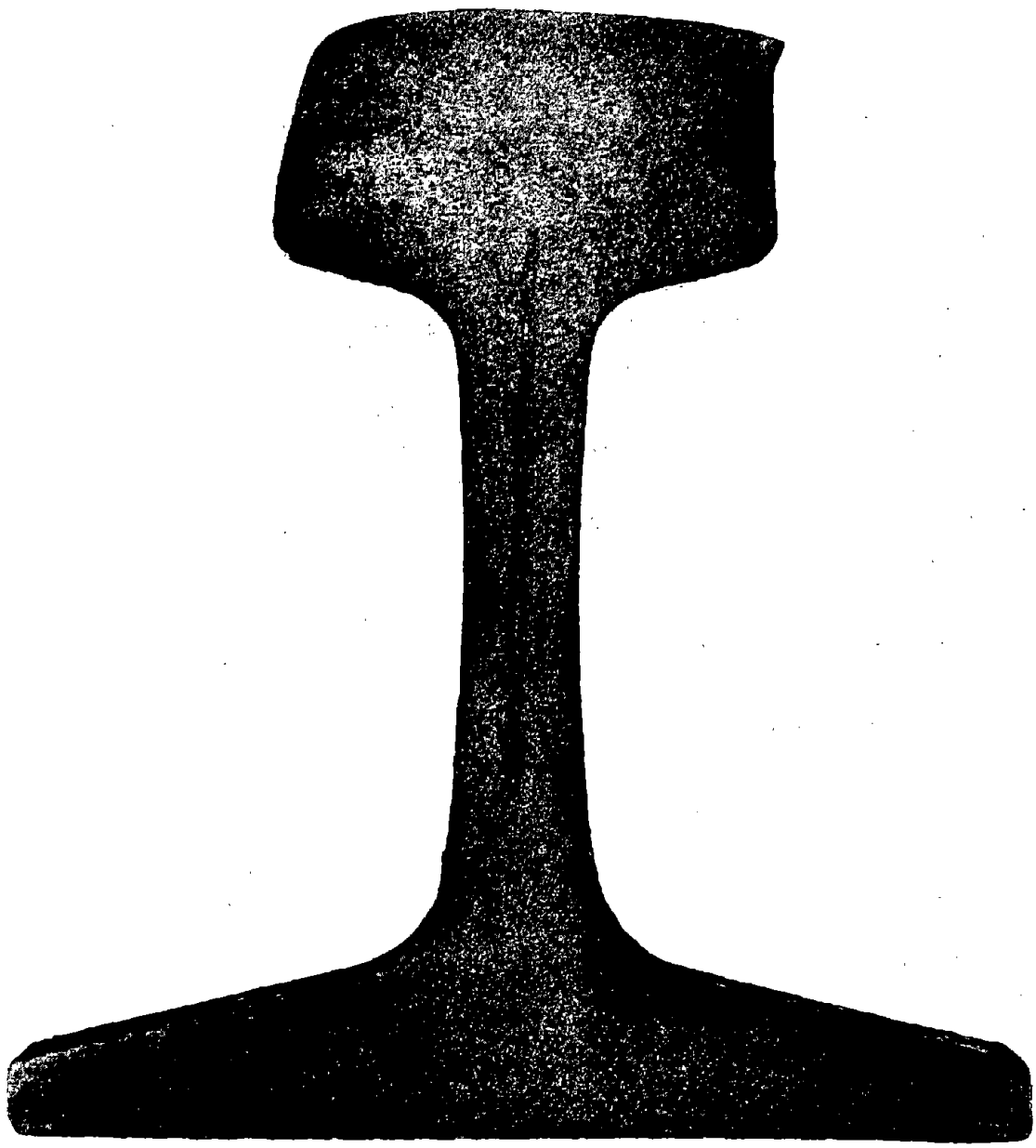

1X

FIGURE 10. MACROSTRUCTURE OF RAIL SAMPLE 003
Note segregation in the web.

3.3 MICROSTRUCTURES

Microscopic examinations of longitudinal metallographic specimens of the rail samples showed that the microstructures of 48 rails consisted of essentially 100 percent fine pearlite with very minor amounts of free ferrite occurring adjacent to some manganese sulfide inclusions or along a few prior austenite grain boundaries. A typical microstructure is shown by the photomicrograph of Sample 051 in Figure 11. The microstructures of Samples 004, 010, 013, 028, 038, 041, 045, 047, and 052 consisted of 85 to 95 percent (visual estimates) fine pearlite with the remainder being free ferrite located primarily along prior austenite grain boundaries. Rail Samples 004 and 045 contained the most free ferrite in the form of a ferrite network along prior austenite grain boundaries. Figure 12 shows the microstructure of Sample 004. The remaining Rail Samples, 002, 036, 037, 043, 054, 058, 064, 065, and 066, had microstructures consisting of about 96 to 99 percent (visual estimates) fine pearlite with the remainder being free ferrite scattered along prior austenite grain boundaries and adjacent to some sulfide inclusions. The microstructure of Sample 058 (shown in Figure 13) had much finer pearlite and considerably smaller pearlite colonies than any of the other rails. This type of microstructure was suggested already by its fine macrostructure. The very small pearlite colony size is obvious by comparison with the pearlite colony size in Figure 11. This fine structure suggests Sample 058 was heat treated following hot rolling.

Internal cracks in Sample 001, which were evident during macroscopic observations, were clearly apparent during microscopic observations. Three principal cracks running generally parallel to the longitudinal direction of the rail were observed in the longitudinal metallographic specimen examined. An example of one of the cracks observed is shown in Figure 14. The cracks propagated primarily across pearlite colonies, but also some propagation was observed along pearlite colony interfaces. In the specimen examined, the cracks were located below the running surface about ½ inch and deeper. The longest crack observed was approximately 200 mils. The cracks are believed to be the result of a high hydrogen content in the steel when the rail was manufactured.

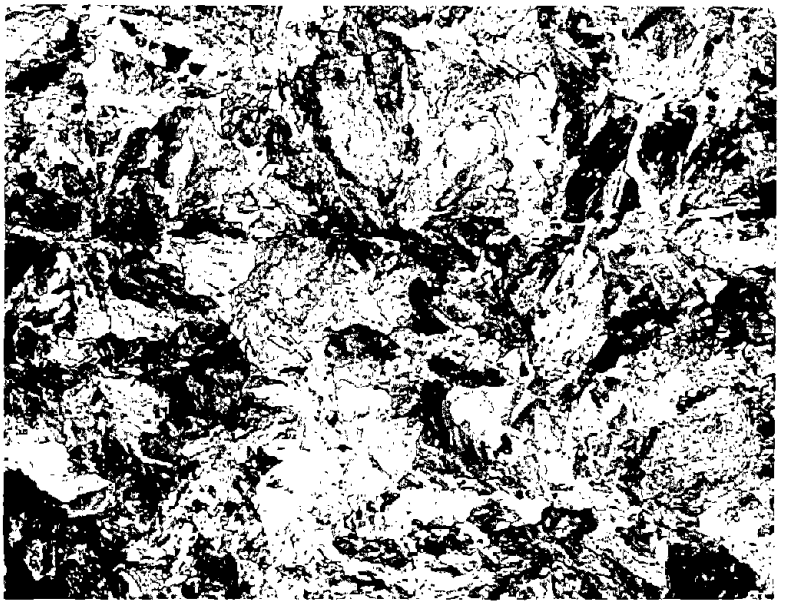

100X

FIGURE 11. PEARLITIC MICROSTRUCTURE TYPICAL OF THE MAJORITY OF RAILS - SAMPLE 051L

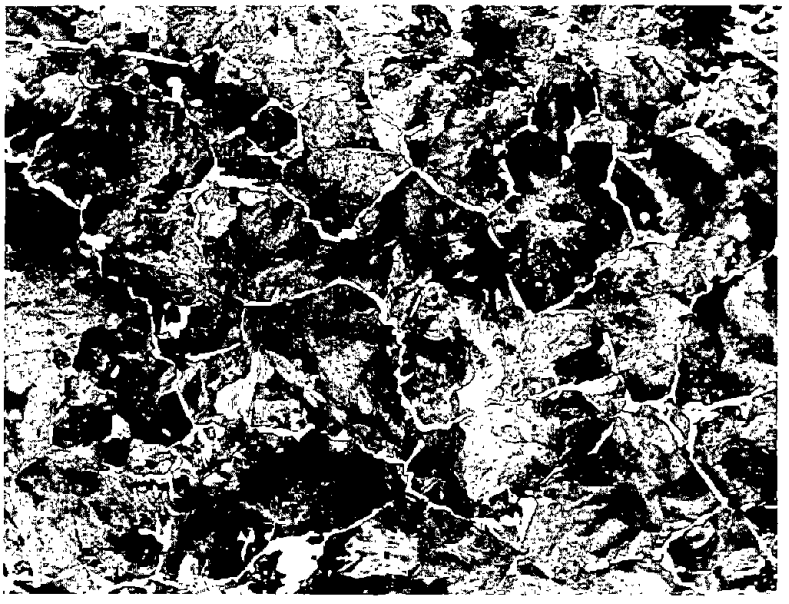

100X

FIGURE 12. FERRITE NETWORK IN A MATRIX OF PEARLITE - SAMPLE 004

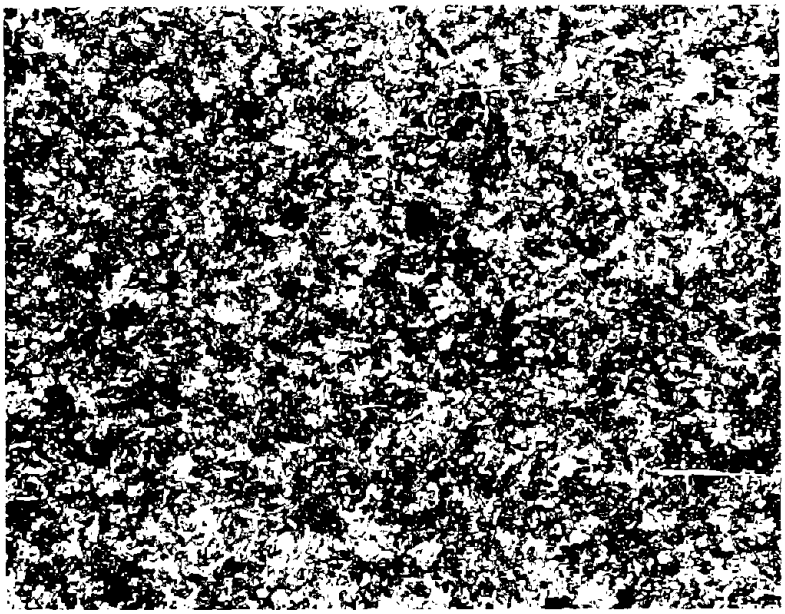

100X

FIGURE 13. HEAT-TREATED PEARLITIC MICROSTRUCTURE OF RAIL SAMPLE 058L

100X

FIGURE 14. INTERNAL CRACK IN RAIL SAMPLE 001L

4. EXPERIMENTAL DETAILS

4.1 SPECIMENS

One tensile specimen and one fatigue-crack-growth specimen were machined from each rail sample. The orientation of the specimens is shown in Figure 15. Charpy V specimens were taken from six rail samples — 023 and 030 which exhibited a high rate of fatigue-crack growth, 019 and 031 with medium crack-growth rates, and 001 and 036 with low growth rates. Forty-five Charpy specimens were made, 15 from each of the three growth-rate categories. From each category, five specimens were taken in each of the three directions shown in Figure 15. The specimens were taken from the center of the rail head.

The tensile specimens were standard ASTM 0.25-inch-diameter specimens. Charpy specimens were also of standard dimensions; i.e., 2.165-inch long, 0.394-inch thick with a square cross section.

Fatigue-crack-growth specimens were of the compact tension (CT) type. Their dimensions are shown in Figure 16. The specimens were provided with a 1.650-inch deep chevron notch (0.900 inch from the load line). Details of the notch can best be observed in Figure 17 which shows two specimens, one before and one after testing.

4.2 TESTING PROCEDURES

Tensile and Charpy tests were performed in accordance with standard procedures.

To expedite the crack-growth tests, specimens were precracked in a Krause fatigue machine. Crack-growth experiments were conducted in a 25-kip-capacity electrohydraulic servocontrolled fatigue machine. Figure 18 shows a specimen mounted in the fatigue machine. The tests were performed at constant amplitude, the load cycling between 0 and 2500 pounds, resulting in a stress ratio of $R = 0$. Cycling frequency was 40 Hz, but was reduced to 4 Hz toward the end of a test to enable more accurate recording of the crack size giving final failure. The laboratory air was kept at 68 F and 50 percent relative humidity.

Crack growth was measured visually, using a 30 power traveling microscope. The cracks were allowed to grow in increments of 0.050 inch, after which the test was stopped for an accurate crack size measurements. Crack size was recorded as a function of the number of load cycles.

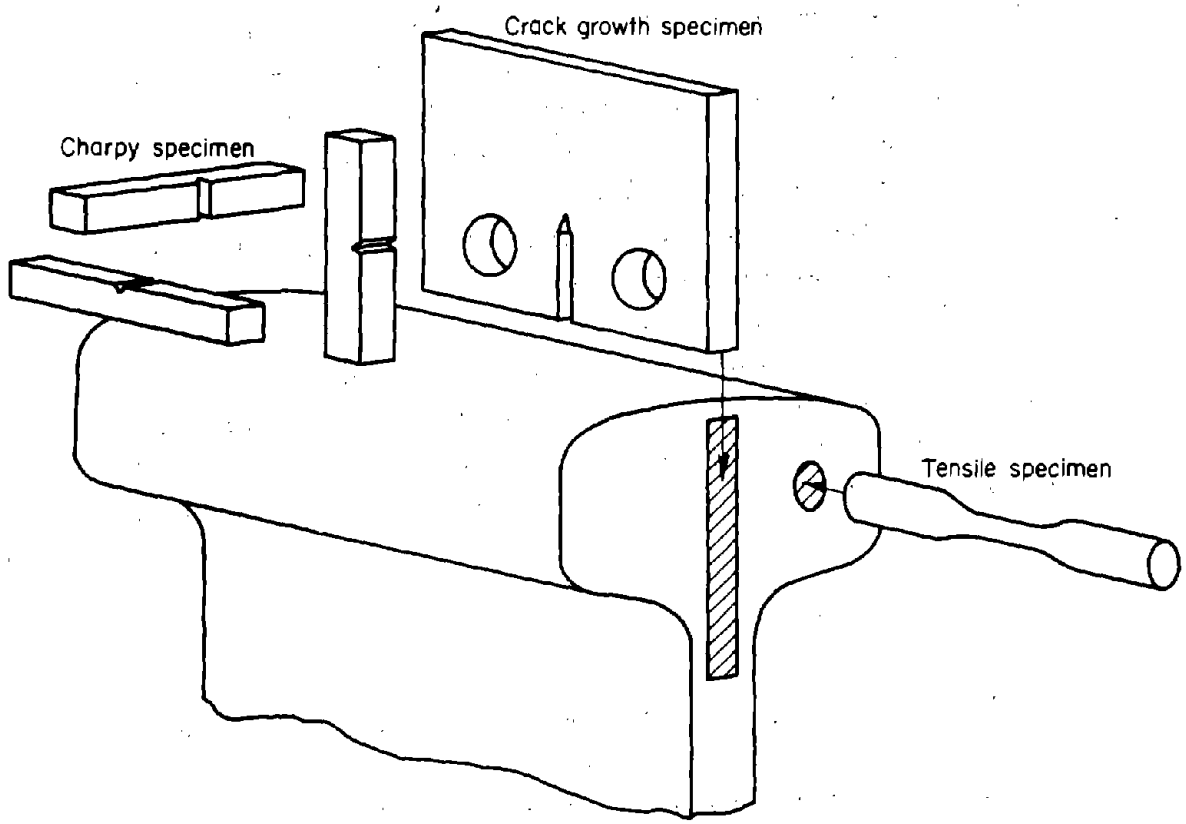

FIGURE 15. ORIENTATION OF SPECIMENS

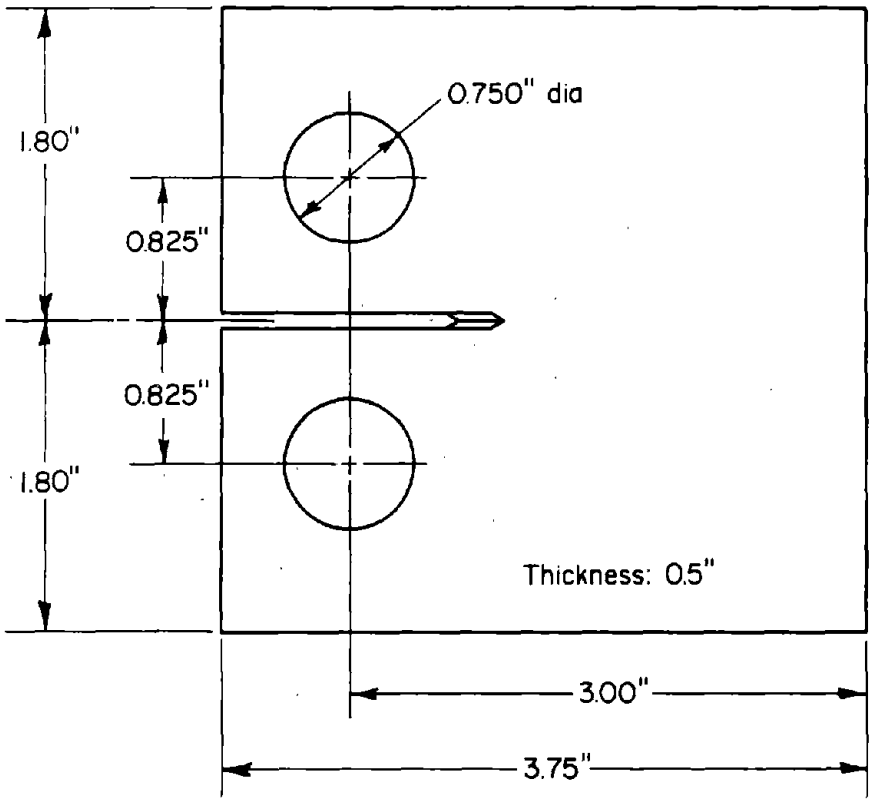

FIGURE 16. COMPACT TENSION FATIGUE CRACK GROWTH SPECIMEN

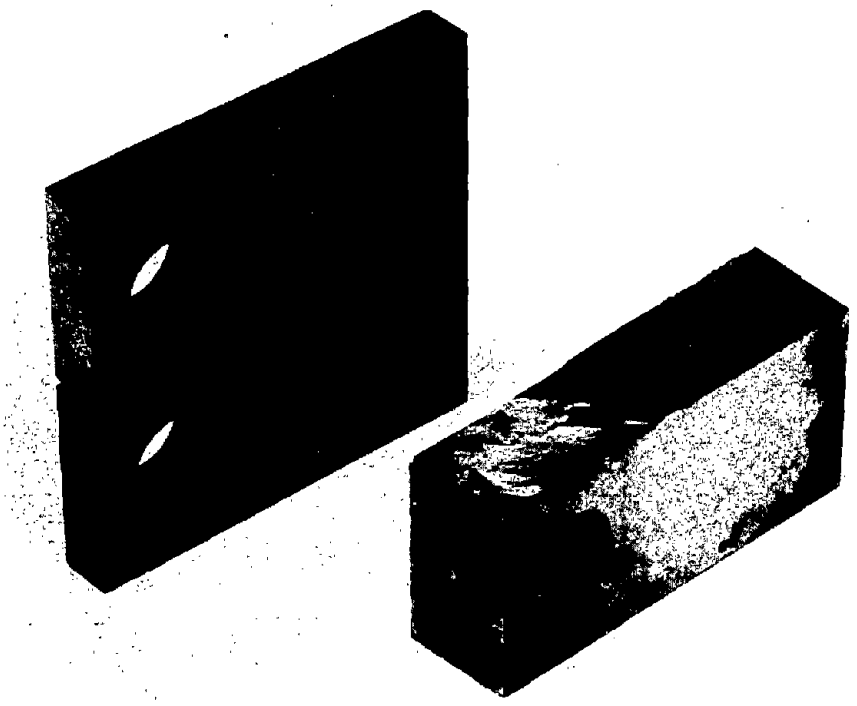

FIGURE 17. COMPACT TENSION SPECIMENS BEFORE AND AFTER TESTING

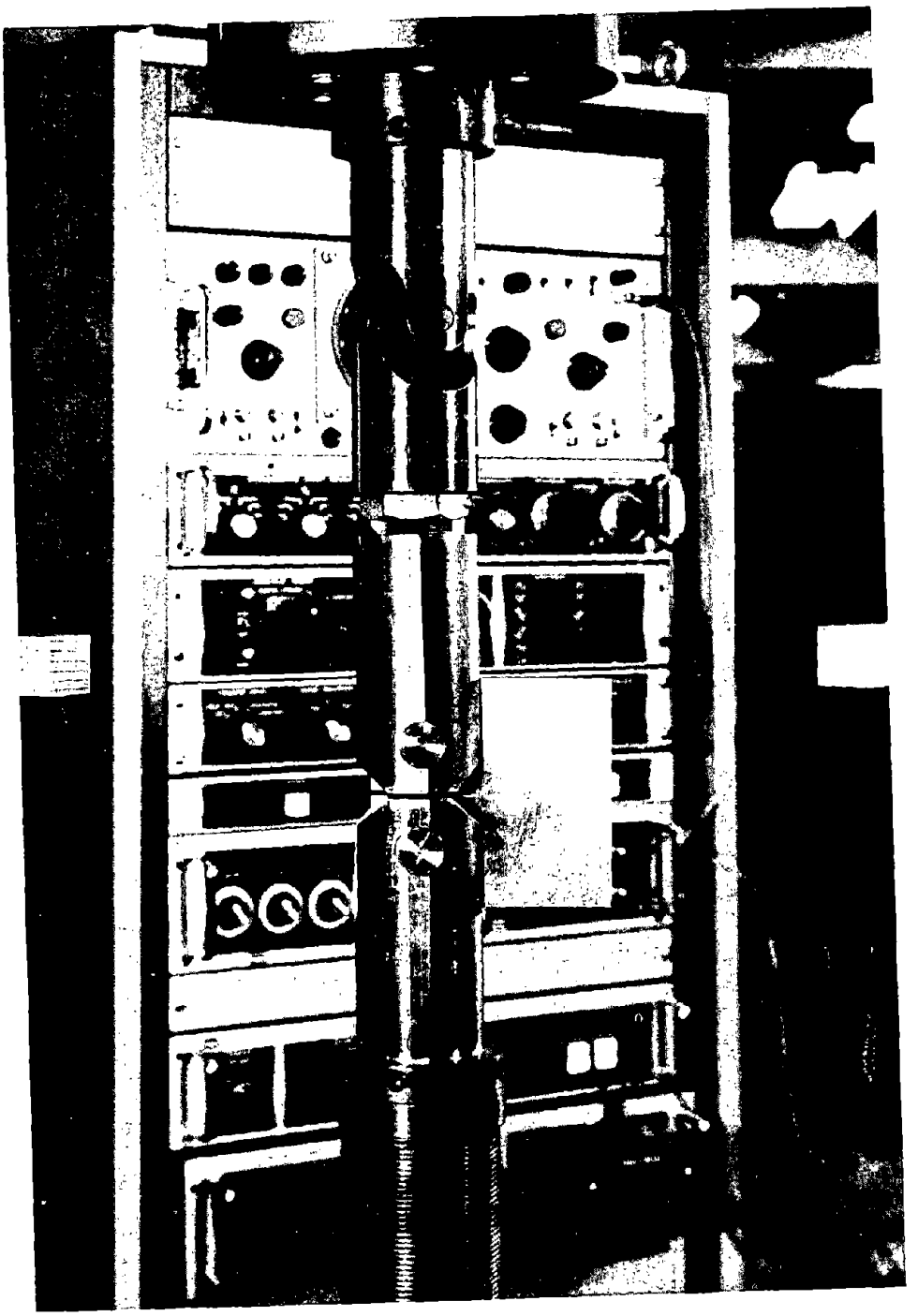

FIGURE 18. COMPACT TENSION SPECIMEN IN FATIGUE MACHINE

5. TEST RESULTS

The tensile properties of the 66 rail samples are presented in Table 4. With a few exceptions, the tensile ultimate strength (TUS) and the tensile yield strength (TYS) are in the order of 130 ksi and 75 ksi, respectively. One heat treated rail showed a high TUS of 188.3 ksi and a TYS of 127.3 ksi. Two tensile specimens (030 and 045) contained longitudinal cracks as became apparent after fracture, since the fracture path partly followed these cracks. This resulted in the strength of those samples being low. It should be noted that these samples were different from the ones reported cracked in Section 3.2.

The Charpy data are presented in Tables 5, 6, and 7. They show that in the range of ambient temperatures the Charpy energy is essentially the same for all these steels. Transition temperatures and upper shelf behavior show some variation, but these are of limited interest under operational conditions.

Some typical fatigue-crack-propagation curves are given in Figure 19. The curves show that the number of cycles to grow a 1-inch crack to failure showed a wide variation for the rails from which the specimens were taken. This will be reflected in the rate of growth, which is the basis on which the materials will be compared in the next section. Also the final crack size at failure showed quite a wide variation which will be reflected in the toughness number. The raw test data (crack size versus cycle number) of all specimens are given in Appendix A.

6. DATA ANALYSIS

In order to develop a failure model for track rail, one must identify and quantify the damage processes, couple them appropriately, provide a means for accumulating the damage (i.e., compile the crack growth), and establish the criterion for failure or fracture. The first step in implementing these tasks is the baseline effort of crack-growth characterization and metallurgical studies previously described. In the following sections, the approach to interpretation, quantification, and correlation of these data is discussed. In the next phase, this will be broadened to consider additional variables.

TABLE 4. TENSION TEST RESULTS FOR 66 RAIL SAMPLES

Rail Number	TUS, ksi	TYS, ksi	Elongation in 1 Inch, percent	Reduction in Area, percent	E, 10^3 ksi	True Fracture Stress, ksi	True Fracture Strain, ϵ_t	Ramberg-Osgood Exponent, n	Work Hardening Exponent, 1/n
001	136.4	76.5	13.5	28.0	34.0	171.2	.1266	7.8	.128
002	134.4	74.7	12.0	20.6	30.8	159.4	.1133	7.7	.130
003	137.4	73.6	12.0	17.7	30.3	160.1	.1133	13.1	.076
004	116.0	59.9	15.0	24.0	28.6	144.6	.1397	10.4	.096
005	134.8	76.4	13.5	26.0	31.8	154.9	.1266	11.5	.081
006	135.0	71.2	11.0	21.2	30.2	161.9	.1043	11.5	.087
007	135.8	70.0	12.0	17.6	30.3	156.9	.1133	12.5	.080
008	125.1	67.0	14.0	25.0	30.1	155.9	.1310	10.8	.093
009	139.8	81.8	14.0	29.4	32.0	180.0	.1310	12.0	.083
010	111.5	58.7	17.0	27.2	29.3	143.1	.1570	9.8	.102
011	126.9	73.2	12.5	20.8	33.8	144.3	.1177	10.3	.097
012	134.7	78.3	10.5	17.0	32.4	153.1	.0998	8.4	.119
013	129.3	72.8	12.5	29.1	29.1	160.8	.1177	7.9	.126
014	135.4	75.9	12.0	18.0	33.1	158.7	.1133	7.5	.133
015	131.6	71.5	11.0	16.5	30.6	150.0	.1043	6.0	.167
016	138.6	75.6	9.5	15.0	28.8	154.4	.0907	6.3	.159
017	137.1	74.4	10.0	19.5	28.2	163.6	.0953	6.4	.156
018	133.2	70.6	11.0	19.9	27.5		.1043		
019	131.2	73.4	12.0	19.2	34.5	152.8	.1133	8.5	.118
020	131.4	72.0	11.0	18.4	30.4	152.6	.1043	6.5	.154
021	132.3	77.2	12.0	18.4	32.6	153.9	.1133	9.8	.102
022	130.7	76.0	13.0	22.7	31.7	157.9	.1222	8.2	.122
023	135.1	77.3	10.5	17.9	32.2	155.7	.0998	7.7	.130

TABLE 4. (Continued)

Rail Number	TUS, ksi	TYS, ksi	Elongation in 1 Inch, percent	Reduction in Area, percent	E, 10^3 ksi	True Fracture Stress, ksi	True Fracture Strain, ϵ_t	Ramberg-Osgood Exponent, n	Work Hardening Exponent, 1/n
024	136.7	74.6	10.0	16.2	32.4	158.7	.0953	6.3	.159
025	141.1	75.7	9.5	18.8	26.5	164.9	.0907	6.3	.159
026	135.0	74.4	11.0	17.5	29.9	153.1	.1043	8.2	.122
027	136.4	69.4	10.0	13.6	29.0	150.1	.0953	6.2	.161
028	129.1	70.5	11.5	18.9	31.8	119.8	.1088	7.5	.133
029	125.5	61.7	12.0	19.9	29.4	146.6	.1133	6.8	.147
030	110.0[a]	76.8	--	--	28.2	--	--	7.1	.140
031	133.4	75.6	11.0	17.6	31.6	149.4	.1043	8.6	.116
032	139.5	80.0	12.0	19.5	34.8	165.3	.1133	8.0	.125
033	135.0	73.3	10.0	13.9	28.6	--	.0953		
034	137.3	77.3	10.5	20.7	30.2	164.3	.0998	6.0	.167
035	128.1	69.3	12.5	19.6	33.6	154.1	.1177	7.2	.139
036	132.1	74.6	12.0	21.4	31.1	155.3	.1133	10.0	.100
037	127.7	68.6	16.0	25.9	32.6	156.8	.1484	9.4	.106
038	124.2	74.9	17.0	42.3	33.7	185.3	.1570	11.5	.087
039	130.7	75.0	14.5	21.6	30.9	155.9	.1354	7.5	.133
040	138.8	83.3	9.5	15.0	26.9	156.5	.0907	7.7	.130
041	132.0	73.6	11.5	22.0	28.6	156.1	.1088	7.7	.130
042	133.0	74.7	10.5	15.9	29.6	151.1	.0998	6.8	.147
043	133.2	75.6	13.0	20.5	32.8	156.9	.1222	6.9	.145
044	139.7	80.0	10.0	15.3	29.3	158.7	.0953	11.5	.087
045	96.8[a]	66.0	8.0	16.3	33.8	98.0	.0769	10.2	.098
046	130.6	75.9	14.5	20.6	28.9	160.5	.1354	25.0	.040

TABLE 4. (Continued)

Rail Number	TUS, ksi	TYS, ksi	Elongation in 1 Inch, percent	Reduction in Area, percent	E, 10^3 ksi	True Fracture Stress, ksi	True Fracture Strain, ϵ_t	Ramberg-Osgood Exponent, n	Work Hardening Exponent, 1/n
047	123.8	60.4	14.0	21.0	29.2	150.1	.1310	24.0	.041
048	132.4	75.5	11.5	17.5	29.9	152.9	.1088	10.5	.095
049	132.0	72.4	11.5	20.1	30.5	157.8	.1088	7.2	.139
050	132.4	73.8	12.0	21.0	29.9	157.5	.1133	7.8	.128
051	141.5	81.2	9.5	13.3	31.2	159.1	.0907	11.8	.085
052	126.0	64.0	13.5	21.3	29.7	151.0	.1266	14.0	.071
053	140.2	75.8	9.5	13.3	30.3	159.4	.0907	8.9	.112
054	135.9	76.5	12.0	18.8	30.9	159.5	.1133	9.2	.109
055	137.4	77.9	9.0	14.2	29.5	156.1	.0861	7.7	.130
056	136.0	72.6	9.5	13.2	29.6	149.6	.0907	9.2	.109
057	136.6	72.9	10.5	18.2	27.1	158.9	.0998	8.2	.122
058	188.7[b]	127.3	11.5	31.7	29.6	239.4	.1088	30.	.033
059	137.2	79.1	11.0	15.4	28.3		.1043		
060	135.3	74.2	12.0	16.5	30.9	153.4	.1133	13.0	.077
061	132.5	70.7	11.5	17.1	31.2	154.4	.1088	17.5	.057
062	141.3	76.9	11.0	19.3	32.0	167.5	.1043	13.5	.074
063	135.6	73.5	11.0	18.8	29.6	155.3	.1043	14.0	.071
064	133.1	69.1	13.0	21.1	30.5	159.4	.1222	14.8	.067
065	131.3	73.3	11.0	17.7	31.0	157.5	.1043	4.4	.227
066	134.2	70.0	12.0	20.7	30.5	159.9	.1133	13.0	.077

(a) Longitudinal cracks in specimen.

(b) Heat treated rail.

TABLE 5. CHARPY IMPACT TEST RESULTS FOR CATEGORY 1 RAILS (HIGH GROWTH RATE)

Specimen Orientation	Temperature, F	Energy, ft/lb	Shear Area, percent
L	32	5	0
L	RT	4	0
L	RT	5	0
L	212	5.5	20
L	300	18.5	99
T	32	2	0
T	RT	2	0
T	RT	2	0
T	212	2	40
T	300	3	98
ST	32	3	0
ST	RT	4	0
ST	RT	4	0
ST	212	5	20
ST	300	11.5	95

TABLE 6. CHARPY IMPACT TEST RESULTS FOR CATEGORY 2 RAILS (MEDIUM GROWTH RATE)

Specimen Orientation	Temperature, F	Energy, ft/lb	Shear Area, percent
L	32	3.5	0
L	RT	4	0
L	RT	4	0
L	212	10	10
L	300	13	45
T	32	2	0
T	RT	2	0
T	RT	2	0
T	212	3.5	5
T	300	6.5	45
ST	32	3.5	0
ST	RT	3	0
ST	RT	4	0
ST	212	7	25
ST	300	12	95

TABLE 7. CHARPY IMPACT TEST RESULTS FOR CATEGORY 3 RAILS (LOW GROWTH RATE)

Specimen Orientation	Temperature, F	Energy, ft/lb	Shear Area, percent
L	32	3	0
L	RT	4	0
L	RT	5.5	0
L	212	11	45
L	300	14	70
T	32	3	0
T	RT	2	0
T	RT	2	0
T	212	4.5	0
T	300	10.5	65
ST	32	2	0
ST	RT	3	0
ST	RT	3	0
ST	212	5.5	15
ST	300	13	95

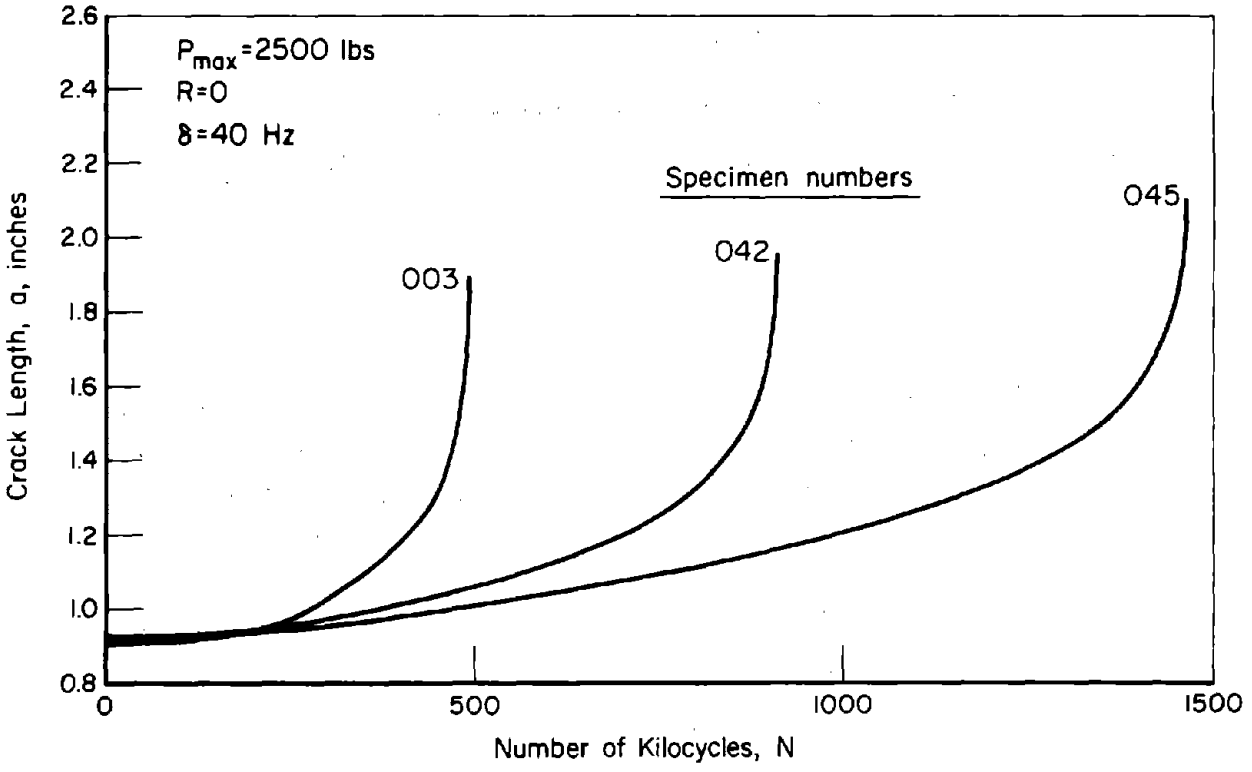

FIGURE 19. TYPICAL FATIGUE CRACK PROPAGATION CURVES

6.1 ANALYSIS OF RATE DATA

The rate of fatigue-crack propagation can be expressed as a function of the stress-intensity factor K. The stress-intensity factor (unit ksi/in.) is a measure for the stress singularity at the crack tip. If two cracks in the same material but under entirely different circumstances are subjected to the same stress intensity, their behavior will be the same. For the CT specimen used in this investigation, the stress intensity can be given as

$$K = \frac{P}{2BW^{1/2}} (1+a/W)(1-a/W)^{-3/2}[7.000-7.050(a/W)+4.275(a/W)^2] \qquad (1)$$

in which P is the load on the specimen, B is the specimen thickness, W is the specimen width, and a is the crack size.

The rate of crack growth is related to K through

$$\frac{da}{dN} = f(\Delta K, R) \qquad (2)$$

where N is the cycle number, R is the ratio between minimum and maximum load in a cycle, and ΔK is the range through which K varies during the cycle. Thus, ΔK is found by substituting the load range ΔP into Equation (1). In the present tests, the load varied between 0 and 2500 pounds so that $\Delta P = 2500$ pounds and $R = 0$.

Over a wide range of growth rates in steels and for fixed R, Equation (2) can be approximated by

$$\frac{da}{dN} = C(\Delta K)^n \qquad (3)$$

where C and n are constants for a given material. Hence, the various rail steels can be compared on the basis of their C and n values.

Equation (3) implies that a plot of da/dN versus ΔK on double-log paper is a straight line. In reality there will be an upswing in the rate of crack growth towards the end of the test, because the failure conditions are being approached. This is reflected in the following equation:

$$\frac{da}{dN} = C \frac{(\Delta K)^n}{(1-R)\ K_{Ic}-\Delta K} \qquad (4)$$

Not only does this equation take into account the effect of the stress ratio R, it also shows that the crack-growth rate becomes infinite if the stress intensity

at maximum load becomes equal to K_{Ic}. The quantity K_{Ic} is the fracture toughness of the material, which is the value of K at which fracture occurs. For the special case of R = 0, the equation reduces to

$$\frac{da}{dN} = C \frac{\Delta K^n}{K_{Ic} - \Delta K} \quad . \tag{5}$$

Both Equations (3) and (5) were evaluated for their applicability to the present data base. For this purpose, da/dN was calculated from the measured crack-growth data through the weighted average incremental slope approximation,

$$\frac{da}{dN} \approx \left(\frac{\Delta a}{\Delta N}\right)_i + \frac{\Delta N_i}{(N_{i+1} - N_{i-1})} \left[\left(\frac{\Delta a}{\Delta N}\right)_{i+1} - \left(\frac{\Delta a}{\Delta N}\right)_i\right] \quad . \tag{6}$$

The results were plotted as a function of ΔK as determined by Equation (1). Subsequently, curves were fitted through the data to give values for C and n. A special computer program was used to find the best fit.

Examples of the resulting plots of da/dN versus ΔK are given in Figure 20. An example of a computer printout giving the basic crack-growth data, crack-growth rate, and the stress-intensity factor, is shown in Table 8. The variability of crack-growth rates in the 66 samples can be appreciated from Figure 20. The heat-treated rail appeared to have the lowest crack-growth rates. It did fall to the right of the scatter band containing all other samples. All the curve fitting data, in terms of C, n, and the correlation parameter, R^2, are presented in Table 9. The correlation parameter is generally close to unity which is an indication of the goodness of the fits. These results have been derived from the basic crack-growth data listed in Appendix A.

Also presented in this table are the apparent toughness, defined as the stress-intensity factor, determined by Expression (1), for the last recorded crack measurement, and a life parameter,

$$N_L = \left[\left(\frac{n}{2} - 1\right) \cdot \left(da/dN\right)_{\Delta K=20}\right]^{-1} \quad ,$$

which is a coupled function of C and n used to rank the growth rates.

Very few crack-growth data for rail steels have been reported in the literature. The data reported in References 1 and 2* are useful for a comparison with the present results. The British rail steel tested contained 0.56 percent C, 1.02 percent Mn, 0.13 percent Si, and less than 0.05 of P and S each. The steel had a 0.1 percent yield strength of 67 ksi and an ultimate tensile strength of 121 ksi. Test results for center cracked panels showed a value of 4 for the exponent n in Equation (3) for the case of R = 0 (Reference 1). Experiments at various R-

* References are listed on page 70.

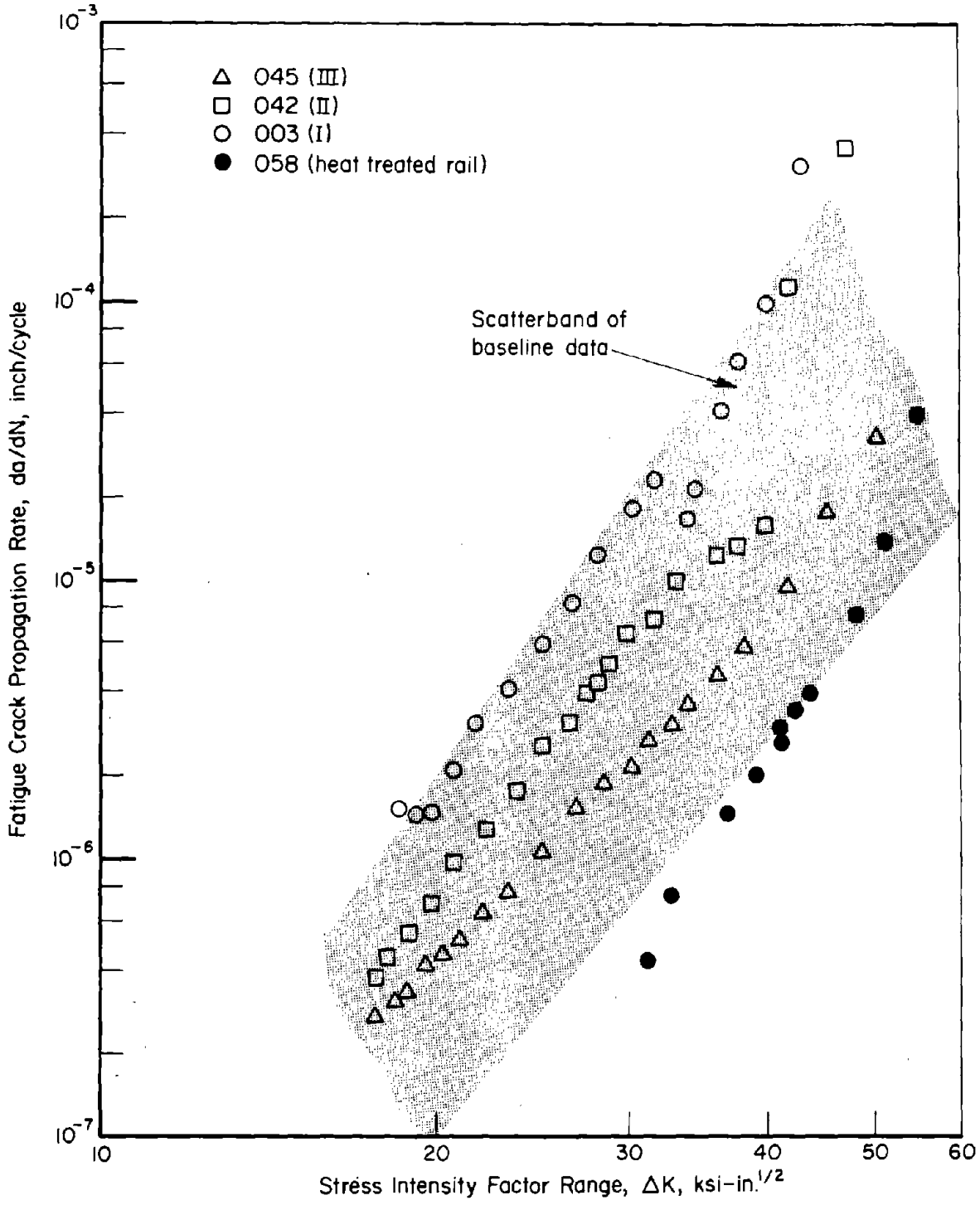

FIGURE 20. VARIABILITY OF FATIGUE CRACK PROPAGATION RATE BEHAVIOR

TABLE 8. SAMPLE OF COMPUTER PRINTOUT OF BASIC DATA ALONG WITH FIRST STAGE OF RATE ANALYSIS

SPECIMEN IDENTIFICATION =009
GRAIN DIRECTION =LT
SPECIMEN CONFIGURATION =CT
THICKNESS = .502 INCH
WIDTH = 3.00 INCH
MAXIMUM LOAD = 2.50 KIPS
LOAD RATIO = .00
TEST FREQUENCY = 40.00 HZ.
TEST TEMPERATURE = 70.00 DEGREE F
DATE OF ANALYSIS = 2 21 0

OVERALL WIDTH = 3.75 INCH
HEIGHT = 3.20 INCH

BASIC DATA		RATE CALCULATIONS		DAMAGE PARA.	
CRACK LENGTH, A,INCH	CYCLE COUNT, N,KC	TWO POINT SLOPE	THREE POINT SLOPE	K(MAX) KSI-SQRT(INCH)	DELTA K
.913	320.00	.634E-06	.000E+00	16.99	16.99
1.002	460.00	.739E-06	.698E-06	18.10	18.10
1.069	550.00	.891E-06	.815E-06	19.01	19.01
1.149	640.00	.118E-05	.106E-05	20.23	20.23
1.220	700.00	.187E-05	.148E-05	21.43	21.43
1.369	780.00	.336E-05	.286E-05	24.44	24.44
1.504	820.00	.626E-05	.568E-05	27.85	27.85
1.566	830.00	.101E-04	.900E-05	29.74	29.74
1.607	834.00	.184E-04	.156E-04	31.08	31.08
1.644	836.00	.232E-04	.216E-04	32.39	32.39
1.667	837.00	.538E-04	.385E-04	33.26	33.26
1.720	838.00	.417E-04	.445E-04	35.47	35.47
1.733	838.30	.235E-03	.120E-03	36.02	36.02
1.836	838.74	.000E+00	.000E+00	41.12	41.12

TABLE 9. SUMMARY OF CRACK BEHAVIOR PARAMETERS FOR BASELINE RAIL MATERIAL SPECIMENS

Rail Sample Number	Linear Model				Modified Linear Model				Apparent Toughness, K_{app}, ksi-in.$^{\frac{1}{2}}$	Life Parameter, N_L, cycles	Crack Growth Life From 1-in. to Failure, kilocycles
	Coefficient, C	Exponent, n	Correlation Coefficient, R^2	Computed Life Margin	Coefficient, C'	Exponent, n'	Correlation Coefficient, R^2	Computed Life Margin			
001	$.279 \times 10^{-16}$	7.09	.785	-.321	$.127 \times 10^{-11}$	5.63	.797	-.176	69.4	8.40×10^{8}	736
002	$.256 \times 10^{-10}$	3.70	.978	+.020	$.459 \times 10^{-8}$	1.63	.895	+.123	50.8	7.01×10^{8}	270
003	$.580 \times 10^{-13}$	5.73	.954	-.111	$.489 \times 10^{-8}$	3.08	.969	+.039	44.0	3.24×10^{8}	211
004	$.340 \times 10^{-11}$	4.27	.986	+.012	$.913 \times 10^{-7}$	2.14	.921	+.264	54.7	7.21×10^{8}	348
005	$.927 \times 10^{-12}$	4.77	.983	-.074	$.138 \times 10^{-7}$	2.72	.936	+.037	48.6	4.85×10^{8}	271
006	$.654 \times 10^{-13}$	5.44	.966	-.056	$.130 \times 10^{-8}$	3.32	.978	+.127	49.5	7.44×10^{8}	490
007	$.911 \times 10^{-13}$	5.23	.976	-.019	$.389 \times 10^{-8}$	2.89	.926	+.153	52.5	1.07×10^{9}	796
008	$.487 \times 10^{-11}$	4.21	.984	-.040	$.177 \times 10^{-7}$	2.66	.992	+.006	52.7	6.19×10^{8}	294
009	$.154 \times 10^{-14}$	6.76	.951	-.128	$.148 \times 10^{-10}$	4.73	.967	-.054	41.1	4.38×10^{8}	391
010	$.183 \times 10^{-10}$	3.78	.987	-.057	$.150 \times 10^{-8}$	2.08	.950	+.047	62.3	7.42×10^{8}	277
011	$.136 \times 10^{-13}$	6.08	.922	-.145	$.938 \times 10^{-10}$	4.41	.945	-.010	55.4	3.82×10^{8}	262
012	$.463 \times 10^{-11}$	4.39	.993	-.046	$.965 \times 10^{-7}$	2.18	.968	+.101	43.7	3.51×10^{8}	172
013	$.148 \times 10^{-9}$	3.21	.985	-.058	$.415 \times 10^{-8}$	1.84	.958	-.017	62.4	7.44×10^{8}	216
014	$.266 \times 10^{-11}$	4.43	.976	-.052	$.218 \times 10^{-7}$	2.38	.988	+.029	49.4	5.33×10^{8}	269
015	$.112 \times 10^{-11}$	4.58	.870	-.125	$.385 \times 10^{-8}$	3.05	.926	-.059	52.2	7.61×10^{8}	395
016	$.435 \times 10^{-10}$	3.69	.907	-.083	$.143 \times 10^{-6}$	0.58	.967	+.037	42.3	4.41×10^{8}	150
017	$.386 \times 10^{-13}$	5.81	.857	-.106	$.422 \times 10^{-9}$	3.84	.921	-.050	47.8	3.76×10^{8}	288
018	$.105 \times 10^{-13}$	6.10	.949	-.070	$.106 \times 10^{-9}$	4.12	.985	+.056	46.8	5.38×10^{8}	384
019	$.293 \times 10^{-12}$	4.99	.920	-.144	$.628 \times 10^{-8}$	2.80	.960	-.044	46.9	7.34×10^{8}	435
020	$.373 \times 10^{-16}$	6.83	.971	+.041	$.138 \times 10^{-11}$	5.29	.945	+.227	53.8	1.44×10^{9}	1302
021	$.218 \times 10^{-11}$	4.33	.926	-.059	$.414 \times 10^{-7}$	2.29	.991	+.044	54.2	9.16×10^{8}	419
022	$.682 \times 10^{-10}$	5.23	.864	-.246	$.768 \times 10^{-9}$	3.38	.970	-.114	56.8	1.42×10^{9}	803
023	$.646 \times 10^{-10}$	3.48	.911	-.084	$.768 \times 10^{-6}$	0.856	.756	+.048	47.0	4.74×10^{8}	155
024	$.211 \times 10^{-14}$	6.58	.915	-.071	$.435 \times 10^{-11}$	5.11	.955	-.034	46.8	5.69×10^{8}	495
025	$.804 \times 10^{-11}$	4.23	.838	-.144	$.313 \times 10^{-8}$	1.97	.946	-.028	55.0	3.50×10^{8}	153
026	$.144 \times 10^{-11}$	4.63	.978	+.100	$.172 \times 10^{-7}$	2.48	.892	+.181	39.1	5.00×10^{8}	233
027[a]	$.319 \times 10^{-13}$	5.76	.993	-.045	$.274 \times 10^{-9}$	3.68	.972	+.094	39.3	5.35×10^{7}	--
027A	$.204 \times 10^{-13}$	5.65	.973	-.087	$.159 \times 10^{-8}$	3.78	.977	+.001	46.7	1.20×10^{8}	890
028	$.131 \times 10^{-11}$	4.47	.991	+.196	$.979 \times 10^{-9}$	3.55	.981	+.267	65.3	9.45×10^{8}	536
029A	$.111 \times 10^{-14}$	6.50	.987	-.085	$.298 \times 10^{-10}$	4.26	.981	+.021	49.6	1.40×10^{9}	1256

TABLE 9. (CONTINUED)

Rail Sample Number	Linear Model				Modified Linear Model				Apparent Toughness, K_{app}, ksi-in.$^{\frac{1}{2}}$	Life Parameter, N_L, cycles	Crack Growth Life From 1-in. to Failure, kilocycles
	Coefficient, C	Exponent, n	Correlation Coefficient, R^2	Computed Life Margin	Coefficient, C′	Exponent, n′	Correlation Coefficient, R^2	Computed Life Margin			
030	$.168 \times 10^{-10}$	3.91	.927	+.045	$.361 \times 10^{-7}$	3.53	.962	+.130	53.7	5.10×10^{5}	197
031	$.214 \times 10^{-12}$	5.02	.895	-.088	$.208 \times 10^{-8}$	3.15	.961	+.004	52.4	9.11×10^{6}	596
032	$.732 \times 10^{-13}$	5.45	.957	-.021	$.108 \times 10^{-9}$	4.12	.970	+.019	48.3	6.43×10^{6}	404
033	$.113 \times 10^{-11}$	4.67	.956	-.236	$.233 \times 10^{-8}$	1.81	.846	+.014	47.7	5.57×10^{5}	261
034	$.166 \times 10^{-11}$	4.61	.976	-.098	$.747 \times 10^{-7}$	2.14	.966	-.001	42.6	4.64×10^{5}	221
035	$.380 \times 10^{-13}$	5.32	.962	-.131	$.254 \times 10^{-9}$	3.61	.986	-.006	54.3	1.90×10^{6}	1218
036	$.138 \times 10^{-13}$	6.37	.933	-.164	$.678 \times 10^{-11}$	4.72	.967	-.096	52.0	1.71×10^{6}	1269
037	$.812 \times 10^{-12}$	4.54	.933	-.136	$.104 \times 10^{-8}$	3.42	.965	-.097	63.0	1.20×10^{6}	617
038	$.345 \times 10^{-11}$	3.90	.838	-.132	$.381 \times 10^{-8}$	2.86	.895	-.092	66.2	2.57×10^{6}	1047
039	$.161 \times 10^{-12}$	4.90	.874	-.243	$.173 \times 10^{-9}$	3.06	.967	-.127	55.7	1.81×10^{6}	910
040	$.387 \times 10^{-11}$	4.20	.909	-.137	$.287 \times 10^{-8}$	1.67	.978	-.047	49.1	8.06×10^{5}	323
041	$.805 \times 10^{-13}$	4.45	.993	-.058	$.211 \times 10^{-9}$	3.19	.969	+.062	72.1	1.65×10^{6}	867
042	$.125 \times 10^{-13}$	5.92	.926	-.086	$.172 \times 10^{-9}$	3.91	.969	+.053	48.9	8.11×10^{6}	546
043	$.218 \times 10^{-10}$	3.64	.941	-.058	$.692 \times 10^{-7}$	2.19	.981	-.004	56.9	1.03×10^{6}	380
044	$.789 \times 10^{-14}$	6.11	.985	-.114	$.108 \times 10^{-9}$	4.10	.961	+.035	48.6	6.93×10^{5}	525
045	$.441 \times 10^{-12}$	4.57	.988	-.045	$.106 \times 10^{-8}$	3.26	.996	+.032	62.7	2.00×10^{6}	1019
046[b]	$.335 \times 10^{-4}$	11.4	.942	+.313	$.103 \times 10^{-17}$	8.17	.934	+.334	61.4	9.36×10^{6}	--
047	$.294 \times 10^{-13}$	5.39	.984	-.018	$.169 \times 10^{-9}$	3.66	.973	+.056	51.0	1.95×10^{6}	1424
048	$.127 \times 10^{-12}$	3.91	.941	-.061	$.916 \times 10^{-7}$	2.21	.956	+.053	58.9	6.75×10^{5}	254
049	$.168 \times 10^{-11}$	4.43	.989	-.077	$.701 \times 10^{-8}$	2.86	.977	-.004	54.6	8.44×10^{5}	440
050	$.369 \times 10^{-13}$	5.46	.986	+.021	$.132 \times 10^{-9}$	3.91	.989	+.118	51.3	1.23×10^{6}	820
051	$.140 \times 10^{-15}$	7.12	.951	+.033	$.187 \times 10^{-13}$	5.95	.958	+.064	51.4	1.18×10^{6}	1047
052	$.508 \times 10^{-13}$	5.49	.957	-.189	$.412 \times 10^{-9}$	3.73	.991	-.059	57.2	8.12×10^{5}	540
053	$.881 \times 10^{-14}$	5.99	.951	+.008	$.588 \times 10^{-9}$	3.40	.901	+.145	44.7	9.16×10^{5}	788
054	$.517 \times 10^{-14}$	6.05	.855	-.198	$.109 \times 10^{-11}$	4.74	.917	-.129	58.7	1.29×10^{6}	881
055	$.260 \times 10^{-13}$	4.78	.861	-.142	$.919 \times 10^{-9}$	3.27	.938	-.072	55.2	1.67×10^{6}	923
056	$.288 \times 10^{-15}$	5.45	.995	-.010	$.763 \times 10^{-11}$	4.01	.986	+.070	52.6	1.63×10^{6}	1150
057	$.854 \times 10^{-14}$	5.25	.963	-.009	$.229 \times 10^{-9}$	3.80	.979	+.041	53.3	1.07×10^{6}	712
058[c]	$.801 \times 10^{-12}$	7.23	.948	+.085	$.792 \times 10^{-11}$	3.58	.963	+.233	56.3	1.87×10^{7}	--
059	$.291 \times 10^{-13}$	5.27	.872	-.037	$.116 \times 10^{-9}$	3.74	.925	+.077	56.5	2.93×10^{6}	2317
060	$.144 \times 10^{-11}$	4.64	.971	-.069	$.673 \times 10^{-8}$	2.95	.993	-.006	46.9	4.83×10^{5}	247

TABLE 9. (CONTINUED)

Rail Sample Number	Linear Model				Modified Linear Model				Apparent Toughness, K_{app}, ksi-in.$^{\frac{1}{4}}$	Life Parameter, N_L, cycles	Crack Growth Life From 1-in. to Failure, kilocycles
	Coefficient, C	Exponent, n	Correlation Coefficient, R^2	Computed Life Margin	Coefficient, C'	Exponent, n'	Correlation Coefficient, R^2	Computed Life Margin			
061	$.154 \times 10^{-11}$	4.67	.937	-.097	$.455 \times 10^{-8}$	3.19	.985	-.032	52.8	4.09×10^{5}	211
062	$.327 \times 10^{-12}$	5.14	.935	-.135	$.175 \times 10^{-8}$	3.40	.982	-.053	46.7	4.00×10^{5}	217
063	$.243 \times 10^{-11}$	4.50	.933	-.152	$.656 \times 10^{-8}$	3.10	.960	-.085	56.1	5.03×10^{6}	217
064	$.862 \times 10^{-14}$	5.89	.986	-.114	$.554 \times 10^{-10}$	4.16	.977	+.010	52.3	1.30×10^{8}	1005
065	$.578 \times 10^{-16}$	6.76	.991	+.092	$.336 \times 10^{-11}$	5.01	.986	+.203	48.9	1.17×10^{8}	1118
066	$.105 \times 10^{-13}$	5.72	.986	+.104	$.134 \times 10^{-10}$	4.56	.981	+.158	59.1	1.85×10^{8}	1661

(a) 2 kip CT.
(b) 5 kip CT.
(c) 4.5 kip CT.

ratios indicated that n = 2.69 in Equation (4) gave the best fit. It appears that the material compares with the materials showing the lower growth rates in the present investigation.

6.2 SYNTHESIS OF CRACK-GROWTH DATA

As validation of the rate analysis, the crack-growth curves were reconstructed by integrating the rate data according to both the linear (Equation (3)) and the modified-linear (Equation (5)) fatigue-crack-propagation models. In simple terms the integration can be expressed as

$$a = \int \frac{da}{dN}\, dN \tag{7}$$

$$N = \int \frac{da}{dN}^{-1}\, da \quad . \tag{8}$$

Since the crack-growth model cannot generally be integrated in closed form, the solution of the above expressions is accomplished by a numerical integration or summation procedure wherein the computational steps must be defined in detail. Basic sources of error include experimental error, material anomalies, and simplicity of the model.

An incremental definition of Equation (8) can be expressed as

$$N = \sum_{i=1}^{k} \left(\frac{da}{dN}\right)^{-1} \Delta a \tag{9}$$

where $da/dN = f(C, n, \Delta K)$

$\Delta a = (a_f - a_o)/k$

k = number of increments, arbitarily set at 100.

Two alternative schemes of crack-growth prediction are being adopted in the basic data analysis computer program. One scheme predicts the number of cycles to grow the crack from a precrack length, a_o, to a final crack length, a_f; the other predicts the final crack length, a_f, which results from cycling the precrack, a_o, N_f times. If the analysis as well as the data models provided a perfect correlation, the results would, of course, agree perfectly with the experiment. In reality, however, perfect correlation will not be achieved due to experimental error, material variation and mere oversimplicity (i.e., inadequacy) of the analysis. The contrast in the results of the two computational schemes will provide further insight to the source and degree of errors.

The measure of the effectiveness of these two schemes of analysis is expressed in the "cyclic life margin of safety" which is expressed as

$$M.S._{life} = \frac{N_{actual}}{N_{computed}} - 1 \quad . \tag{10}$$

and in the cyclic crack growth margin, which is expressed as

$$M.S._a = \frac{a_{actual}}{a_{computed}} - 1 \quad . \tag{11}$$

Positive values of either of these margins infer that the computed value is less than the actual and, hence, conservative. The degree of conservatism (+) or unconservatism (-) is reflected in the variation of margin from unity (1.0). (Note at the present time, only the life margin, Expression (10), has been tabulated in Table 9.)

Synthesis Results

The preceding crack-growth-synthesis procedure was applied to the 66 baseline data sets to obtain a set of life margins which in turn were analyzed statistically. These results are presented in Table 10.

TABLE 10. RESULTS OF CRACK-GROWTH SYNTHESIS

Model	Predicted Mean Life	Predicted Life Margin Statistics		
		Mean Life Margin	Variance	Standard Deviation
Linear	0.936	-0.064	0.010	0.100
Modified Linear (Forman)	1.035	+0.035	0.011	0.104

From these results, several interesting observations can be made. First, it appears that the linear model tends to be unconservative in that it predicts, on the average, a larger crack lifetime than was encountered in the test. This is evidenced by the negative value of the mean life margin. In contrast, the modified linear model provides a conservative estimate of life and for that reason may be a more preferable model to use. Second, since the variance and standard deviation are nearly equivalent for each model, it is judged that lifetime scatter about the mean is not particularly affected by the model.

6.3 CORRELATION OF RATE DATA WITH OTHER PROPERTIES

6.3.1. General Approach

One of the basic objectives of this research program is to discern whether the crack behavior of rail materials can be linked to more fundamental mechanical, metallurgical, and processing variables. As a result, a key activity in data analysis is the broad scale assessment and evaluation of rate data with respect to other material properties. The following sections describe the initial efforts which have been undertaken and the results which have been ascertained to date.

The detection and isolation of primary variables affecting crack behavior would be a straightforward procedure if all of the variables were truly independent. In reality, however, most of the mechanical, metallurgical, and processing variables are not mutually independent and interact in a very complex manner. As a result, the discrimination of the dominant factors and the determination of their order of precedence requires a deliberate search and involves considerable trial-and-error data scanning.

For the baseline fatigue-crack-propagation specimens of this program, a broad matrix of data was assembled. This consisted of the background, mechanical property, metallurgical and derived crack-behavior variables determined for each material sample. These were extensively examined by computerized analysis as well as by more intuitive technical review (i.e., engineering judgments). While some general trends were discerned, more in-depth probing, analysis, and data generation will be necessary to strength and more positively identify the trends. It appears that the broad scatter of the data will require more diligent screening and examination of individual tests. The following discussion of procedures and results presents the current status of this effort.

6.3.2 Automatic Interaction Detector (AID) Analysis

The AID computer program is a statistical tool for assessing the relative influence of a set of independent variables (termed predictors) on the behavior of a specified dependent variable. The correlation (or lack thereof) between the dependent variable and any given predictor is established by decomposing the total variance of the dependent variable (fixed for a given body of data) into a within-subset and a between-subset variance of successive splits (i.e., two-part divisions) of the set of values of the dependent variable.

For each predictor, the set of values of the dependent variable are ordered by either the order of the predictor (if a monotonic predictor) or the order of the dependent variable (if a free predictor). The set of values of the dependent variable is then divided (or split) successively into two subsets along the domain of the predictor. At each split, the within-subset variance and between-subset variance is computed. The split which produces the largest ratio of between-subset variance to within-subset variance (i.e., F ratio or signal-to-noise ratio) is considered the optimum split for that predictor. The predictor which exhibits the largest ratio of between-subsets variance to total variance is the dominant or primary predictor for the dependent variable.

The computational scheme is semiquantitative in that the independent variables are linearly scaled and coded to integral values from 0 to 63. However, since known correlations do not exist, a method that compares data on such a normalized basis can provide a clearer discrimination of the dominance (if such exists) of the primary independent variables.

Once the optimum split of the primary variable has been defined, the procedure is repeated for the two groups at each side of the split and so on. The resulting cascade of splits which is generated in this repetitive procedure can be graphically displayed in the AID "tree", a sample of which is shown in Figure 21. Only the salient features of the analysis are included in this pictorial summary.

In this particular illustration, the influence of a range of compositional variables--the carbon equivalents (CE), later discussed--on the logarithm of crack life (the dependent variable or criterion scale) is evaluated. The body of data consisted of 57 specimens (selectively called from a total data set of 67 specimens). The primary variable, CE1, revealed an optimum split into two groups of 37 and 20 at a life value of 5.90. These two resulting groups subsequently split on predictors CE4 and CE6. The mean and standard deviation values are given along with the coded predictor values. Subsequent splits and their related numerical details are also given. Note that the dependent variable is noted as the common logarithm of the life parameter.

At the outset of this task, the widest variety of independent variables was chosen and put into the AID "hopper" to see what would be sorted out. These variables included

- Rail weight } Background
- Year produced }
- Tensile ultimate strength }
- Tensile yield strength }
- Elongation } Mechanical Properties
- Reduction of area }
- Elastic modulus }
- Hardness }
- Carbon }
- Manganese }
- Silicon }
- Sulfur } Metallurgical
- Oxygen }
- Hydrogen }
- Pearlite. }

These were then related to the life parameter, N_L, as a dependent variable.

AUTOMATIC INTERACTION DETECTOR
DOT REGRESSION

BINARY TREE STRUCTURE

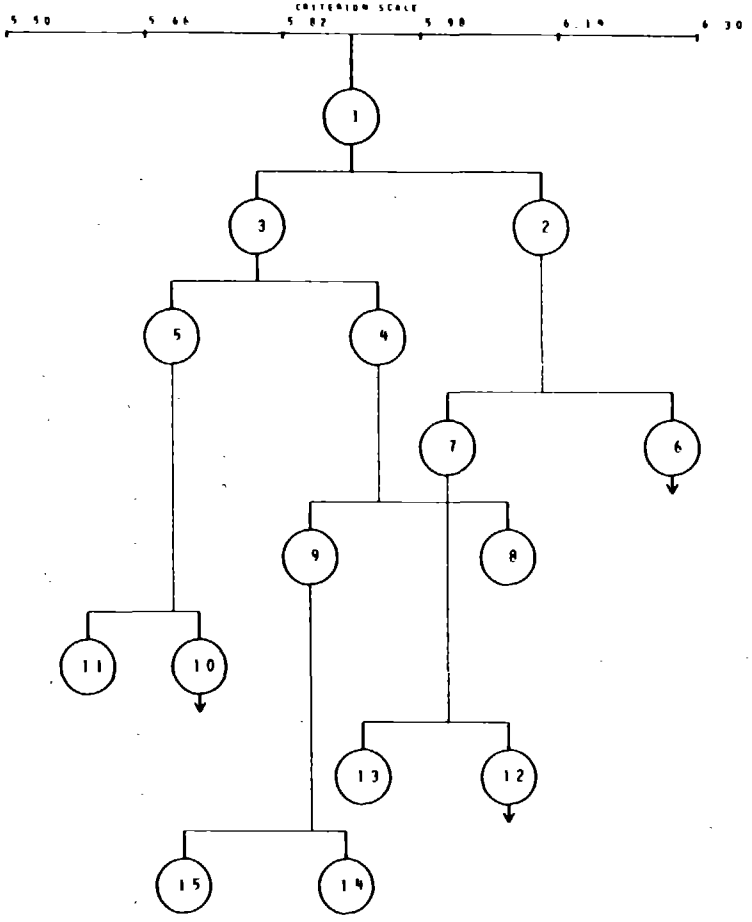

SUMMARY TABLE

---TOTAL GROUP---

CRITERION - LIFE

TOTAL GROUP N = 57
MEAN = 5.90
STD. DEV. = 0.23

PARENT 1 SPLITTING VARIABLE - CE1

MEAN= 5.79 S.D.= 0.17 N= 37
PREDICTOR VALUES -- 0 12 13 18 23 25 29 36 37 39 41 43 45 48 49 50 53 55

MEAN= 6.12 S.D.= 0.16 N= 20
PREDICTOR VALUES -- 15 16 31 39 38 40 42 44 46 47 51 52

PARENT 3 SPLITTING VARIABLE - CE4

MEAN= 5.69 S.D.= 0.00 N= 22
PREDICTOR VALUES -- 32 35 38 41 42 44 48 50 51 53 54 45 47 50

MEAN= 5.93 S.D.= 0.16 N= 15
PREDICTOR VALUES -- 0 10 13 19 40 43 44 47 49 63

PARENT 2 SPLITTING VARIABLE - CE6

MEAN= 6.01 S.D.= 0.11 N= 11
PREDICTOR VALUES -- 30 32 33 36 37 40 42 46

MEAN= 5.87 S.D.= 0.07 N= 9
PREDICTOR VALUES -- 6 9 26 31 38 41 46

PARENT 4 SPLITTING VARIABLE - CE10

MEAN= 5.85 S.D.= 0.10 N= 10
PREDICTOR VALUES -- 0 9 7 13 19 30 32 36 43

FINAL GROUP

MEAN= 6.00 S.D.= 0.13 N= 9
PREDICTOR VALUES -- 31 33 34 35

FINAL GROUP

PARENT 5 SPLITTING VARIABLE - CE8

MEAN= 5.99 S.D.= 0.05 N= 5
PREDICTOR VALUES -- 26 32 39 50

FINAL GROUP

MEAN= 5.77 S.D.= 0.07 N= 17
PREDICTOR VALUES -- 28 29 31 33 34 35 37 38 40 46 56

PARENT 7 SPLITTING VARIABLE - CE3

MEAN= 5.91 S.D.= 0.05 N= 5
PREDICTOR VALUES -- 30 41 42 56

FINAL GROUP

MEAN= 6.00 S.D.= 0.00 N= 6
PREDICTOR VALUES -- 34 42 43 44 50

PARENT 9 SPLITTING VARIABLE - CE8

MEAN= 5.78 S.D.= 0.15 N= 2
PREDICTOR VALUES -- 0 33

FINAL GROUP

MEAN= 5.89 S.D.= 0.02 N= 8
PREDICTOR VALUES -- 2 6 17 23 31 32 34 63

FINAL GROUP

FIGURE 21. SAMPLE GRAPHICAL OUTPUT FROM PROGRAM AID

6.3.3. Process of Analysis

The AID analysis proceeded through several stages. It became obvious at the outset that the variables were not mutually independent. An interspersion of various metallurgical and mechanical variables became apparent when all the variables were considered. This inferred that the mechanical property variables were, in essence, a restatement of the compositional variables (or vice-versa)--a not too surprising result. This led to selective regrouping and fitting of the variables to discern those that were most dominant.

6.3.4. Results of Analysis

The dominance of a particular independent variable may be expressed as the percentage contribution of its BSS to the TSS of the dependent variable. The results of the AID analysis of independent variables for leading contenders can be summarized as follows:

Category	Variable	Contribution to Variance, percent
Mechanical Property	Tensile Ultimate Strength	13
	Hardness	14
Metallurgical	% Pearlite	19
	% Carbon	8
	% Oxygen	8
	% Sulfur	5
	% Manganese	4.

For the mechanical property category, the nearly equivalent dominance of strength and hardness is not surprising because of their well-documented interrelationship. However, the statistical impact is lessened when one then views the graphical relationship of strength and life as shown in Figure 22(a).

A similar disillusionment is encountered when one observes the display of percent pearlite versus life in Figure 22(b). The latter part of the above tabulation suggested the consideration of a carbon equivalent (CE) which was expressed as

$$\% \text{ CE} = \% \text{ C} + \alpha \text{ [\% Mn-1.7 (\% S)]} \quad .$$

The factor 1.7 is the ratio between the atomic weights of Mn and S. As a result, the term between brackets is the percentage of free Mn, i.e., total Mn minus the fraction tied up in the compound MnS. The free Mn is in solid solution where it

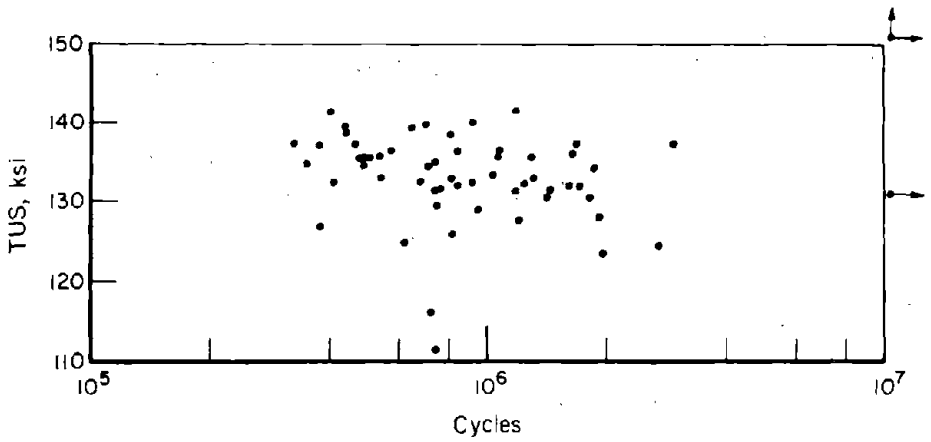

(a) Effect of Tensile Ultimate Strength

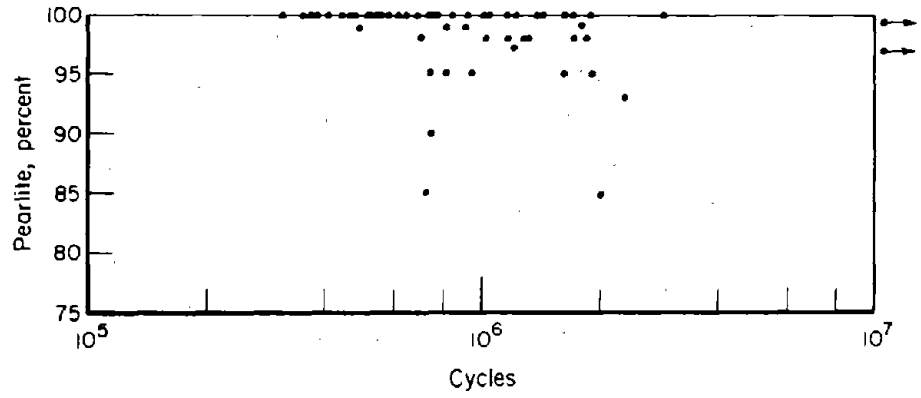

(b) Effect of Pearlite

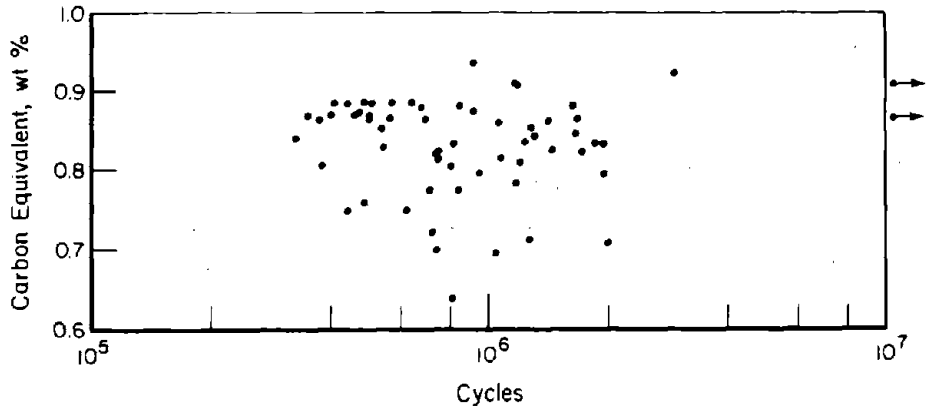

(c) Effect of Carbon Equivalent

FIGURE 22. VARIATION OF LIFE WITH LEADING PREDICTORS

has a similar, but less effective, strengthening effect as Carbon. This is reflected by the factor α. An AID analysis for incremental values of α was conducted from which a value of $\alpha = 0.1$ was obtained as providing a 21 percent contribution to variances. Again, however, the statistical analysis was poorly supported with the "shotgun" pattern of Figure 22(c).

6.3.5. Correlation Analysis

The contrast between the statistical AID analysis and the weak evidence of the graphical displays suggests that any numerical correlation is a coincidence of "noise" in the data. At the same time, however, the complexity of a carbon or other equivalent as suggested by other investigators[3] requires that other microstructural details be included. In Reference (3), correlation functions were derived between the TUS, TYS, and 20 ft-lb Charpy impact temperature for ferrite-pearlite steels. The functions are complex equations containing the percentage of the various chemical constituents, volume fraction of pearlite, interlamellar spacing and cementite plate thickness. At the present time, a positive conclusion is not tendered. The analysis will be advanced as additional metallurgical details are generated. However, the complex correlation functions as derived in Reference (3) suggest that any correlation function may be very artificial. Consequently, the generality of such functions is doubtful.

7. CATEGORIES FOR FURTHER RESEARCH

7.1 SELECTION OF CATEGORIES

The present test data provide the baseline information for the computational failure model to be developed during the second phase of this research program. However, for a complete failure model, more information is needed concerning crack growth under various circumstances. The effect of the following parameters will have to be evaluated:

(a) Stress ratio, R

(b) Cycling frequency, F

(c) Temperature, T

(d) Specimen orientation.

In addition, the behavior of elliptical flaws and the behavior under mixed-mode loading and variable-amplitude loading should be studied.

It is prohibitive to perform all this experimentation on all 66 rail materials. Therefore, it is necessary to make a selection of a few materials to be studied in more detail, under the assumption that the results obtained can be generalized relative to the baseline behavior as observed in the present tests. Although various possibilities exist to select the materials, the most obvious criterion for selection is the rate of crack growth, because the differences in crack-growth rates were so large.

Therefore, three categories were selected for further characterization, consisting of materials with high (I), medium (II), and low (III) growth rates, respectively. The basis for categorization was the crack propagation life from a 1-inch crack size to failure. This reflects the combined effects of n, C, and K_{app} in a natural way. As a practical concern, the length of the sample available for specimen manufacture was also a consideration.

The materials selected for Category I have crack growth lives (from 1 inch to failure) varying from 150 to 270 kilocycles. In Category II the lives vary from 380-600 kilocycles, and in Category III the lives are 700 kilocycles and higher. An appreciation of the crack growth behavior of the materials in the three categories can be obtained from Figure 20. Specimen 3 in Figure 20 had a life of 211 kilocycles which is typical for Category I. The life of Specimen 42 was 546 kilocycles, typical for Category II, and the life of Specimen 45 was 1,018 kilocycles, which is typical for Category III.

The samples selected for each category are listed in Table 11. Subsequent testing will be done primarily on those materials. A more detailed metallographic and fractographic characterization of these materials will be required. This effort is already under way and some preliminary results are presented in the following sections.

Some additional samples will be used for more detailed characterization and testing. These samples will be selected on the basis of the AID analysis. The criteria for selection will be discussed in Section 7.4. A test matrix and experimental plan for the second phase of this program is presented in Section 7.5.

TABLE 11. THE THREE CATEGORIES FOR PHASE II

Category	Rail Sample Number	C	Mn	Crack Growth Life From 1 Inch to Failure, kilocycles
I	002	.74	.61	270
	013	.74	.89	216
	014	.78	.74	269
	016	.81	.93	150
	023	.79	.92	155
	025	.80	.91	153
	030	.80	.90	197
II	006	.72	.97	490
	009	.61	1.46	381
	018	.75	.89	384
	019	.74	.88	435
	024	.81	.83	495
	031	.79	.76	596
	032	.80	.94	404
III	001	.63	1.48	736
	007	.73	.93	796
	020	.75	.83	1302
	022	.78	.87	803
	029	.72	.89	1256
	035	.76	.80	1218
	036	.75	.80	1269

7.2 MICROSTRUCTURAL ANALYSIS OF THREE CATEGORIES

7.2.1. Rail Samples Used

From the three categories of rails established on the basis of crack-growth rate, five rail samples were chosen for more detailed microstructural analyses. They were Samples 002 and 030 from Group I, Samples 006 and 024 from Group II, and Sample 001 from Group III. The selection of the two samples from Groups I and III was based primarily on major differences in their chemistry. Sample 001 was selected because of the presence of internal fissures. Sample 004, which was not categorized, was selected for further microstructural analysis, since its microstructure consisted of a relatively high percentage (~ 15%) of ferrite in a network morphology.

7.2.2. Grain-Size Measurements

Since standard metallographic preparation techniques do not reveal prior austenite grain boundaries in pearlitic steels, an attempt was made to heat treat the samples in such a way that the grain sizes could be measured. The heat treatment employed was a partial isothermal transformation at approximately 1100 F, designed to develop a structure consisting of a network of fine pearlite nodules at austenite grain boundaries in a martensitic matrix. Partial isothermal transformation was successful using very small specimens, but the nucleation sites of pearlite nodules were too random to discern a grain-boundary network. Attempts to reveal prior austenite grains were made also using special etching reagents on quenched and tempered specimens of rail samples. The reagents used were (1) Vilella's reagent, an alcoholic solution of 1% picric - 5% hydrochloric acids, (2) a saturated aqueous solution of picric acid containing 1 gram of sodium triolecyl benzene sulfonate per 100 ml of solution, (3) a saturated aqueous solution of picric acid containing 2 ml of Teepol (sodium alkyl sulfonate) per 100 ml of solution, and (4) a solution of 1 gram of potassium metabisulfite and 2 drops of Teepol in 100 ml of water. None of these etchants revealed prior austenite grains satisfactorily for grain size measurements. Special etching techniques were also used on quenched and tempered specimens of rail samples in attempts to reveal the prior austenite grains, but these too were unsuccessful.

The prior austenite grains were revealed in Sample 004 by the ferrite network present in its microstructure. A similar network was present in the other five samples at the rail surfaces where decarburization occurred during hot

rolling. The depth of decarburization was sufficient to produce a ferrite network zone below the surface. The width of the zone generally encompassed several prior austenite grains. Therefore, grain-size determinations on the other five rails were made in the decarburized surface zones.

Grain sizes were determined by the line intercept method. The number of grains at 100X magnification intersected by a test line 10 cm long was obtained three times on each specimen. The ASTM grain size, G, was calculated from Hilliard's equation:

$$G = 10.00 - 6.64 \log L_a \qquad (12)$$

where $L_a = \dfrac{\text{Total length of test lines}}{\text{Total no. intersections x magnification}}$.

The results of prior austenite grain size measurements of the six rail samples, and values computed from the grain-size measurements for average grain diameters and average number of grains per unit volume also are given in Table 12.

TABLE 12. PRIOR AUSTENITE GRAIN-SIZE MEASUREMENTS

Rail Group and/or Sample No.	ASTM Grain Size No.	Calculated Diameter of Average Grain, mm	Average No. of Grains per mm^3
Group I –			
002	4.3	0.081	1880
030	4.7	0.071	2850
Group II –			
006	3.5	0.107	820
024	4.9	0.066	3500
Group III –			
001	4.4	0.078	2100
004	3.2	0.12	600

7.2.3. Pearlite Interlamellar Spacing

True interlamellar spacing, S_o, is the perpendicular distance between the planes of a single pair of contiguous lamellae. Because true spacing is difficult to measure directly on metallographically prepared cross sections, the mean random spacing, σ, of the pearlite lamellae observed in the six samples was measured. The mean random spacing is defined as the reciprocal of N_L, where N_L is

the number of alternate lamellae intersected per unit length of random test lines. True spacing was then calculated using $S_o = \frac{\sigma}{2}$, the validity of which has been confirmed experimentally.

The mean random spacing of pearlite lamellae was measured on scanning electron microscope (SEM) micrographs of the pearlite structures photographed at 5000X. No unresolved pearlite lamellae were observed at this magnification. Examples of the pearlite, as revealed by the SEM micrographs, are shown in Figure 23.

Thirteen random fields on each specimen were photographed using the SEM. Intercept measurements were made along six different test lines on each micrograph. Each test line was 10 cm long. Thus, a total of 78 (6 x 13) test-line measurements were made on each rail sample. A statistical analysis of the data for each sample indicated the accuracy of the interlammelar spacings obtained to be ±10 to 14 percent.

The results of interlamellar spacing measurements are presented in Table 13.

TABLE 13. PEARLITE INTERLAMELLAR SPACING

Rail Group and/or Sample No.	Number of Intersections per mm, N_L	True Spacing, S_o, A	Accuracy, ± percent
Group I –			
002	1705	2932	10.2
030	1385.5	3608	10.6
Group II –			
006	1861.5	2686	10.9
024	1464.5	3414	13.8
Group III –			
001	2025	2470	10.4
004	1202	4159	12.2

7.2.4. Other Microstructural Parameters

Determinations of the pearlite colony size and characterizations of the nonmetallic inclusions in the six rail samples are planned but, as yet, have not been made. Visual estimates of the volume fraction of free ferrite in the samples are reported elsewhere. More precise determinations of volume fractions of ferrite using established quantitative metallographic techniques also are planned.

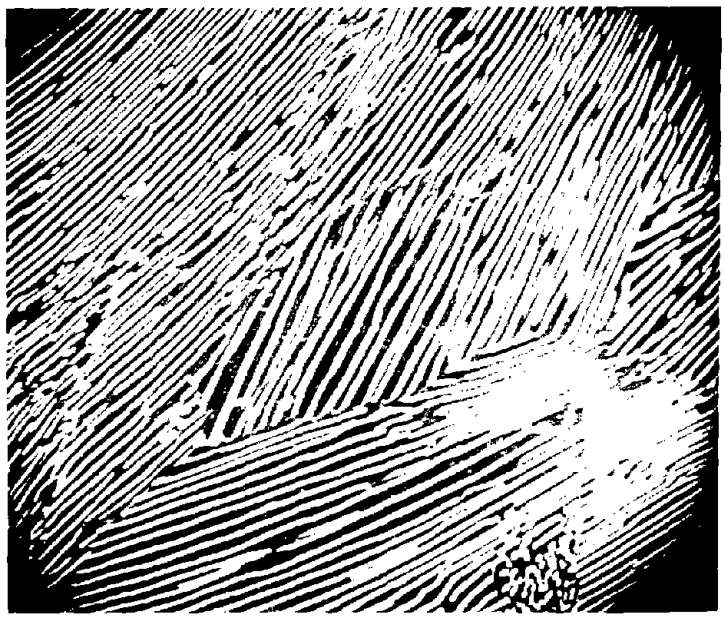

5000X

(a) Sample 002L, Field 7

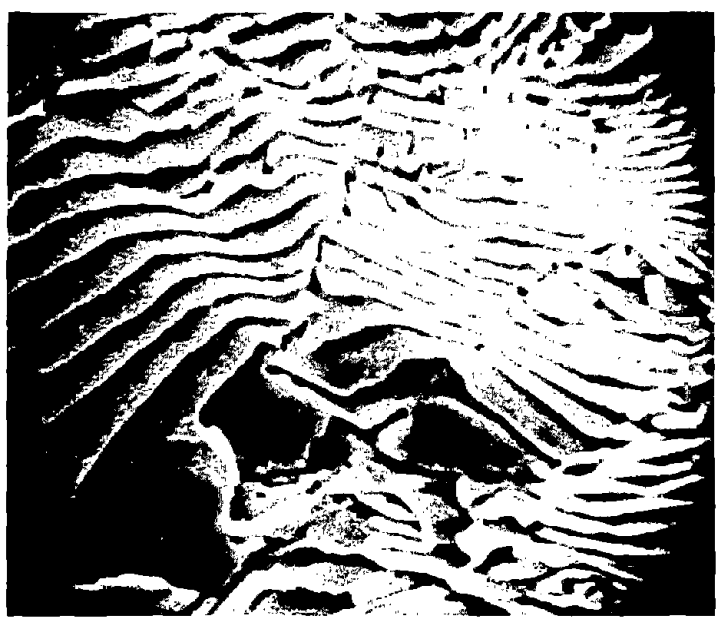

5000X

(b) Sample 006L, Field 13

FIGURE 23. TYPICAL SCANNING ELECTRON MICROSCOPE VIEWS OF PEARLITE IN RAIL SAMPLES

7.3 FRACTOGRAPHY

A photomacrograph of the fatigue-test fracture surfaces of the six rails is shown in Figure 24. The encircled areas on the fracture surfaces denote the fracture surface locations along the direction of fatigue-crack propagation where fractographic studies are being made. The locations were selected from the plots of crack lengths versus the number of load cycles and correspond to the approximate midpoints of significant changes in the slopes (crack-growth rates) of the curves. In addition to these locations, the following fracture surface locations also are being examined: (1) the precrack fatigue origin, (2) the approximate midpoint of the length of precrack propagation, (3) the approximate beginning of constant cyclic load crack propagation, (4) a location approximately midway between the point where the load frequency was lowered and the point of unstable crack propagation, and (5) an area of unstable crack propagation. The locations in terms of distance from the tip (origin of the precrack) of the notch on the test specimen are given in Table 14.

TABLE 14. LOCATIONS OF FRACTOGRAPHIC STUDIES

Sequence of Location	Sample Identification					
	004	002	030	006	001	024
1st	0	0	0	0	0	0
2nd	0.18	0.17	0.17	0.17	0.18	0.18
3rd	0.31	0.33	0.30	0.26	0.31	0.27
4th	0.41	0.43	0.58	0.32	0.46	0.37
5th	0.86	0.79	1.15	0.47	0.64	0.56
6th	1.26	1.25	1.41	0.81	0.96	0.82
7th	--	--	--	1.22	1.36	1.20
8th	--	--	--	--	--	1.38

NOTE: Numbers shown represent distance from notch root in inches.

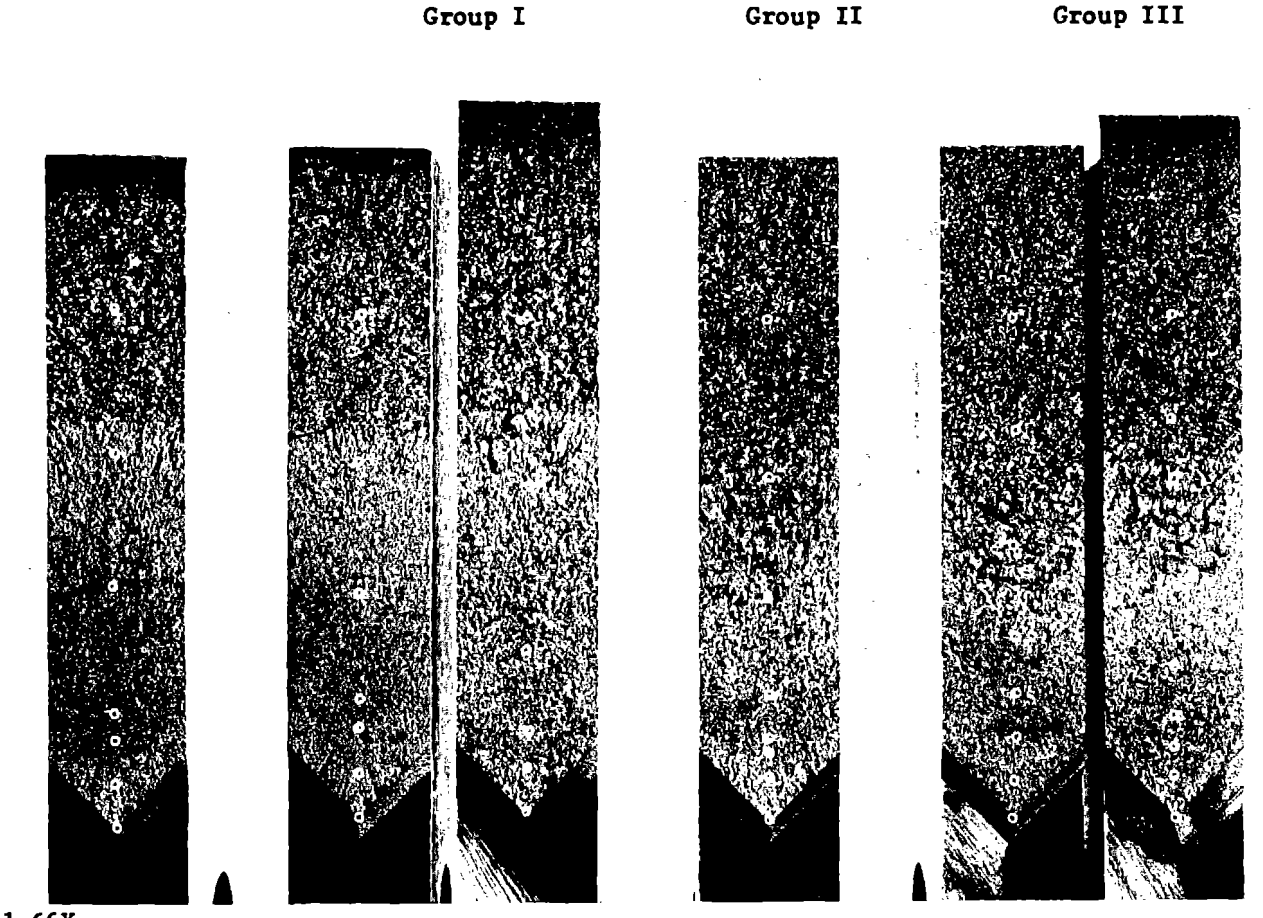

Rail Sample (Category)	004 (I-II)	002 (I)	030 (I)	006 (II)	001 (III)	024 (II)
K_{app} at Failure ($ksi\sqrt{in}$)	55	51	54	50	70	47

FIGURE 24. FATIGUE TEST FRACTURE SURFACES

Encircled areas denote locations of fractographic studies.

Some general fracture surface characteristics are apparent in the fracture surfaces shown in Figure 24. Significant observations made at magnifications up to 100X using optical microscopy are described in Table 15.

TABLE 15. GENERAL FRACTURE-SURFACE CHARACTERISTICS

Rail Sample Number	Low-Magnification Observations
004	• The length of the fatigue crack zone was ~30 mm. • A cleavage facet was located very near the tip (precrack origin area) of the notch. • Some scattered cleavage facets were located throughout the fatigue-crack zone. • The fatigue-crack zone terminated abruptly and was followed by unstable cleavage fracture. • Final rupture, about 2 – 3 mm in length, was ductile.
002	• The length of the fatigue-crack zone was ~28 mm. • A cleavage facet was located a little below, and on one side of, the notch tip. • Some scattered cleavage facets were located throughout the fatigue-crack zone to a crack length of ~20 mm. Several cleavage facets were located from 20 mm to the end of the fatigue-crack zone. • The fatigue-crack zone terminated fairly abruptly and was followed by unstable cleavage fracture. • Final rupture, about 1 – 2 mm in length, was ductile.
030	• The length of the fatigue-crack zone was ~30 mm. • Cleavage fracture was predominant at the tip of the notch. • Some scattered cleavage facets were located throughout the fatigue-crack zone to a crack length of ~15 mm. At approximately 18, 23, 25, and 27 mm of crack length, there appeared to be arrest zones containing increasing amounts of cleavage fracture in each successive zone. • The fatigue-crack zone terminated fairly abruptly and was followed by unstable cleavage fracture. • Final rupture, about 2 mm in length, was ductile.

TABLE 15. (Continued)

Rail Sample Number	Low-Magnification Observations
006	• The length of the fatigue-crack zone was ~25 mm.
	• Several cleavage facets were located a short distance from the notch tip.
	• Some scattered cleavage facets were located throughout the fatigue-crack zone to a crack length of ~12 mm. Beyond 12 mm, the amount of cleavage fracture increased rapidly to more than 50 percent at the termination of the fatigue-crack zone. From 17 to 25 mm of crack length there was some tendency for cleavage to concentrate in apparent arrest zones.
	• The fatigue-crack zone seemed to terminate by a gradual transition from fatigue to cleavage fracture over the last 13 mm of fatigue-crack length and was followed by unstable cleavage fracture.
	• Final rupture, about 0.5 mm or less in length, was ductile.
001	• The length of the fatigue-crack zone was ~21 mm.
	• Some cleavage facets were located in the area of the notch tip. However, fracture-surface features were partially obliterated by corrosion.
	• Some scattered cleavage facets were located throughout the fatigue-crack zone to a crack length of ~10 mm. The amount of cleavage increased between 10 and 21 mm of crack length. Cleavage tended to be concentrated in ~3 arrest zones between 15 and 19 mm of crack length.
	• The fatigue-crack zone terminated in a rapid transition from fatigue to cleavage over the last 6 mm of fatigue-crack length.
	• Final rupture, less than 0.5 mm in length, was ductile.
024	• The length of the fatigue-crack zone was ~25 mm.
	• Very little cleavage was located in or near the notch tip.
	• Some scattered cleavage facets were located throughout the fatigue-crack zone to a crack length of ~13 mm. Beyond 13 mm, cleavage occurred in increasing amounts.
	• The fatigue-crack zone terminated in a rapid transition from fatigue to cleavage over the last 7 – 8 mm of crack length.
	• Final rupture, ~1.5 mm in length, was ductile.

Fractographic studies of the six rails using electron microscopy are incomplete. Initial scanning electron microscopic (SEM) examinations resulted in some confusion with respect to the interpretation of detailed fracture features. Similar difficulties were encountered during replication transmission electron microscopic (RTEM) examinations. However, it is anticipated that continued examinations by both techniques will bring clarification.

Observations of the fracture surface at the tip of the notch (the fatigue precrack origin) made during SEM examinations of the six rails are shown in Figures 25 through 30. Cleavage facets, indicated by the letter "C" in the figures, are apparent in some cases. Fatigue striations do not seem to be discernible at the lower magnifications. The features which appear to be bubbles at the top and to the right in most of the micrographs are globules of molten metal on the electrical discharge machined surface of each test specimen. The globules are most evident in Figure 30.

Two SEM views of an area of the fracture surface located 0.17 inch from the notch tip of Sample 002 are shown in Figure 31. The views are considered to be typical of the appearance of the fracture surface areas of most of the samples when using the SEM. Note the fibrous striated brittle appearance of the crack surface. The lines in Figure 31 appear to be fatigue striations but they are actually pearlite lamellae on the fracture surface. Note the similarity between the pearlite interlamellar spacing shown in Figure 23(a) at 5000X magnification and the spacing of the lines in Figure 31 at 5000X magnification.

Some random RTEM views of fracture surfaces are shown in Figures 32 through 35. The RTEM micrograph in Figure 32 has an appearance similar to the SEM micrograph in Figure 31; however, the magnifications differ by a factor of 4. Some striations observed in Sample 004 which appear to be clearly fatigue striations are shown in Figure 33(a). These striations may be located in ferrite, since Sample 004 contained a high percentage of ferrite in the microstructure. On the other hand, similar striations in Figure 33(b) were observed on the fracture surface of Sample 030 which contained essentially no ferrite.

Occasionally, cross-hatched lines were observed as shown in Figure 34. Since the replicas were shadowed in a direction toward the crack origin, the lines in Figure 34 most nearly perpendicular to the direction of shadowing are likely to be fatigue striations. (These are the striations running approximately up and down in Figure 34.) The other lines, those that are parallel to the direction of shadowing, are likely to be pearlite lamellae.

The RTEM view presented in Figure 35 shows primarily cleavage fracturing. No evidence of ductile overload cracking has been observed in any of the fatigue fracture zones.

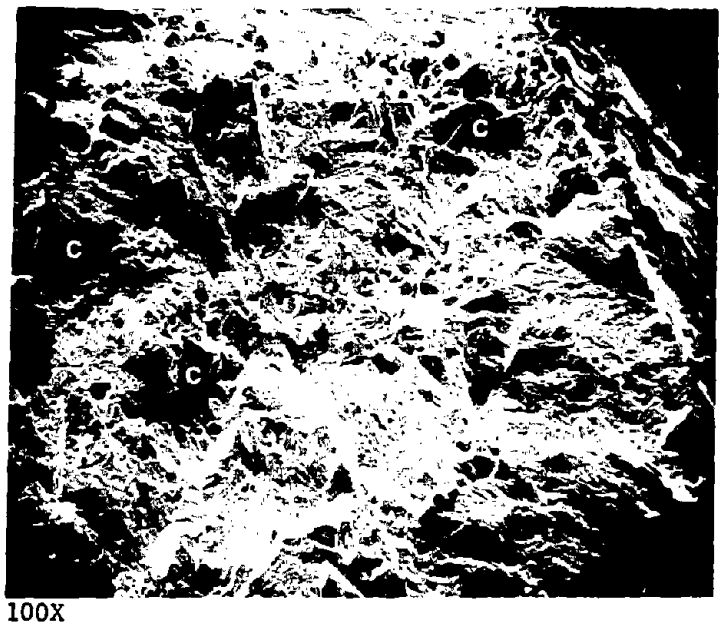

100X

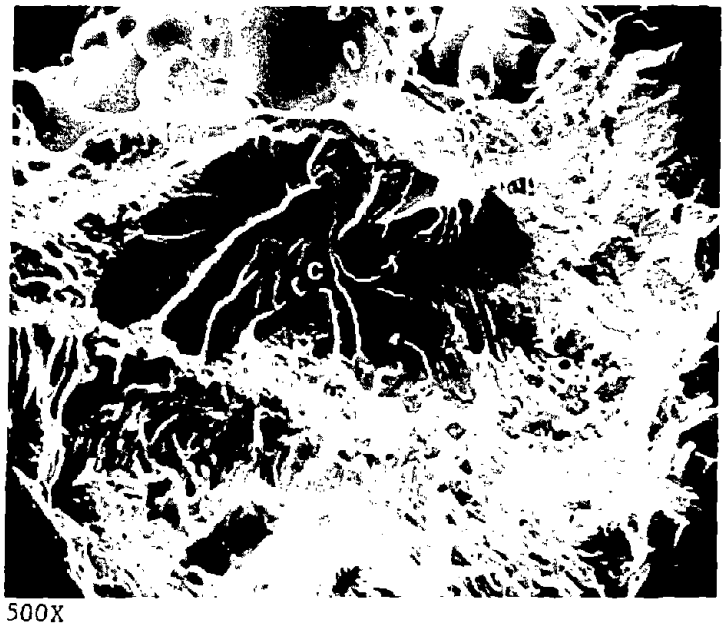

500X

FIGURE 25. FRACTURE SURFACE OF SAMPLE 004 AT THE NOTCH TIP

"C" denotes cleavage fracture.
Tip of notch is at upper right.

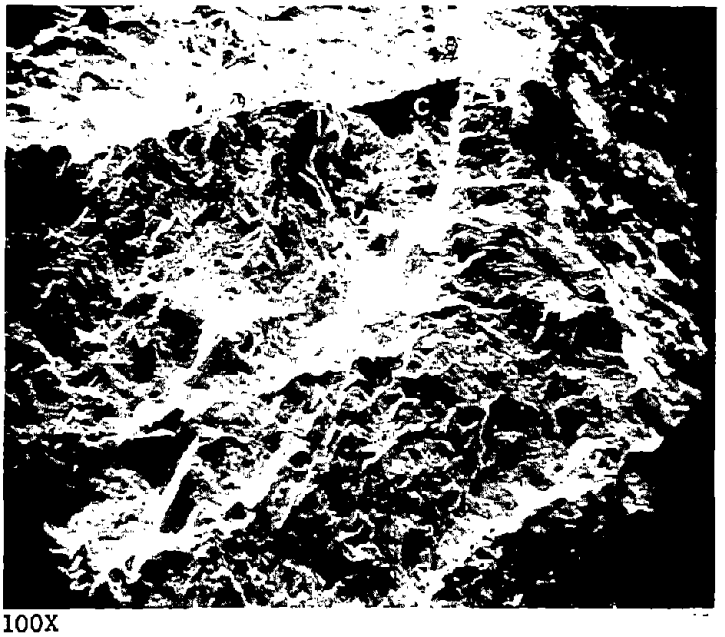

100X

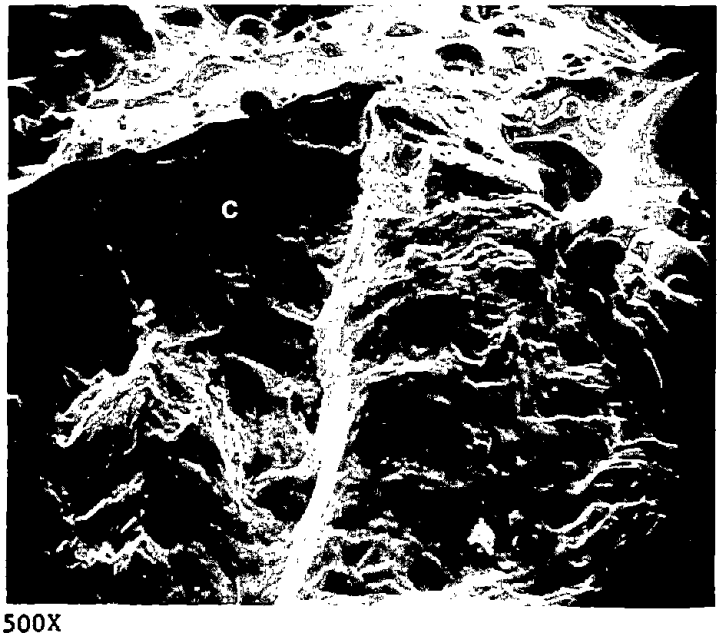

500X

FIGURE 26. FRACTURE SURFACE OF SAMPLE 002 AT THE NOTCH TIP

"C" denotes cleavage fracture.
Tip of notch is at upper right.

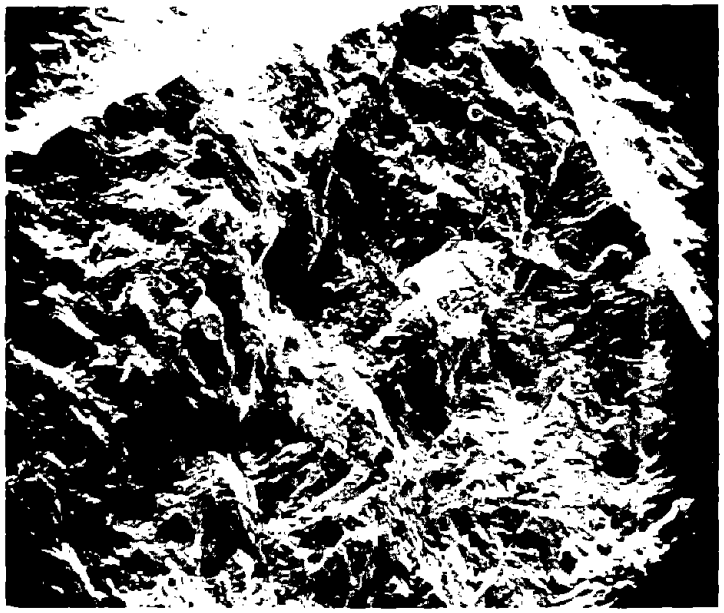

100X

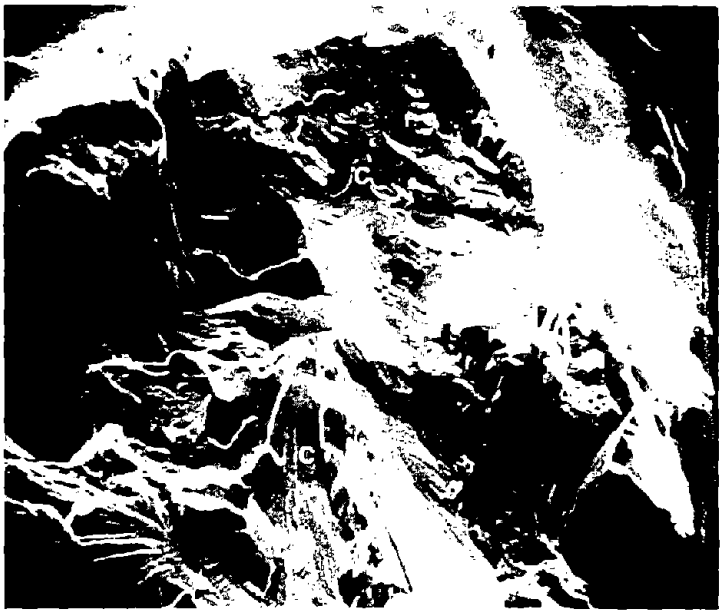

500X

FIGURE 27. FRACTURE SURFACE OF SAMPLE 030 AT THE NOTCH TIP

"C" denotes cleavage fracture.
Tip of notch is at upper right.

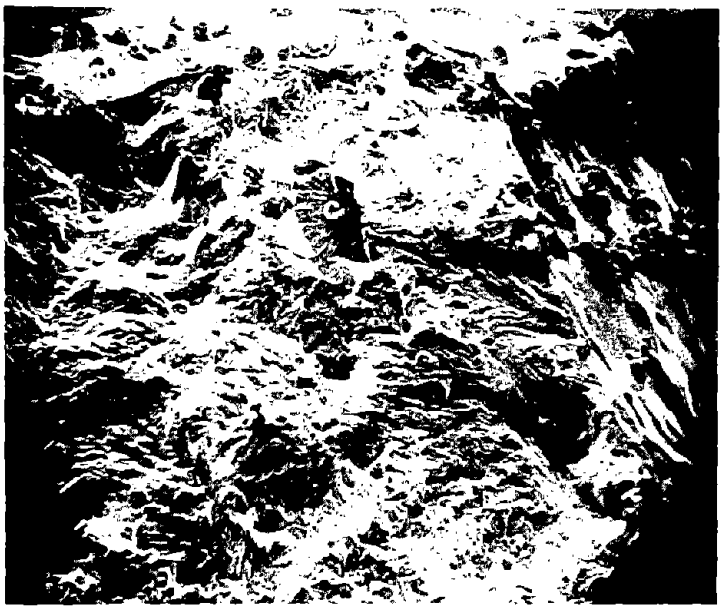

100X

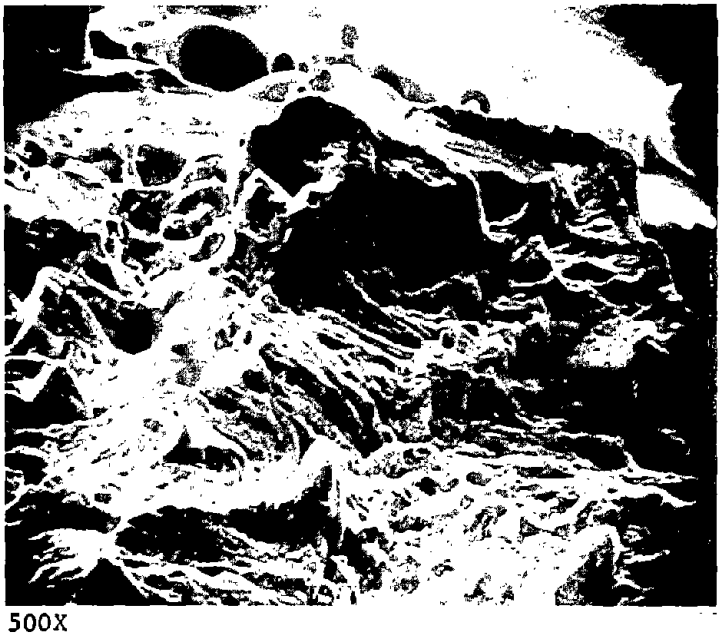

500X

FIGURE 28. FRACTURE SURFACE OF SAMPLE 006 AT THE NOTCH TIP

"C" denotes cleavage fracture.
Tip of notch is at upper right.

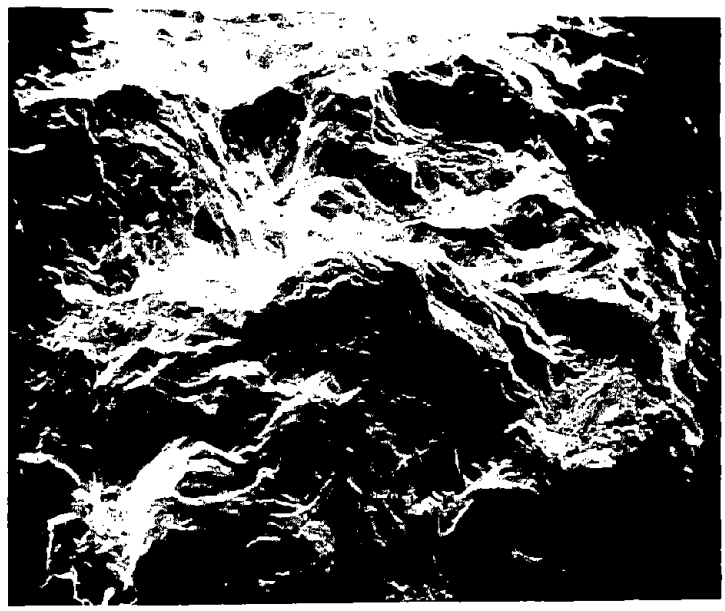

100X

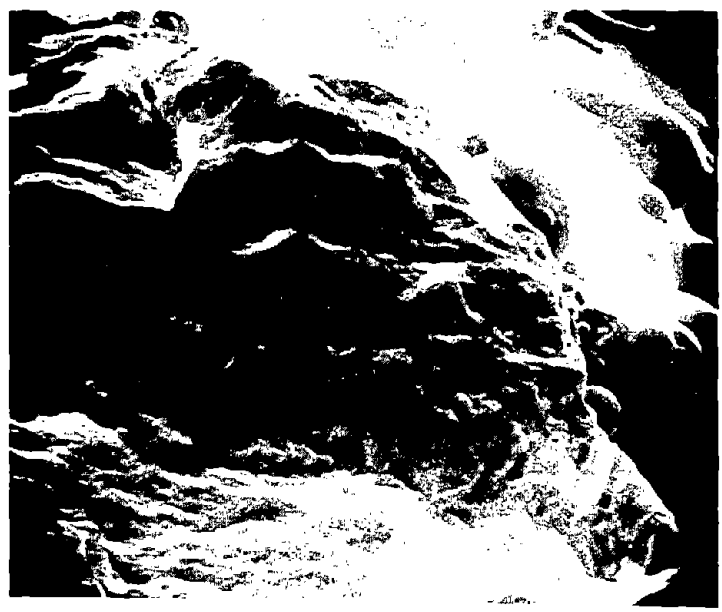

500X

FIGURE 29. FRACTURE SURFACE OF SAMPLE 001 AT THE NOTCH TIP

Tip of notch is at upper right.

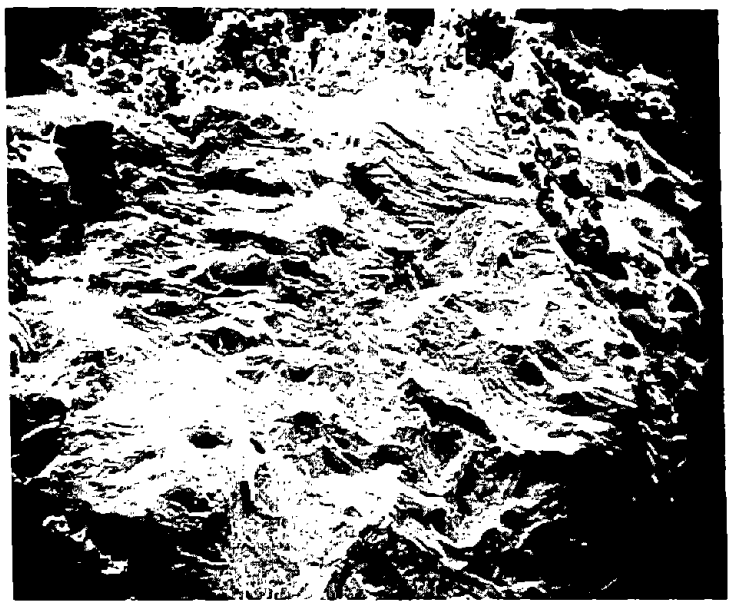

100X

500X

FIGURE 30. FRACTURE SURFACE OF SAMPLE 024 AT THE NOTCH TIP

Tip of notch is at upper right.

1000X

5000X

FIGURE 31. FRACTURE SURFACE OF SAMPLE 002 0.17 INCH FROM THE NOTCH TIP, $\Delta K \approx 17$ ksi-in.$^{\frac{1}{2}}$

Compare lines at 5000X with Figure 23(a).

4000X

FIGURE 32. FRACTURE SURFACE OF SAMPLE 024 0.56 INCH FROM THE NOTCH TIP, $\Delta K \approx 22$ KSI-IN.$^{\frac{1}{2}}$

9500X

(a) Sample 004, 0.86 inch From Notch Tip, $\Delta K \approx$ 29 ksi-in.$^{\frac{1}{2}}$

9500X

(b) Sample 030, 1.15 inches From Notch Tip, $\Delta K \approx 43$ ksi-in.$^{\frac{1}{2}}$

FIGURE 33. EXAMPLES OF FRACTURE SURFACE STRIATIONS

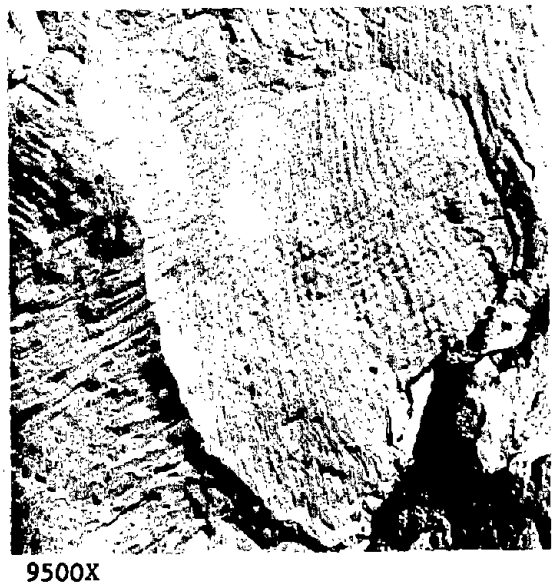

9500X

FIGURE 34. CROSS-HATCHED LINE PATTERN - SAMPLE 024, 1.21 INCHES FROM NOTCH TIP, $\Delta K \approx 45$ KSI-IN.$^{\frac{1}{2}}$

2800X

FIGURE 35. CLEAVAGE FRACTURE - SAMPLE 024, 1.21 INCHES FROM NOTCH TIP, $\Delta K \approx$ 45 KSI-IN.$^{\frac{1}{2}}$

The fractographic results obtained so far are in agreement with those reported in references 1 and 2. The two referenced publications indicate that the topography of the examined fatigue fractures is as complex with an irregular occurrence of striations, transgranular pearlite cracking, and some cleavage.

The observation of a gradual increase in the amount of cleavage fracture is in agreement with other reports.[4,5] During Phase II of the program, quantitative estimates will be made of the amount of cleavage encountered during the fatigue crack growth in various rail steels.

The scattered cleavage facets observed close to the notch tip in various specimens will also be a point of further examination. A two-component mechanism for crack extension at very low growth rates was proposed in reference 6. This mechanism accounts for planar fracture damage (controlled by ΔK) in favorably oriented grains, followed by failure of the unbroken grains (controlled by K_{max}). It is expected that the tests at different R-ratios and the threshold experiments may shed some further light on this matter.

7.4. PROJECTED EXPERIMENTS FOR PHASE II

The objective of Phase II is to obtain the more detailed information on fatigue-crack propagation necessary for the development of the failure model. As pointed out in the foregoing sections, this information will be generated for a limited number of rail samples. For this purpose, three groups of samples were selected with low, medium, and high crack propagation rates. It was attempted to compose each group of rail samples with nearly the same carbon and manganese content (Table 11).

In addition to these three groups, other samples were to be selected for further testing on the basis of the data analysis. However, no clear-cut correlations with other properties as might appear from between fatigue-crack growth rates and metallurgical variables emerged. Therefore, the selection of the additional samples were somewhat arbitrary. The weak correlations found with carbon and manganese content, carbon equivalent, and fraction of pearlite were used as a starting point for the selection.

The 10 samples chosen are listed in Table 16. Reasons for selection are indicated, and it is also shown in which growth rate category each sample would belong. Two additional experiments will be performed on each sample in order to obtain further information for the AID analysis. In addition, detailed metallography and fractography will be performed on 20 samples used in Phase II. This work involved the determination of pearlite lamella size, pearlite colony size,

TABLE 16. SAMPLES SELECTED FOR ADDITIONAL TESTING

Rail Sample Number	Category	C	Mn	Reason for Selection
004	I-II	.61	.62	85% pearlite, high sulfur
010	I	.63	.74	90% pearlite, low sulfur
014	I	.78	.74	low sulfur
026	I	.78	.94	low sulfur
027	III	.78	.87	low ratio, TYS/TUS
037	II	.72	.93	low sulfur
038	III	.57	1.48	93% pearlite, low C, high Mn
040	I-II	.58	.64	99% pearlite, low C, low Mn
045	III	.65	.65	85% pearlite, low sulfur
058	III	.83	.84	heat treated

TABLE 17. EXPERIMENTS IN PHASE III

Test Type	Parameters	Specimen Types	Number of Tests per Category
Orientation	Orientations TL, SL	CT	2
Stress Ratio	R = -1.0, 0.5	CT, SEN	8
Temperature	-40, +140 F	CT	11
	R = 0, 0.5		
	Frequency 2, 20 Hz		
Surface Flaw	R = 0, 75 F	SF	2
Mixed Mode	I-II, I-III	Bend	8
Threshold	R = -1.0, 0, 0.5	CT, SEN	2
Variable Amplitude		CT, SEN	10
		Total	43
		Total for 3 Categories	129
Check tests on 10 additional samples listed in table			
R = 0, Orientation LT and TL			20
		Total Number of Tests	149

prior austenite grain size, inclusion content and fraction of various fracture mechanisms. This will permit an exercise of complex correlation functions as presented in reference 3.

The test matrix for Phase II is presented in Table 17. The top part shows the detail testing to be performed on the three categories. The parameters for investigation are indicated. All this information will be used in the development of the failure model. It requires 129 crack growth tests.

The bottom part of Table 17 shows the experiments to be performed on the 10 additional samples listed in Table 16. Hence, a total of 149 experiments will be performed in Phase II. All experimental data will be used for a further evaluation with the AID program.

8. REFERENCES

1. Evans, P. R. V., Owen, N. B., and Hopkins, B. E., "Fatigue Crack Growth and Sudden Fast Fracture in a Rail Steel", J. of the Iron and Steel Inst., June 1970, pp 560-567.

2. Evans, P. R. V., Owen, N. B., and McCartney, L. N., "Mean Stress Effects on Fatigue Crack Growth and Failure in a Rail Steel", Eng. Fracture Mechanics, 6, 1974, pp 183-193.

3. Gladman, T., McIvor, I. D., and Pickering, F. B., "Some Aspects of the Structure-Property Relationships in High-Carbon Ferrite-Pearlite Steels", J. of the Iron and Steel Inst., Dec. 1972, pp 916-930.

4. Beevers, C. J., et al., "Some Considerations of the Influence of Subcritical Change Growth During Fatigue Crack Propagation in Steel", Metal Science, 9,3 (1975), pp 119-126.

5. Cooke, R. J., and Beevers, C. J., "Low Fatigue Crack Propagation in Pearlitic Steels", Mat. Science Engineering, 13 (1974), pp 201-210.

6. Robinson, G. L., and Beevers, C. J., "The Effects of Load Ratio, Interstitial Content and Grain Rise on Low-Stress Fatigue-Crack Propagation in α-Titanium", Metal Science, 7,9 (1973), pp 153-159.

APPENDIX A

BASELINE CRACK-GROWTH DATA

The following tabulations present the crack length measurements and associated cycle count for the 66 material samples received for evaluation in this program. A total of 67 data sets are presented with a reproducibility demonstration provided in duplicate testing of Specimen Nos. 027 and 027A. Specimen No. 029A replaced Specimen No. 029 for which unanticipated crack growth to failure occurred during an untended cycling period.

These crack growth data sets are presented sequentially in ascending order of sample number. The first measurement point represents the precrack length on the specimen surface after crack initiation and generation out of the chevron notch. The final crack length represents the last crack length that could be monitored by visual following with a traveling microscope.

Note: Specimen 27 was cycled at 2 kips, Specimen 46 at 5 kips, Specimen 58 at 4.5 kips. All other specimens were cycled at 2.5 kips. R = 0 for all tests.

CRACK LENGTH, A, INCH	CYCLE COUNT, N, KC
SPECIMEN 001	
.910	470.00
.947	540.00
1.021	610.00
1.060	672.00
1.105	750.00
1.135	800.00
1.186	905.00
1.238	1000.00
1.309	1102.00
1.347	1150.00
1.394	1200.00
1.476	1260.00
1.532	1285.00
1.592	1300.00
1.622	1306.00
1.648	1312.00
1.713	1320.00
1.745	1323.00
1.789	1326.00
1.843	1327.30
2.137	1327.35
2.162	1327.57

CRACK LENGTH, A, INCH	CYCLE COUNT, N, KC
SPECIMEN 002	
.936	350.00
.980	390.00
1.027	430.00
1.082	470.00
1.122	500.00
1.170	530.00
1.224	560.00
1.295	590.00
1.356	610.00
1.435	630.00
1.492	640.00
1.526	645.00
1.560	650.00
1.606	655.00
1.654	660.00
1.709	664.00
1.753	667.00
1.789	669.00
1.804	670.00
1.828	671.00
1.859	673.00
1.908	675.00
1.964	677.00
1.980	677.19

CRACK LENGTH, A, INCH	CYCLE COUNT, N, KC
SPECIMEN 003	
.974	265.00
1.045	310.00
1.089	340.00
1.131	370.00
1.178	400.00
1.254	430.00
1.324	450.00
1.396	465.00
1.462	475.00
1.515	480.00
1.588	485.00
1.628	487.00
1.681	489.00
1.894	490.00
1.741	491.36
1.770	492.00
1.807	492.50
1.869	493.00
1.885	493.05

CRACK LENGTH, A, INCH	CYCLE COUNT, N, KC
SPECIMEN 004	
.933	260.00
1.019	400.00
1.107	500.00
1.170	550.00
1.252	600.00
1.316	630.00
1.445	670.00
1.521	685.00
1.553	690.00
1.583	695.00
1.624	700.00
1.658	705.00
1.714	710.00
1.737	712.00
1.780	715.00
1.827	717.00
1.851	718.00
1.918	720.00
2.006	722.10
2.020	722.21

CRACK LENGTH, A, INCH	CYCLE COUNT, N, KC
SPECIMEN 005	
.905	225.00
.980	300.00
1.041	350.00
1.074	375.00
1.099	400.00
1.137	430.00
1.197	460.00
1.236	480.00
1.282	500.00
1.320	515.00
1.363	530.00
1.424	545.00
1.469	555.00
1.524	565.00
1.610	575.00
1.652	580.00
1.696	582.00
1.755	584.00
1.795	585.00
1.861	586.00
1.884	586.50
1.918	587.00
1.954	587.52

CRACK LENGTH, A, INCH	CYCLE COUNT, N, KC
SPECIMEN 006	
.896	260.00
.938	400.00
.998	500.00
1.055	600.00
1.117	700.00
1.152	760.00
1.212	820.00
1.291	880.00
1.404	930.00
1.540	965.00
1.570	970.00
1.608	975.00
1.638	978.00
1.656	980.00
1.672	982.00
1.686	984.00
1.706	986.00
1.733	988.00
1.797	991.00
1.820	992.00
1.875	993.36
1.917	994.01
1.945	994.22
1.963	994.29

CRACK LENGTH, A, INCH	CYCLE COUNT, N, KC
SPECIMEN 007	
.918	400.00
.955	460.00
.986	520.00
1.024	600.00
1.058	700.00
1.098	800.00
1.153	900.00
1.210	1000.00
1.268	1100.00
1.323	1160.00
1.392	1240.00
1.443	1270.00
1.495	1290.00
1.559	1310.00
1.605	1320.00
1.632	1325.00
1.666	1330.00
1.722	1335.00
1.763	1338.00
1.821	1341.00
1.882	1343.00
1.921	1344.00
1.951	1344.50
1.970	1345.00
1.994	1345.50
2.002	1345.55

CRACK LENGTH, A, INCH	CYCLE COUNT, N, KC
SPECIMEN 008	
.940	130.00
.989	175.00
1.035	210.00
1.068	235.00
1.104	260.00
1.134	280.00
1.178	310.00
1.228	340.00
1.267	360.00
1.310	380.00
1.360	400.00
1.425	420.00
1.456	430.00
1.503	440.00
1.560	451.00
1.668	465.00
1.734	470.00
1.771	472.00
1.816	474.00
1.844	475.00
1.896	476.00
1.934	477.00
2.003	477.78

CRACK LENGTH, A, INCH	CYCLE COUNT, N, KC
SPECIMEN 009	
.913	320.00
1.002	460.00
1.069	550.00
1.143	640.00
1.220	700.00
1.369	780.00
1.504	820.00
1.566	830.00
1.607	834.00
1.644	836.00
1.667	837.00
1.720	838.00
1.733	838.30
1.836	838.74

CRACK LENGTH, A, INCH	CYCLE COUNT, N, KC
SPECIMEN 010	
.919	175.00
.972	215.00
.993	245.00
1.032	275.00
1.065	300.00
1.104	325.00
1.143	350.00
1.185	375.00
1.229	400.00
1.293	425.00
1.361	450.00
1.438	470.00
1.482	480.00
1.537	490.00
1.570	495.00
1.606	500.00
1.643	505.00
1.690	510.00
1.727	514.00
1.777	518.00
1.835	521.00
1.869	522.50
1.906	524.00
1.961	525.50
2.037	527.00
2.092	527.63
2.104	527.69

CRACK LENGTH, A, INCH	CYCLE COUNT, N, KC
SPECIMEN 011	
.920	205.00
.954	250.00
.981	300.00
1.036	335.00
1.111	400.00
1.198	460.00
1.236	480.00
1.287	500.00
1.334	515.00
1.392	530.00
1.439	540.00
1.464	545.00
1.494	550.00
1.537	555.00
1.574	560.00
1.628	565.00
1.660	568.00
1.703	571.00
1.813	574.00
1.865	574.65
2.004	574.65
2.036	574.89

CRACK LENGTH, A, INCH	CYCLE COUNT, N, KC
SPECIMEN 012	
.923	165.00
1.020	220.00
1.094	260.00
1.199	305.00
1.341	340.00
1.392	350.00
1.423	355.00
1.464	360.00
1.513	365.00
1.545	368.00
1.586	371.00
1.631	374.00
1.686	377.00
1.736	379.00
1.776	380.00
1.818	381.00
1.878	381.80

CRACK LENGTH, A, INCH	CYCLE COUNT, N, KC
SPECIMEN 013	
.927	135.00
.995	165.00
1.024	180.00
1.065	200.00
1.075	210.00
1.100	220.00
1.121	230.00
1.148	240.00
1.203	260.00
1.252	280.00
1.316	300.00
1.360	315.00
1.420	330.00
1.470	340.00
1.530	350.00
1.601	360.00
1.654	365.20
1.710	370.00
1.734	373.00
1.770	375.00
1.810	377.00
1.858	379.00
1.915	381.00
1.967	382.50
2.014	383.50
2.060	384.40
2.106	384.90

CRACK LENGTH, A, INCH	CYCLE COUNT, N, KC
SPECIMEN 014	
.915	270.00
1.001	350.00
1.058	400.00
1.123	450.00
1.200	500.00
1.347	555.00
1.521	590.00
1.614	602.00
1.693	610.00
1.717	612.00
1.757	614.00
1.778	615.00
1.799	616.00
1.841	617.00
1.875	618.00
1.914	618.57
1.964	618.96

CRACK LENGTH, A, INCH	CYCLE COUNT, N, KC
SPECIMEN 015	
.920	160.00
.974	220.00
1.014	260.00
1.059	300.00
1.105	340.00
1.143	380.00
1.190	420.00
1.246	460.00
1.276	490.00
1.318	520.00
1.372	550.00
1.433	570.00
1.465	580.00
1.502	590.00
1.539	600.00
1.588	610.00
1.642	620.00
1.709	628.00
1.737	632.00
1.796	636.00
1.838	638.00
1.872	640.00
1.930	641.50
2.000	641.68

CRACK LENGTH, A, INCH	CYCLE COUNT, N, KC
SPECIMEN 016	
1.000	160.00
1.122	200.00
1.152	210.00
1.192	220.00
1.247	235.00
1.319	250.00
1.387	265.00
1.442	275.00
1.501	285.00
1.537	290.00
1.593	295.00
1.645	301.00
1.695	304.00
1.728	306.00
1.773	308.00
1.807	310.00
1.835	310.50
1.855	310.74

CRACK LENGTH, A, INCH	CYCLE COUNT, N, KC
SPECIMEN 017	
.947	155.00
.997	180.00
1.023	200.00
1.053	220.00
1.082	240.00
1.110	260.00
1.154	290.00
1.205	320.00
1.250	350.00
1.322	380.00
11.389	405.00
1.474	430.00
1.571	450.00
1.647	460.00
1.704	465.00
1.736	467.00
1.798	469.00
1.827	469.30
1.849	469.60
1.868	470.00
1.898	470.16
1.944	470.18

CRACK LENGTH, A, INCH	CYCLE COUNT, N, KC
SPECIMEN 018	
.801	485.00
.835	600.00
.871	700.00
.901	800.00
.936	900.00
.976	1000.00
1.024	1100.00
1.094	1200.00
1.207	1300.00
1.303	1350.00
1.387	1380.00
1.422	1390.00
1.463	1400.00
1.492	1405.10
1.522	1410.00
1.565	1416.00
1.617	1421.00
1.661	1425.00
1.722	1430.00
1.789	1432.50
1.832	1433.70
1.903	1434.65
1.923	1434.67

CRACK LENGTH, A, INCH	CYCLE COUNT, N, KC
SPECIMEN 019	
.927	270.00
.964	320.00
1.034	371.00
1.082	420.00
1.123	470.00
1.171	520.00
1.230	570.00
1.280	610.00
1.326	640.00
1.363	670.00
1.430	700.00
1.511	730.00
1.605	750.00
1.633	755.00
1.670	760.00
1.710	765.00
1.762	769.00
1.847	772.00
1.904	772.58
1.930	772.86

CRACK LENGTH, A, INCH	CYCLE COUNT, N, KC
SPECIMEN 020	
.818	8741.00
.840	9200.00
.883	9740.00
.921	10140.00
.979	10600.00
1.071	11230.00
1.223	11720.00
1.286	11830.00
1.334	11890.00
1.381	11930.00
1.395	11940.00
1.408	11950.00
1.471	11980.00
1.522	12000.00
1.577	12015.00
1.600	12020.00
1.626	12025.00
1.657	12030.00
1.693	12035.00
1.732	12040.00
1.776	12043.00
1.832	12045.00
1.984	12045.70
2.014	12046.00

CRACK LENGTH, A, INCH	CYCLE COUNT, N, KC
SPECIMEN 021	
.980	208.00
.997	230.00
1.025	260.00
1.060	300.00
1.102	350.00
1.150	400.00
1.194	450.00
1.306	520.00
1.342	540.00
1.398	560.00
1.443	576.00
1.497	593.00
1.551	606.00
1.592	615.00
1.618	620.00
1.642	625.00
1.682	630.00
1.718	635.00
1.761	640.00
1.822	645.00
1.859	648.00
1.898	650.00
1.962	652.00
2.010	652.70
2.026	652.74

CRACK LENGTH, A, INCH	CYCLE COUNT, N, KC
SPECIMEN 022	
.938	305.00
.987	350.00
1.042	460.00
1.054	500.00
1.088	580.00
1.122	660.00
1.171	770.00
1.244	850.00
1.306	930.00
1.375	1000.00
1.409	1050.00
1.495	1110.00
1.564	1140.00
1.636	1160.00
1.684	1170.00
1.703	1174.00
1.722	1178.00
1.743	1182.00
1.764	1186.00
1.783	1190.00
1.797	1192.00
1.829	1196.00
1.891	1200.00
1.959	1201.70
2.041	1202.33
2.050	1202.34

CRACK LENGTH, A, INCH	CYCLE COUNT, N, KC
SPECIMEN 023	
.936	130.00
1.001	150.00
1.058	170.00
1.121	190.00
1.190	210.00
1.250	230.00
1.336	250.00
1.446	270.00
1.503	280.00
1.600	290.00
1.626	293.00
1.661	296.00
1.702	298.00
1.730	300.00
1.744	301.00
1.767	302.00
1.791	303.00
1.813	304.00
1.859	304.70
1.925	305.43
1.936	305.49

CRACK LENGTH, A, INCH	CYCLE COUNT, N, KC
SPECIMEN 024	
.792	322.40
.812	400.00
.840	500.00
.865	600.00
.887	700.00
.916	800.00
.965	950.00
1.019	1100.00
1.070	1200.00
1.127	1300.00
1.218	1400.00
1.289	1450.00
1.426	1500.00
1.547	1520.00
1.572	1524.00
1.601	1528.00
1.626	1532.00
1.650	1535.00
1.697	1538.00
1.752	1541.00
1.860	1542.60
1.924	1542.66

CRACK LENGTH, A, INCH	CYCLE COUNT, N, KC
SPECIMEN 025	
.942	133.00
1.058	170.00
1.094	180.00
1.129	190.00
1.166	200.00
1.201	210.00
1.239	220.00
1.281	230.00
1.323	240.00
1.372	250.00
1.423	260.00
1.484	270.00
1.548	280.00
1.625	290.00
1.668	295.00
1.739	300.00
2.011	304.00

CRACK LENGTH, A, INCH	CYCLE COUNT, N, KC
SPECIMEN 026	
.791	240.00
.831	340.00
.881	440.00
.912	500.00
.979	600.00
1.033	650.00
1.094	700.00
1.145	730.00
1.213	760.00
1.270	780.00
1.336	800.00
1.382	810.00
1.435	820.00
1.466	825.00
1.497	830.00
1.553	835.00
1.582	838.00
1.615	841.00
1.642	844.00
1.690	847.00
1.751	850.00
1.794	852.00

CRACK LENGTH, A, INCH	CYCLE COUNT, N, KC
SPECIMEN 027	
.921	3250.00
.970	3485.00
1.019	3775.00
1.054	3975.00
1.106	4200.00
1.184	4475.00
1.245	4650.00
1.297	4750.00
1.362	4860.00
1.451	4940.00
1.511	4970.00
1.555	4990.00
1.615	5010.00
1.657	5020.00
1.714	5030.00
1.753	5035.00
1.789	5040.00
1.886	5045.00
1.922	5046.00

CRACK LENGTH, A, INCH	CYCLE COUNT, N, KC
SPECIMEN 027A	
.928	450.00
.980	550.00
1.020	650.00
1.078	800.00
1.139	950.00
1.200	1100.00
1.249	1200.00
1.299	1280.00
1.343	1350.00
1.421	1400.00
1.542	1450.00
1.578	1460.00
1.609	1465.00
1.634	1470.00
1.668	1475.00
1.702	1480.00
1.763	1485.00
1.802	1487.00
1.833	1488.00
1.858	1489.00
1.906	1490.00
1.925	1490.17

CRACK LENGTH, A, INCH	CYCLE COUNT, N, KC
SPECIMEN 028	
.918	561.00
.948	700.00
.989	790.00
1.142	1070.00
1.225	1160.00
1.267	1200.00
1.331	1235.00
1.360	1250.00
1.403	1265.00
1.446	1280.00
1.480	1290.00
1.519	1300.50
1.541	1305.00
1.564	1310.00
1.590	1315.10
1.623	1320.00
1.660	1325.00
1.703	1330.00
1.731	1332.50
1.756	1335.00
1.796	1338.50
1.821	1340.00
1.877	1342.00
1.904	1343.00
1.934	1344.00
2.130	1346.56

CRACK LENGTH, A, INCH	CYCLE COUNT, N, KC
SPECIMEN 029A	
.914	730.00
.958	900.00
1.008	1110.00
1.042	1270.00
1.080	1450.00
1.099	1530.00
1.161	1730.00
1.214	1880.00
1.270	2000.00
1.359	2150.00
1.458	2250.00
1.608	2305.00
1.744	2325.00
1.783	2327.50
1.820	2329.00
1.845	2330.00
1.858	2330.60
1.887	2331.10
1.920	2331.50
1.951	2332.00
1.965	2332.07

CRACK LENGTH, A, INCH	CYCLE COUNT, N, KC
SPECIMEN 030	
.794	305.00
.854	405.00
.923	480.00
.970	520.00
1.007	540.00
1.042	560.00
1.086	580.00
1.130	600.00
1.179	620.00
1.239	640.00
1.265	650.00
1.321	665.00
1.386	680.00
1.435	690.00
1.500	700.00
1.534	705.00
1.568	710.00
1.607	715.00
1.632	718.00
1.662	721.00
1.694	724.00
1.741	727.00
1.776	729.00
1.804	730.00
1.841	731.00
1.858	732.00
1.886	733.00
1.945	733.50
2.014	733.77

CRACK LENGTH, A, INCH	CYCLE COUNT, N, KC
SPECIMEN 031	
.922	250.00
.985	320.00
1.023	350.00
1.048	380.00
1.072	410.00
1.099	450.00
1.128	500.00
1.153	550.00
1.177	600.00
1.238	700.00
1.358	800.00
1.437	850.00
1.493	870.00
1.529	880.00
1.570	890.00
1.627	902.00
1.685	911.00
1.711	915.00
1.765	920.00
1.800	923.00
1.829	925.00
1.861	927.00
1.942	928.50
1.977	928.87
2.001	928.92

CRACK LENGTH, A, INCH	CYCLE COUNT, N, KC
SPECIMEN 032	
.765	300.00
.787	400.00
.811	500.00
.833	600.00
.860	700.00
.900	800.00
.941	900.00
.984	1000.00
1.049	1100.00
1.125	1200.00
1.241	1300.00
1.327	1340.00
1.381	1360.00
1.412	1370.00
1.448	1380.00
1.487	1390.00
1.539	1400.00
1.571	1406.00
1.598	1410.00
1.642	1415.00
1.692	1420.00
1.761	1425.00
1.812	1427.00
1.859	1439.00
1.949	1429.35

CRACK LENGTH, A, INCH	CYCLE COUNT, N, KC
SPECIMEN 033	
.933	215.00
1.066	300.00
1.134	340.00
1.169	360.00
1.203	380.00
1.226	400.00
1.274	420.00
1.326	440.00
1.390	460.00
1.477	480.00
1.523	490.00
1.565	496.00
1.605	502.00
1.636	506.00
1.654	508.00
1.676	510.00
1.705	512.00
1.738	514.00
1.778	516.00
1.829	518.00
1.865	519.00
1.935	519.44
1.940	519.48

CRACK LENGTH, A, INCH	CYCLE COUNT, N, KC
SPECIMEN 034	
.995	185.00
1.076	230.00
1.110	250.00
1.157	275.00
1.195	295.00
1.240	315.00
1.286	335.00
1.349	355.00
1.433	375.00
1.494	385.00
1.543	391.00
1.575	395.00
1.603	398.00
1.620	400.00
1.651	402.00
1.680	404.00
1.717	406.00
1.741	407.00
1.775	408.00
1.830	409.00
1.862	409.53

CRACK LENGTH, A, INCH	CYCLE COUNT, N, KC
SPECIMEN 035	
.940	450.00
1.003	601.00
1.045	720.00
1.084	850.00
1.138	1000.00
1.167	1150.00
1.241	1300.00
1.306	1450.00
1.384	1600.00
1.479	1700.00
1.527	1730.00
1.584	1755.00
1.615	1765.00
1.654	1775.00
1.677	1780.00
1.697	1785.00
1.719	1790.00
1.743	1795.00
1.762	1800.00
1.825	1805.00
1.907	1810.00
1.944	1811.00
1.980	1812.00
2.021	1812.31

CRACK LENGTH, A, INCH	CYCLE COUNT, N, KC
SPECIMEN 036	
.964	430.00
1.014	550.00
1.055	670.00
1.095	805.00
1.121	900.00
1.146	1000.00
1.194	1160.00
1.235	1300.00
1.296	1450.00
1.353	1550.00
1.434	1650.00
1.506	1700.50
1.564	1730.00
1.624	1750.00
1.668	1761.00
1.749	1775.00
1.799	1780.00
1.843	1783.00
1.879	1785.00
1.932	1785.50
1.994	1785.71

CRACK LENGTH, A, INCH	CYCLE COUNT, N, KC
SPECIMEN 037	
.939	245.00
1.005	315.00
1.039	360.00
1.069	400.00
1.105	450.00
1.140	500.00
1.172	550.00
1.207	602.00
1.255	660.00
1.296	710.00
1.354	760.00
1.430	810.00
1.523	855.00
1.598	880.00
1.661	895.00
1.684	900.00
1.703	905.00
1.773	915.00
1.820	920.00
1.851	923.00
1.903	925.00
1.949	926.00
2.001	927.00
2.108	927.53

CRACK LENGTH, A, INCH	CYCLE COUNT, N, KC
SPECIMEN 038	
.934	300.00
.996	385.00
1.036	450.00
1.069	515.00
1.103	580.00
1.145	660.00
1.197	750.00
1.254	850.00
1.314	950.00
1.365	1030.00
1.408	1100.00
1.446	1170.00
1.501	1240.00
1.572	1300.00
1.637	1345.00
1.696	1375.00
1.745	1395.00
1.772	1405.00
1.806	1415.00
1.856	1425.00
1.865	1430.00
1.926	1435.00
1.962	1437.50
2.020	1438.62
2.135	1439.50

CRACK LENGTH, A, INCH	CYCLE COUNT, N, KC
SPECIMEN 039	
.938	280.00
1.025	400.00
1.064	470.00
1.083	520.00
1.128	620.00
1.161	700.00
1.216	800.00
1.270	900.00
1.344	1000.00
1.384	1050.00
1.429	1100.00
1.478	1140.00
1.538	1180.00
1.604	1210.00
1.633	1220.00
1.661	1230.00
1.697	1240.00
1.742	1250.00
1.791	1260.00
1.877	1270.00
1.915	1273.00
1.955	1275.00
2.012	1276.85
2.036	1276.90

CRACK LENGTH, A, INCH	CYCLE COUNT, N, KC
SPECIMEN 040	
.985	174.00
1.084	230.00
1.122	255.00
1.152	275.00
1.189	300.00
1.221	320.00
1.253	340.00
1.286	360.00
1.322	380.00
1.398	415.00
1.579	470.00
1.623	478.00
1.656	484.00
1.693	490.00
1.747	497.00
1.812	502.00
1.875	505.00
1.946	506.50
1.957	506.58

CRACK LENGTH, A, INCH	CYCLE COUNT, N, KC
SPECIMEN 041	
.926	302.00
.979	400.00
1.026	502.00
1.066	600.00
1.110	700.00
1.148	800.00
1.196	900.00
1.253	1000.00
1.322	1080.00
1.386	1151.00
1.434	1190.10
1.487	1220.00
1.540	1241.00
1.569	1252.00
1.593	1260.00
1.631	1270.00
1.672	1280.00
1.733	1290.00
1.782	1297.00
1.825	1302.00
1.869	1305.00
1.906	1307.00
1.950	1309.00
2.011	1311.00
2.071	1312.20
2.147	1313.20
2.180	1313.47

CRACK LENGTH, A, INCH	CYCLE COUNT, N, KC
SPECIMEN 042	
.942	212.00
.975	304.00
1.013	400.00
1.065	505.00
1.120	600.00
1.199	700.00
1.264	760.00
1.338	810.00
1.397	840.00
1.456	860.00
1.493	871.00
1.514	876.00
1.537	881.00
1.570	887.00
1.624	894.00
1.665	900.00
1.728	905.00
1.764	908.00
1.808	911.00
1.842	913.00
1.929	913.60
1.955	913.67

CRACK LENGTH, A, INCH	CYCLE COUNT, N, KC
SPECIMEN 043	
.951	145.00
1.000	180.00
1.035	205.00
1.070	230.00
1.097	255.00
1.150	300.00
1.208	345.00
1.249	380.00
1.294	410.00
1.348	440.00
1.407	465.00
1.467	485.00
1.557	512.00
1.599	520.00
1.620	525.00
1.643	530.00
1.678	535.00
1.708	540.00
1.749	545.00
1.793	550.00
1.856	555.00
1.891	557.00
1.944	558.61
1.990	559.51
2.050	560.52

CRACK LENGTH, A, INCH	CYCLE COUNT, N, KC
SPECIMEN 044	
.949	210.00
1.011	300.00
1.067	400.00
1.122	490.00
1.182	580.00
1.229	640.00
1.266	680.00
1.319	710.00
1.356	730.00
1.394	750.00
1.455	770.00
1.490	780.00
1.543	790.00
1.586	795.00
1.637	800.00
1.684	802.50
1.721	804.00
1.742	805.00
1.779	806.50
1.824	808.00
1.919	809.00
1.951	809.23

CRACK LENGTH, A, INCH	CYCLE COUNT, N, KC
SPECIMEN 045	
.946	250.00
.987	400.00
1.029	550.00
1.062	650.00
1.115	800.00
1.161	900.00
1.207	1000.00
1.264	1100.00
1.320	1180.00
1.397	1270.00
1.471	1330.00
1.522	1360.00
1.574	1385.00
1.608	1400.00
1.655	1415.00
1.686	1425.00
1.733	1436.00
1.778	1445.00
1.848	1455.00
1.902	1460.00
1.969	1463.00
2.051	1465.00
2.106	1465.67

CRACK LENGTH, A, INCH	CYCLE COUNT, N, KC
SPECIMEN 046	
.885	900.00
.885	1550.00
.893	1800.00
.902	1900.00
.927	2100.00
.984	2300.00
1.061	2500.00
1.140	2600.00
1.187	2650.00
1.263	2700.00
1.367	2730.00
1.410	2736.00
1.451	2742.00
1.472	2744.50
1.507	2746.40
1.555	2747.10
1.595	2747.62

CRACK LENGTH, A, INCH	CYCLE COUNT, N, KC
SPECIMEN 047	
.909	375.00
.946	525.00
.980	700.00
1.018	900.00
1.035	1000.00
1.071	1200.00
1.102	1350.00
1.138	1500.00
1.190	1700.00
1.274	1900.00
1.329	2000.00
1.432	2100.00
1.486	2135.00
1.519	2150.00
1.562	2170.00
1.609	2185.00
1.649	2195.00
1.695	2205.00
1.759	2215.00
1.801	2220.00
1.853	2225.00
1.895	2228.00
1.939	2230.10
1.981	2230.73

CRACK LENGTH, A, INCH	CYCLE COUNT, N, KC
SPECIMEN 048	
.891	185.00
.914	215.00
.943	251.00
.979	290.00
1.033	340.00
1.094	380.00
1.150	410.00
1.212	440.00
1.263	465.00
1.351	485.00
1.408	500.00
1.484	515.00
1.541	525.00
1.573	530.00
1.604	535.00
1.641	540.00
1.662	545.00
1.720	550.00
1.758	552.50
1.783	555.00
1.809	557.00
1.835	559.00
1.892	561.00
1.948	562.00
2.061	563.60
2.071	563.64

CRACK LENGTH, A, INCH	CYCLE COUNT, N, KC
SPECIMEN 049	
.913	260.00
.984	330.00
1.029	390.00
1.058	430.00
1.092	470.00
1.135	530.00
1.172	570.00
1.231	620.00
1.271	650.00
1.318	680.00
1.382	710.00
1.469	740.00
1.513	750.00
1.563	760.00
1.622	770.00
1.663	775.00
1.709	780.00
1.775	785.00
1.811	787.00
1.863	789.00
1.901	790.00
1.930	791.00
1.964	792.00
2.025	792.59

CRACK LENGTH, A, INCH	CYCLE COUNT, N, KC
SPECIMEN 050	
.926	285.00
.979	510.00
1.023	700.00
1.094	910.00
1.154	1050.00
1.202	1125.00
1.257	1200.00
1.335	1275.00
1.392	1315.00
1.453	1345.00
1.493	1360.00
1.538	1375.00
1.576	1385.00
1.624	1395.00
1.688	1405.00
1.731	1410.00
1.763	1413.00
1.802	1416.00
1.850	1419.00
1.912	1421.00
1.967	1421.76

CRACK LENGTH, A, INCH	CYCLE COUNT, N, KC
SPECIMEN 051	
.921	365.00
.945	665.00
.973	865.00
.992	1000.00
1.033	1272.00
1.092	1500.00
1.178	1730.00
1.259	1880.00
1.313	1940.00
1.352	1970.00
1.390	2000.00
1.462	2040.00
1.516	2060.00
1.566	2076.00
1.640	2085.00
1.674	2090.00
1.723	2095.00
1.766	2098.00
1.812	2100.00
1.987	2100.68

CRACK LENGTH, A, INCH	CYCLE COUNT, N, KC
SPECIMEN 052	
.882	275.00
.945	375.00
.984	450.00
1.042	540.00
1.082	600.00
1.117	655.00
1.136	700.00
1.176	760.00
1.233	820.00
1.279	860.00
1.326	890.00
1.384	920.00
1.433	940.00
1.480	955.00
1.537	970.00
1.583	980.00
1.655	990.00
1.719	997.00
1.770	1002.00
1.823	1005.00
1.890	1008.00
1.954	1009.00
2.034	1009.53
2.053	1009.55

CRACK LENGTH, A, INCH	CYCLE COUNT, N, KC
SPECIMEN 053	
.937	415.00
.990	505.00
1.019	600.00
1.057	700.00
1.098	800.00
1.113	950.00
1.149	1050.00
1.216	1160.00
1.270	1210.00
1.361	1262.00
1.467	1285.00
1.540	1295.00
1.570	1300.00
1.595	1305.00
1.637	1310.00
1.677	1315.00
1.731	1320.00
1.772	1323.00
1.818	1325.00
1.863	1326.50
1.893	1326.56

CRACK LENGTH, A, INCH	CYCLE COUNT, N, KC
SPECIMEN 054	
.904	175.00
.951	350.00
.981	440.00
1.011	537.00
1.039	610.00
1.071	700.00
1.125	825.00
1.178	930.00
1.263	1075.00
1.321	1155.00
1.365	1205.00
1.431	1260.00
1.500	1300.00
1.587	1330.00
1.620	1340.00
1.654	1350.00
1.701	1360.00
1.730	1365.00
1.761	1370.00
1.807	1375.00
1.872	1380.00
1.936	1382.00
2.009	1382.48
2.068	1382.49

CRACK LENGTH, A, INCH	CYCLE COUNT, N, KC
SPECIMEN 055	
.921	164.00
.965	250.00
1.004	326.00
1.046	424.00
1.085	504.00
1.130	610.00
1.194	710.00
1.234	800.00
1.296	910.00
1.354	984.00
1.386	1030.00
1.453	1090.00
1.493	1120.00
1.557	1160.00
1.607	1180.00
1.671	1200.00
1.704	1210.00
1.749	1220.00
1.805	1230.00
1.846	1234.00
1.866	1237.00
1.917	1240.00
1.979	1241.68
2.031	1241.81

CRACK LENGTH, A, INCH	CYCLE COUNT, N, KC
SPECIMEN 056	
.914	400.00
.964	610.00
1.007	810.00
1.046	1020.00
1.098	1220.00
1.135	1340.00
1.188	1485.00
1.237	1570.00
1.293	1675.00
1.351	1750.00
1.409	1800.00
1.479	1845.00
1.514	1860.00
1.541	1870.00
1.571	1880.00
1.609	1890.00
1.657	1900.00
1.715	1910.00
1.760	1915.00
1.810	1920.00
1.864	1923.00
1.921	1926.00
2.002	1927.43

CRACK LENGTH, A, INCH	CYCLE COUNT, N, KC
SPECIMEN 057	
.921	285.00
.938	335.00
.963	405.00
.999	500.00
1.048	620.00
1.099	735.00
1.156	846.00
1.203	920.00
1.262	1000.00
1.325	1060.00
1.406	1120.00
1.471	1150.00
1.537	1170.00
1.583	1180.00
1.639	1190.00
1.691	1196.00
1.726	1200.00
1.761	1205.00
1.834	1210.00
1.902	1213.00
1.936	1214.00
2.011	1214.34

CRACK LENGTH, A, INCH	CYCLE COUNT, N, KC
SPECIMEN 058	
.910	500.00
.939	605.00
.994	700.00
1.114	816.00
1.173	850.00
1.195	860.00
1.230	870.00
1.247	880.00
1.280	890.00
1.317	900.00
1.360	910.00
1.420	920.00
1.453	925.00
1.493	930.00
1.572	934.00
1.610	934.70

CRACK LENGTH, A, INCH	CYCLE COUNT, N, KC
SPECIMEN 059	
.924	400.00
.972	500.00
1.039	665.20
1.089	861.70
1.142	1004.90
1.191	1285.40
1.243	1966.00
1.289	2246.80
1.346	2413.00
1.391	2527.10
1.445	2619.80
1.507	2692.70
1.569	2753.90
1.594	2778.30
1.639	2809.20
1.689	2833.80
1.770	2863.50
1.797	2870.10
1.847	2877.60
1.898	2882.70
1.940	2885.10
1.991	2885.80
2.046	2886.30

CRACK LENGTH, A, INCH	CYCLE COUNT, N, KC
SPECIMEN 060	
.908	140.00
1.012	175.00
1.087	230.00
1.125	260.00
1.178	290.00
1.224	310.00
1.277	330.10
1.343	350.00
1.376	360.00
1.414	370.00
1.467	380.00
1.498	385.00
1.526	390.00
1.572	395.00
1.617	400.00
1.673	405.00
1.702	407.00
1.746	409.00
1.794	410.90
1.824	411.50
1.928	412.47

CRACK LENGTH, A, INCH	CYCLE COUNT, N, KC
SPECIMEN 061	
.920	150.00
.951	180.00
.998	210.00
1.055	240.00
1.113	270.00
1.181	300.00
1.223	320.00
1.279	340.00
1.340	360.00
1.378	370.00
1.416	380.00
1.460	390.00
1.528	400.00
1.570	405.00
1.613	410.00
1.687	415.00
1.721	417.00
1.770	419.00
1.844	421.00
1.933	422.00
2.003	422.22

CRACK LENGTH, A, INCH	CYCLE COUNT, N, KC
SPECIMEN 062	
.907	170.00
.938	205.00
.990	255.00
1.064	305.00
1.094	325.00
1.192	372.00
1.277	400.00
1.321	415.00
1.356	425.00
1.395	435.00
1.441	445.00
1.469	450.00
1.500	455.00
1.532	460.00
1.574	465.00
1.613	470.00
1.668	475.00
1.715	477.00
1.808	479.00
1.852	479.50
1.924	479.82

CRACK LENGTH, A, INCH	CYCLE COUNT, N, KC
SPECIMEN 063	
.938	140.00
1.013	175.00
1.059	200.00
1.097	220.00
1.133	240.00
1.176	260.00
1.221	280.00
1.277	300.00
1.343	320.50
1.378	330.00
1.421	340.00
1.470	350.00
1.526	360.00
1.559	365.00
1.604	370.00
1.653	375.00
1.718	380.00
1.746	382.00
1.821	384.00
1.872	385.00
1.969	385.50
2.042	386.25

CRACK LENGTH, A, INCH	CYCLE COUNT, N, KC
SPECIMEN 064	
.916	600.00
.991	810.00
1.044	994.00
1.093	1149.40
1.143	1312.10
1.195	1456.00
1.243	1566.60
1.298	1659.10
1.345	1703.80
1.399	1743.50
1.505	1791.90
1.546	1804.50
1.596	1810.00
1.646	1825.20
1.695	1831.50
1.750	1837.10
1.807	1841.70
1.848	1843.70
1.897	1845.30
1.951	1845.90
1.999	1846.70

CRACK LENGTH, A, INCH	CYCLE COUNT, N, KC
SPECIMEN 065	
.921	280.00
.952	416.00
.996	800.00
1.037	1083.30
1.086	1335.00
1.135	1475.00
1.187	1616.00
1.235	1700.00
1.285	1770.00
1.336	1820.00
1.387	1854.00
1.448	1882.50
1.488	1897.00
1.544	1912.80
1.585	1920.50
1.657	1931.40
1.711	1938.10
1.795	1943.30
1.858	1945.30
1.891	1945.75
1.955	1946.22

CRACK LENGTH, A, INCH	CYCLE COUNT, N, KC
SPECIMEN 066	
.912	1160.00
.934	1270.00
.970	1480.00
1.007	1700.00
1.045	1900.00
1.070	2100.00
1.097	2200.00
1.125	2300.00
1.169	2600.00
1.224	2830.00
1.274	3000.00
1.365	3145.00
1.415	3191.00
1.473	3232.00
1.508	3250.00
1.549	3265.00
1.601	3280.00
1.651	3290.00
1.706	3300.00
1.745	3305.00
1.797	3310.00
1.840	3313.00
1.874	3315.10
1.904	3316.50
1.972	3318.00
2.073	3319.40

APPENDIX B

REPORT OF INVENTIONS

After a diligent review of the work performed to generate the aforementioned information, it is believed that no patentable innovation, or invention was made.

However, this report does contain data on static strength and fatigue-crack-propagation properties of rail steels presently in use in the United States — data which is not widely available. Therefore, it is considered that the data base generated here, although still limited, is a unique compilation of importance for the improvement of safety and performance of railroads in the USA.

220 copies